Centre Eau Terre Environnement

IMPACTS MOLÉCULAIRES DES NANOPLASTIQUES COMBINÉS À L'ARSENIC, EFFETS COMPARÉS ENTRE DES HUÎTRES CARIBÉENNES (*ISOGNOMON ALATUS*) ET CANADIENNES (*CRASSOSTREA VIRGINICA*) EXPOSÉES PAR VOIE TROPHIQUE

Par

Marc Lebordais

Mémoire présenté pour l'obtention du grade de
Maître Sciences (M. Sc.)
en sciences de l'eau

Jury d'évaluation

Président du jury et examinateur interne	Patrice Couture INRS-ETE
Examinateur externe	Elvis Xu University of Southern Denmark
Examinateur externe	Zhe Lu Université du Québec à Rimouski
Directrice de recherche	Valérie Langlois INRS-ETE
Codirectrice de recherche	Magalie Baudrimont Université de Bordeaux

REMERCIEMENTS

Mes remerciements vont en premiers lieux à Agnès Feurtet-Mazel et Nathalie Geneste qui m'ont donné l'opportunité de suivre le parcours Mobbidiq partagé par l'Université de Bordeaux et l'INRS, bénéficiant ainsi d'une immersion en recherche que j'ai pris plaisir à conduire et présenter au cours de ces deux ans.

Pour m'avoir proposé en toute confiance ce sujet novateur et audacieux, j'adresse un grand merci à Magalie Baudrimont qui a encadré mes débuts de travaux à la station marine d'Arcachon puis guidé dans l'avancement du projet sous ses différentes formes. Je remercie aussi Adeline Arini pour sa bienveillance et disponibilité qu'elle m'a accordé avec son expérience sur ce projet. Toute ma gratitude Zélie pour ta constance malgré les obstacles, ton agréable compagnie à toute heure et de m'avoir initié dans la théorie comme dans la pratique à la recherche. Sans oublier le personnel de la station marine d'Arcachon qui m'a formé et permis de mener à bien mes six premiers mois d'expérience.

Je tiens à grandement remercier Valérie Langlois qui m'a accueilli dans son équipe de recherche et supervisé à l'INRS. J'y ai trouvé l'autonomie et le soutien nécessaires pour y conduire mes travaux, ainsi que de belles opportunités pour m'ouvrir aux différentes pratiques de la recherche. A ce titre je remercie très chaleureusement Joy G., Julie R., Lara L.J., Molly L.R., Paisley T., Roxanne B., Sarah W., Scott H., Tuan T. et Vincent B. qui ont aussi bien été sources de critiques et de conseils, que d'inspiration et d'équilibre, si ce n'est un véritable soutien pour mon épanouissement. À Juan qui m'a accompagné tout au long du projet à l'INRS, merci pour ton professionnalisme, ta pédagogie et ta camaraderie j'ai pu acquérir de précieuses compétences aux côtés de ton expertise, tu as toute mon admiration !

Je ne peux finir sans adresser ma profonde amitié aux étudiantes et étudiants notamment des équipes Couture, Fortin, Lavoie et Pasquier, avec qui nous avons partagé les victoires des uns et difficultés des autres (non sans quelques chocolatines et pintes), mais aussi l'euphorie des congrès. À ce titre, Marie et Océane, mes très estimées collègues Mobbidiq je me réjouis vraiment d'avoir été à vos côtés pour cette expédition. Enfin, je garderai un excellent souvenir de nos lunch au 3e qui étaient un concentré d'échanges culturels, de railleries bienveillantes et d'interminables débats socio-environnementaux !

RÉSUMÉ

Compte tenu de la contamination majeure de notre environnement en plastiques, la présence des nanoplastiques (NP) inquiète. Les NP étant capables de traverser les barrières biologiques ils représentent un risque pour les organismes aquatiques. Toutefois leur toxicité est peu connue, notamment en présence d'autres contaminants. En effet, les NP peuvent adsorber des métaux et augmenter leur biodisponibilité pour des organismes filtreurs comme les bivalves.

J'ai donc exposé des huîtres caribéennes (*Isognomon alatus*) et canadiennes (*Crassostrea virginica*) par voie trophique à des concentrations environnementales de NP (10 et 100 µg L^{-1}). Trois types de NP ont été utilisés pour comparer leur toxicité, seuls ou combinés à l'arsenic présent dans l'eau (1 mg L^{-1}). Les interactions des NP sur la bioaccumulation de l'arsenic ont été évaluées, ainsi que l'expression des gènes dans les branchies et masses viscérales des deux espèces. Nos résultats montrent que les traitements de NP combinés à l'arsenic ont déclenché des effets protecteurs sur le niveau d'expression des gènes chez *I. alatus* et des effets synergiques chez *C. virginica*. Cette étude environnementalement pertinente met en avant l'écotoxicité des NP en comparant leurs impacts sur une espèce d'huîtres sauvages et d'élevages.

Mots-clés : nanoplastiques, arsenic, expression de gènes, bioaccumulation, adsorption, voie trophique, huîtres, microalgues

ABSTRACT

Considering plastics are major contaminations in our environment, the presence of nanoplastics (NPs) raises concern. NPs pose a risk to aquatic organisms as they could cross biological barriers. However little is known about NPs toxicity, particularly in the presence of other contaminants. Indeed, NPs can adsorb metallic contaminants and increase their bioavailability to filter-feeding organisms, such as bivalves.

I therefore exposed Caribbean oysters (*Isognomon alatus*) and Canadian oysters (*Crassostrea virginica*) by trophic way to NPs at environmental concentrations (10 and 100 µg L^{-1}). Three types of NPs were used to compare their toxicity, alone or in combination with arsenic in the water (1 mg L^{-1}). Interactions of NPs on arsenic bioaccumulation were studied, along with the expression of genes in gills and visceral mass of both species. Our results show that NP treatments combined with arsenic triggered protective effects on gene expression levels in *I. alatus* and synergetic effects in *C. virginica*. This is an environmentally relevant study that showcases ecotoxicity of NPs by comparing their impacts on wild and cultured oyster species.

Keywords : nanoplastics, arsenic, gene expression, bioaccumulation, trophic pathway, oysters, micro algae

TABLE DES MATIÈRES

LISTE DES FIGURES

LISTE DES TABLEAUX

LISTE DES ÉQUATIONS

$$CI = \frac{\text{leftover tissues} * \text{weight}}{\text{shells weight}} \times 100$$

* leftover tissues : whole body excluding gills and visceral mass

$$BAF = \frac{[As]_{\text{wet tissue}}}{[As]_{\text{water}}}$$

$[As]_{\text{wet tissue}}$: in µg/Kg

$[As]_{\text{water}}$: in µg/L

LISTE DES ABRÉVIATIONS

12S : mitochondrial encoded 12S rRNA

As : arsenic

βactine : actin beta

BAF : BioAccumulation Factor

bax : Bcl-2-associated X apoptosis regulator

bcl-2 : apoptosis regulator

cat : catalase

cav : cavéoline

cDNA : complementary DeoxyriboNucleic Acid

CI : Condition Index

cltc : clathrin heavy chain

COT : Carbone Organique Total

cox1 : mitochondrial encoded cytochrome c oxidase 1

cyp1A : cytochrome P450 family 1 sub-family A1

DLS : Dynamic Light Scattering

ef1α : elongation factor 1 alpha

gadd45 : growth arrest DNA damage

gapdh : glyceraldehyde-3-phosphate-dehydrogenase

ICP-MS : Inductively Coupled Plasma - Mass Spectrometry

ICP-OES : Inductively Coupled Plasma - Optical Emission Spectrometry

MAIL : Modèle d'Activité de l'Ion Libre

mdr : multidrug resistance

MES : Matière En Suspension

MLB : Modèle du Ligang Biotique

MPs : microplastics

mRNA : messenger RiboNucleic Acid

mt : metallothionein

NOM : Natural Organic Matter

NRT : No Reverse Transcriptase control

NTC : No Template Control

NPG : mixed nanoplastics of Guadeloupe

NPs : nanoplastics

p53 : tumor protein P53

PSC : crushed polystyrene nanoparticles

PSL : carboxylated polystyrene nanoparticles of latex

PS NPs : polystyrene nanoplastics

PVC : polyvinylchloride

qPCR : quantitative Polymerase Chain Reaction

rpl7: ribosomal protein L7

rRNA : ribosomic RiboNucleic Acid

RT : Reverse Transcription

SEM : Scanning Electron Microscopy

sod1 : superoxide dismutase Cu-Zn intracellular

sod3 : superoxide dismutase Cu-Zn extracellular

TOC : Total Organic Carbon

vit : vitellogenin

1 REVUE DE LITTÉRATURE

1.1 Productions et déchets plastiques au XXI° siècle

1.1.1 La contamination des océans

Les déchets plastiques sont des contaminants retrouvés dans les écosystèmes, et principalement dans les hydrosystèmes (Carpenter and Smith, 1972; Law *et al.*, 2010; Bank and Hansson, 2019). En effet les hydrosystèmes agissent comme des réceptacles naturels aux contaminants, et de nombreux polymères plastiques y perdurent plusieurs centaines d'années, partiellement dégradés (Briand, 2014; Scherer *et al.*, 2017). Cette contamination en déchets plastiques est visible à tout niveau trophique. Elle est notamment documentée pour les organismes aquatiques qui ingèrent ces débris plastiques et présentent plusieurs effets nocifs (Gregory, 2009; Gall and Thompson, 2015; Lusher *et al.*, 2017). La reconnaissance du caractère polluant des déchets plastiques mène ainsi à des prises de conscience et d'action (UNEP, 2001). Par exemple, une hausse de 80% du recyclage des plastiques en Europe a été notée (pour 11 % de déchets collectés supplémentaires; Plastics Europe, 2018). Néanmoins, une majorité des plastiques produits échappent au recyclage. En effet en 2017, 70% de la masse totale des macroplastiques accumulés dans les océans (émissions continentales et océaniques confondues) étaient issus d'équipement de pêche (**Figure 1.1**).

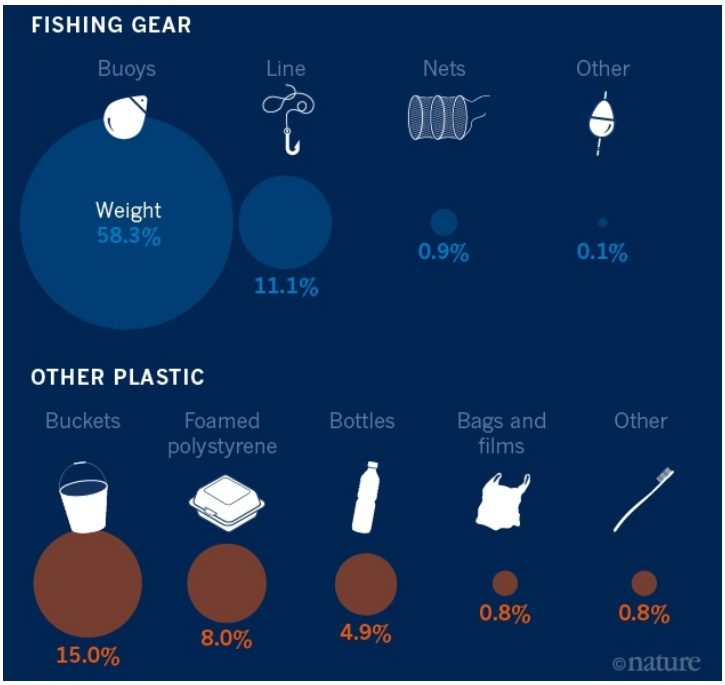

Figure 1.1 : Pourcentage de déchets plastiques dans les océans du globe représentés par leur masse (Cressey, 2016). Données combinées en macroplastiques (> 200 mm) dans les océans Pacifique, Atlantique Sud, Indien et la mer Méditerranéenne.

Les hydrosystèmes ont ainsi accumulé ces dernières décennies une contamination sans précédent de débris plastiques. Ces derniers sont appelés microplastiques (MP) lorsqu'ils sont inférieurs à 5 mm (NOAA, 2008). De nombreux MP sont en effet manufacturés en quantités industrielles comme composants de produits pharmaceutiques de soins personnels, telles que les microbilles présentes dans les cosmétiques (Rochman *et al.*, 2013, Napper *et al.*, 2015).. Ces MP représentent alors un réservoir pour la formation de nanoplastiques (NP) par divers modes de fragmentation (O'Brine and Thompson, 2010; Wright and Kelly, 2017) et sont classés comme contaminants émergents (Richardson and Kimura, 2020).

1.1.2 Le cycle des déchets plastiques

Plusieurs voies agissent sur le transport des déchets plastiques qui sont alors emmagasinés ou redirigés dans différents compartiments (Bank and Hansson, 2019). Ce cycle révèle une exposition majeure des hydrosystèmes marins à la fragmentation des plastiques en particules et leur dispersion dans le biota (**Figure 1.2**).

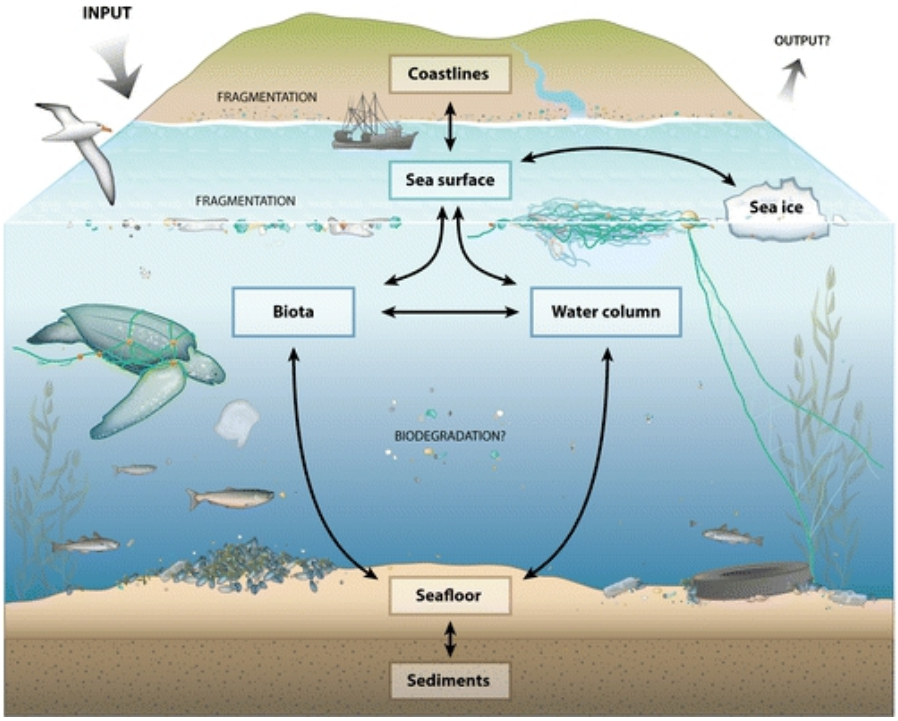

Figure 1.2 : Cycle des plastiques dans l'hydrosystème marin (Law *et al.*, 2017).

Bien que l'ubiquité des MP soit démontrée à la surface des océans (**Figure 1.3**), les concentrations mesurées en plastiques et MP sous-évaluent de plusieurs milliers de tonnes les valeurs attendues (Cózar *et al.*, 2014). Cette observation admise par la communauté scientifique a été nommée la fraction manquante des plastiques (Woodall *et al.*, 2014). À ce titre, plusieurs hypothèses tendent à l'expliquer telle que l'accumulation des MP dans les fonds marins et sédiments (Van Cauwenberghe *et al.*, 2013; Chiba *et al.*, 2018). Ou encore leur nanofragmentation en NP qui échappent alors aux techniques d'analyse (Quick *et al.*, 2011; Besseling *et al.*, 2012).

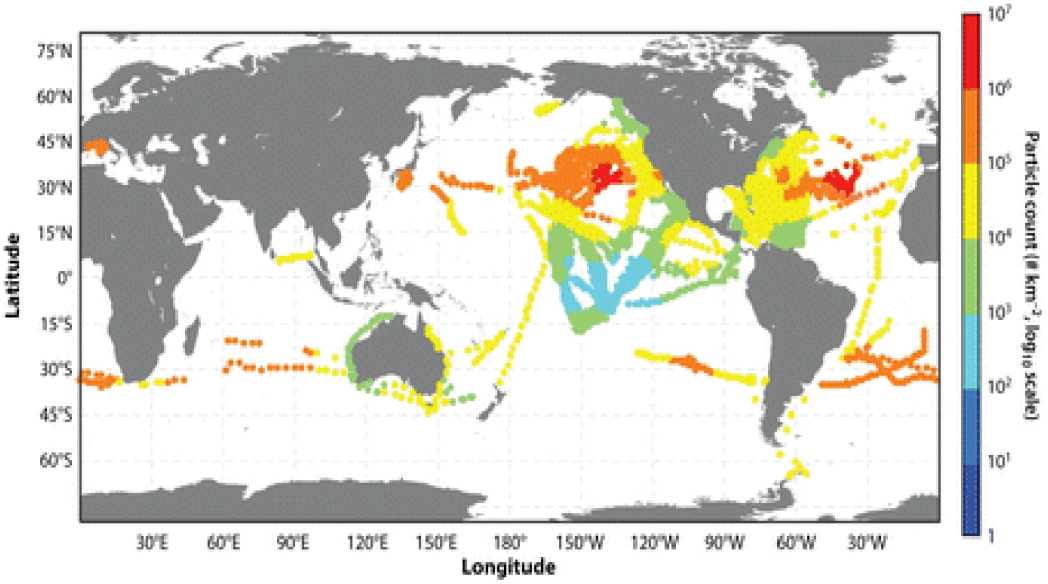

Figure 1.3 : Modélisation de la distribution mondiale du nombre de MP par km² collectés en surface au filet (Law *et al.*, 2017).

Bien qu'à ce jour il n'y ait pas de consensus international pour définir la taille des NP, la limite supérieure reconnue est 1000 nm (Lambert and Wagner, 2016; Gigault *et al.*, 2018). Deux origines sont alors à distinguer. La première sont les NP qui résultent de plus grandes particules qui ont été nanofragmentées (plastiques secondaires, Andrady, 2011; Cózar *et al.*, 2016). Il s'agit soit de déchets plastiques qui ont été altérés par des facteurs environnementaux (**Figure 1.4 A**), soit de résidus secondaires générés à partir du cycle de vie de produits manufacturés en industrie tels que les peintures, matériels biomédicaux et électroniques, adhésifs et revêtements (Koelmans *et al.*, 2015). La seconde origine des NP est synthétique (plastiques primaires). Il s'agit de particules produites en laboratoire dont la composition est connue et les paramètres sont définis (**Figure 1.4 B**).

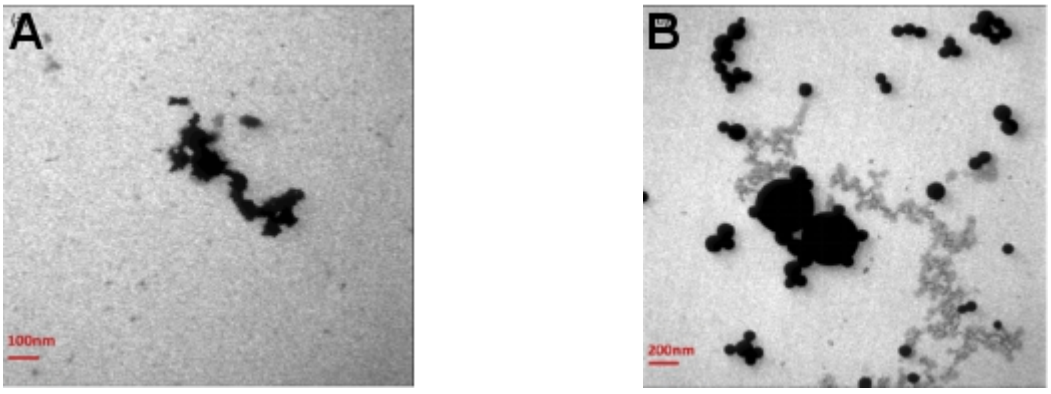

Figure 1.4 : NP vus par microscopie électronique à transmission. NP de polyéthylène issus de microplastiques provenant de l'océan Nord-Atlantique dégradés sous rayonnement UV (A). NP sphériques de polystyrène latex synthétisés en laboratoire (B) (Gigault *et al.*, 2018).

1.1.3 La dispersion multi-échelle des plastiques

Une fois transportées dans un hydrosystème, la dispersion des particules plastiques est déterminée par leur flottaison et sédimentation. Ces deux propriétés sont directement liées à leur densité et forme (Gigault *et al.*, 2018). Lorsque ces dernières atteignent une échelle micrométrique comme les MP, leur flottaison est également affectée par des interactions avec des surfaces polaires tel que le phytoplancton (Lagarde *et al.*, 2016). À échelle nanométrique, s'ajoute la collision avec des particules du milieu tel que la Matière En Suspension (MES) ou d'autres NP. Ces mouvements aléatoires dits "mouvements Browniens" peuvent alors freiner la sédimentation des NP (Hassan *et al.*, 2015).

Le premier enjeu d'étude des NP (primaires et secondaires) est qu'ils échappent aux techniques actuelles de quantification une fois dans l'environnement. En effet, pour mesurer la concentration en NP dans un échantillon, l'analyse se fait par mesure du *Carbone Organique Total* (COT). Mais cette analyse est limitée pour les échantillons environnementaux où la distinction entre le carbone organique des plastiques et celui de la matrice n'est pas possible. D'autant plus que les concentrations environnementales en NP sont inférieures aux limites de détection des instruments. Ceci explique les spéculations et difficultés à évaluer les concentrations réelles en NP dans les hydrosystèmes (Quick *et al.*, 2011; Lenz *et al.*, 2016), malgré de récentes avancées techniques qui permettent des premières analyses concluantes (El Hadri *et al.*, 2020a). Considérant alors la suspension des NP (au moins partielle) dans la

colonne d'eau et l'adsorption des métaux à leur surface, les NP peuvent représenter des vecteurs de contamination métallique pour les organismes aquatiques.

1.2 Le devenir des nanoplastiques pour le vivant

1.2.1 L'adsorption des métaux par les plastiques

La contamination des MP et NP en métaux environnants est à distinguer des métaux volontairement intégrés aux plastiques comme additifs (Nakashima *et al.*, 2012; Alimi *et al.*, 2018). Plusieurs facteurs environnementaux (physique, chimique et biologique) entraînent une perte de stabilité des plastiques. Ces altérations augmentent alors la charge, porosité et hydrophilie des MP et NP (Nowack *et al.*, 2012; Van Sebille *et al.*, 2015) ce qui génère à leur surface des sites actifs d'adsorption (Artham *et al.*, 2009; Tien and Chen, 2013; Rochman *et al.*, 2014), par exemple pour les métaux (Davranche *et al.*, 2019). Les déchets plastiques peuvent alors se retrouver couverts de Pb, Cu, Cd et As respectivement mesurés par Ashton *et al.* (2010), Holmes *et al.* (2012), Rochman *et al.* (2014), El Hadri *et al.* (2020b). En milieu naturel, c'est donc la répétition des nanofragmentations au cours du vieillissement des plastiques qui favorise l'adsorption des métaux à leur surface (**Figure 1.5**). Brennecke *et al.* (2016) démontrent que l'accumulation des métaux à la surface des MP est significativement plus importante pour ceux collectées sur des plages (PVC) plutôt que pour ceux synthétisés (PS). En effet les MP récupérées sur les plages subissent des altérations environnementales (ex. : UV; Gigault *et al.*, 2018; Magrí *et al.*, 2018).

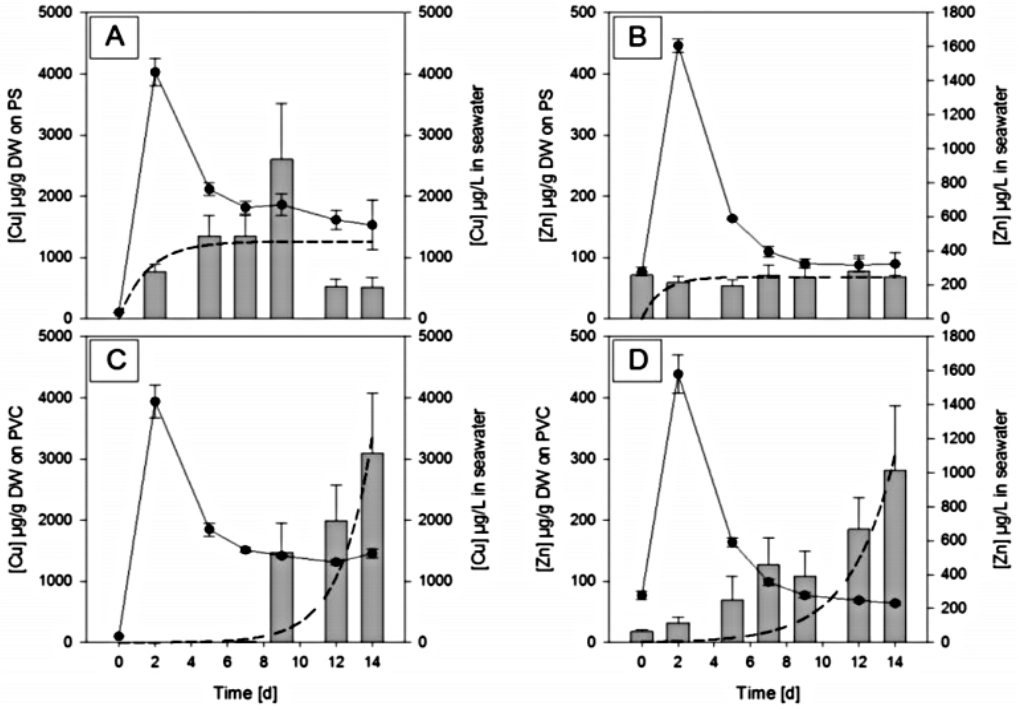

Figure 1.5 : Adsorption de Cu (A) ou Zn (B) sur des MP de polystyrène (PS) de 0.7-0.9 mm en fonction des concentrations nominales en métal et du temps. Adsorption de Cu (C) ou Zn (D) sur des MP de polyvinylchloride (PVC) de 0.8 mm en fonction des concentrations nominales en métal et du temps. Les barres représentent les concentrations de métal adsorbé sur les MPs et modélisées par les lignes en pointillées, les lignes continues représentent les concentrations de métal en solution (Brennecke *et al.*, 2016).

1.2.2 L'absorption des nanoplastiques au niveau cellulaire

Le comportement des NP vis-à-vis du vivant est majoritairement défini par leurs paramètres physico-chimiques schématisés ci-contre (**Figure 1.6**).

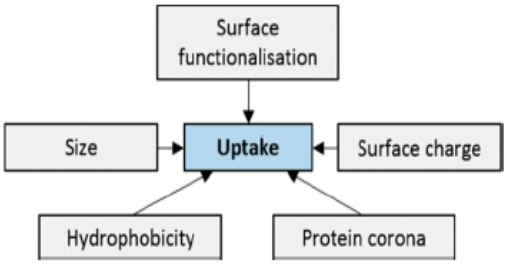

Figure 1.6 : Facteurs influençant la disponibilité des NPs pour une matrice biologique (van Sebille, 2015).

L'exposition des cellules à des NP révèle qu'une saturation de la surface cellulaire est d'autant plus rapide que les tailles des NP sont petites. Les NP peuvent ensuite diffuser à travers les membranes biologiques (Rossi *et al.*, 2014) ou bien les traverser par transport suivant leur charge. En effet, Lunov et son équipe (2011) ont observé un transport par endocytose pour des nanoparticules de polystyrène chargées positivement. Elles étaient alors davantage biodisponibles comparées à celles chargées négativement qui étaient transportées par micropinocytose.

1.2.3 L'impact des nanoplastiques le long d'un réseau trophique

Une fois absorbés par des organismes de bas niveau trophique, les NP peuvent remonter la chaîne alimentaire (Cerdervall *et al.*, 2012). Pour étudier le transfert et la toxicité de nanopolystyrène (nanoPS) fluorescents, Chae *et al.* (2018) ont suivi l'accumulation de ces nanoPS (diamètre < 100 nm) dans la chaîne alimentaire suivante : un producteur primaire (les algues, *Chlamydomonas reinhardtii*), un consommateur primaire (le crustacé, *Daphnia magna*), un second consommateur primaire (le poisson omnivore, *Oryzias sinensis*) et le consommateur terminal (le poisson piscivore, *Zacco temminck*). Le choix de ces organismes d'eau douce garanti la stabilité des nanoPS dans le milieu d'exposition. En effet, l'absence d'agrégation des nanoPS en eau distillée a été vérifiée pour assurer leur biodisponibilité trophique.

L'utilisation de la fluorescence a permis d'observer par microscopie confocale à balayage laser l'adhésion des nanoPS à la surface de *C. reinhardtii* et plus précisément, que ces derniers pénètrent la paroi cellulaire au moment de la cytodiérèse. Les nanoPS ont également été localisés dans les extraits stomacaux et/ou intestinaux des trois consommateurs (*D. magna* en **Figure 1.7A**), ainsi qu'observés dans les fèces d'*O. sinensis* (**Figure 1.7B**). Les principales observations de cette étude sont des dommages sur les microvillosités intestinales de *D. magna* et une accumulation localisée des nanoPS (à l'extrémité intestinale) au cours de leur ingestion. De même, la proportion des nanoPS accumulés chez *Z. temminck* est plus importante dans les extraits intestinaux que stomacaux.

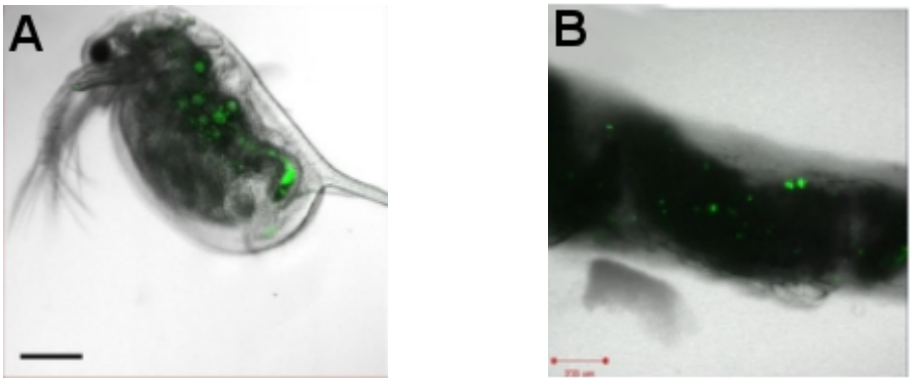

Figure 1.7 : Les nanoPS vus par Microscopie Optique à fluorescence chez *Daphnia magna* (A) et dans les fèces d'*Oryzias sinensis* (B) (Chae *et al.*, 2018).

Néanmoins, ces observations sont à nuancer considérant les concentrations expérimentales de nanoPS exposées au phytoplancton (50 mg/L) qui étaient bien supérieures à celles estimées en milieu naturel (Lenz *et al.*,2016). Mais il s'agit là d'une condition critique à l'observation du transfert trophique des nanoPS. Les auteurs en justifient l'intérêt pour inclure la contamination chronique des NP qui peut avoir lieu en milieu naturel. Par ailleurs, cette étude donne à voir que des NP peuvent être excrétés par les organismes comme cela a été observé pour des MP (Lusher *et al.*, 2013; Sussarellu *et al.*, 2016; Santana *et al.* 2018). Pour mieux cibler la toxicité des NP, il est donc nécessaire d'étudier les effets des contaminants adsorbés/ désorbés à la surface des NP une fois ingérés par les organismes, ainsi que de mesurer l'accumulation des NP dans leurs tissus. Une analyse prometteuse à cet enjeu est le développement de la pyrolyse couplée à la chromatographie gazeuse - spectrométrie de masse.

1.3 La toxicité des métaux pour les bivalves

1.3.1 Les nanoplastiques dans le modèle du ligand biotique ?

Les huîtres sauvages sont des organismes épibenthiques. Ainsi leur contamination en métaux se fait majoritairement par la colonne d'eau (Dumbauld *et al.*, 2009, Cao *et al.*, 2018). Or la colonne d'eau est une matrice variable et complexe considérant la diversité des espèces métalliques et leurs interactions avec les milieux biotique et abiotique. C'est pourquoi la meilleure méthode à ce jour pour étudier la réponse toxicologique d'un métal est le Modèle du Ligand Biotique (MLB; Liao *et al.*, 2007). En effet ce modèle intégrateur permet d'inclure la spéciation du métal, la chimie de l'eau et la physiologie de l'organisme (Paquin *et al.*, 2002). Le

MLB permet alors d'identifier la fraction d'un métal qui est responsable d'une toxicité pour un organisme donné. Généralement, cette toxicité est déterminée par la disponibilité de l'ion libre métallique (**Figure 1.8**). Néanmoins, plusieurs études observent une plus grande bioaccumulation pour certains métaux complexés (ex. : avec la MES) dépendamment des organismes étudiés (Bradac *et al.*, 2010). À ce titre, l'adsorption des métaux en surface des NP représente une voie d'entrée qui ne figure pas dans le MLB. Cette absence des NP s'explique par leur statut de contaminant émergent. En effet, peu d'études ont réussi à quantifier la charge de contaminants métalliques en surface des NP environnementaux (El Hadri *et al.*, 2020b). Et de fait, peu d'études se sont intéressées à la potentielle toxicité des métaux transportés par les NP.

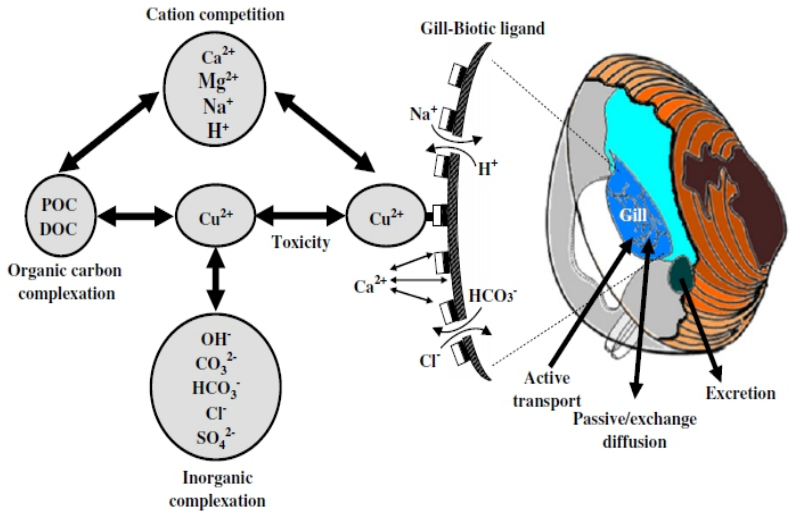

Figure 1.8 : Disponibilité du cuivre pour *Corbicula fluminea* d'après la représentation du Modèle du Ligand Biotique (Liao *et al.*, 2007).

1.3.2 L'accumulation des métaux chez les huîtres

Les bivalves sont un taxon à vaste répartition géographique. Qu'il s'agisse d'eaux douces ou estuariennes (Yap *et al.*, 2011; Ward *et al.*, 2019), ils sont présents dans des eaux sub-tropicales à sub-arctiques (Shumway, 1996; Ozbay *et al.*, 2014). Les bivalves, tels que les huîtres, sont donc des organismes appréciés pour les études comparatives d'écosystèmes. De plus, leur sédentarité et longévité permettent un suivi sur le long terme dans un milieu donné. Enfin, leur acclimatation aux facteurs abiotiques (e.g., température) et biotiques (e.g., alimentation) est relativement tolérante. Ceci amène donc à une meilleure manipulation en

laboratoire pour s'approcher de la complexité environnementale (Cajaraville *et al.*, 2000; Baudrimont *et al.*, 2005; Arini *et al.*, 2019).

Par ailleurs, les huîtres peuvent naturellement accumuler des concentrations élevées de métaux. Cette tolérance en fait ainsi des bioindicateurs privilégiés pour étudier les contaminations métalliques et leurs toxicités (Aguirre-Rubí *et al.*, 2017; Kulkarni *et al.*, 2018). À ce titre, il a été mis en évidence par Wallner-Kersanach *et al.* (2000) que la vitesse d'accumulation des métaux chez l'huître *Crassostrea rhizophorae* variait en fonction du métal considéré et du temps d'exposition (**Figure 1.9**).

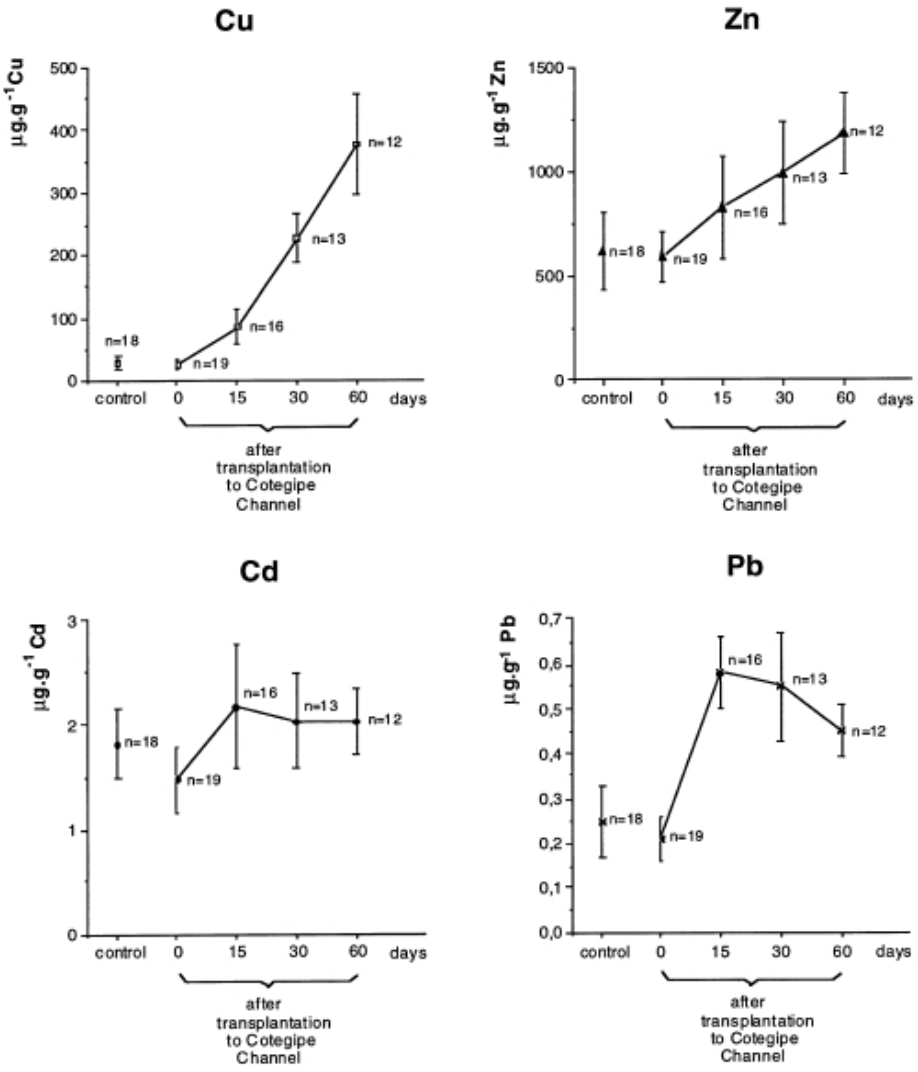

Figure 1.9 : Concentrations de métaux accumulés au cours des 60 jours d'exposition en eau contaminée (Wallner-Kersanach *et al.*, 2000).

Des huîtres contrôles ont été amenées sur un site faiblement contaminé en métaux pour une exposition de 60 jours. Ces dernières ont alors accumulé les métaux non-essentiels à des concentrations approchant celles des huîtres natives du site. Les valeurs mesurées chez les huîtres natives (n = 20) étaient 3.5 µg g^{-1} et 0.6 µg g^{-1} pour le Cd et le Pb respectivement. Il en ressort que les les huîtres amenées sur le site ont donc rapidement saturé autour des quinze premiers jours, ce qui converge avec les études menées en laboratoire sur l'accumulation des métaux non-essentiels. En revanche pour la même période d'exposition sur ce site, d'autres huîtres ont accumulé les métaux essentiels à des concentrations significativement inférieures à celles des huîtres natives. Les valeurs mesurées chez les huîtres natives (n = 20) étaient 1525 µg g^{-1} et 3000 µg g^{-1} pour le Cu et le Zn respectivement. A noter que les masses d'huîtres n'ont pas été suivies pour contrôler l'éventuelle dilution pondérale. Cette étude met en avant les différences de vitesse d'accumulation (plus rapide pour les métaux non-essentiels) et les différences de quantité d'accumulation (plus élevée pour les métaux essentiels). Cette étude souligne également l'importance de la charge initiale d'un métal accumulé chez les huîtres. Cette acclimatation peut alors impacter l'accumulation et la réponse biologique d'huîtres exposées à des métaux.

1.3.3 Enjeux d'étude

La meilleure compréhension d'un contaminant mène progressivement à l'actualisation des divers facteurs déterminants sa toxicité. Ce gain de complexité assure aux études en laboratoire une représentativité environnementale plus robuste des contaminants. D'ailleurs, l'étude des métaux est par exemple passée du Modèle d'Activité de l'Ion Libre (MAIL) au Modèle du Ligand Biotique (MLB) (Paquin *et al.*, 2002). Les NP étant un contaminant émergent de ces dernières années (Richardson and Kimura, 2020), les connaissances fondamentales et compétences analytiques sont incomplètes à ce jour. C'est pourquoi les études écotoxicologiques présentent l'intérêt d'associer les effets biologiques observés des NP à leurs caractéristiques physico-chimiques, générant ainsi de nouvelles connaissances sur leurs propriétés (Handy *et al.*, 2008). Parmi leurs propriétés, comme présenté précédemment, l'adsorption des métaux à la surface des NP est un enjeu d'étude. Toutefois, au vu de la diversité des NP, ces derniers doivent être considérés comme un mélange hétérogène de nanoparticules plastiques. Dans le cadre de ce projet de maîtrise nous avons donc ciblé les potentielles différences de toxicité entre plusieurs NP, et parmi elles, leur interaction avec l'arsenic. Pour cela, l'exposition de deux espèces d'huîtres présente l'avantage supplémentaire de comparer les résultats obtenus pour mieux identifier les patrons d'effets des NP.

2 PREMIER ARTICLE

Molecular impacts of dietary exposure to nanoplastics combined with arsenic in the Caribbean mangrove oysters (*Isognomon alatus*)

Impacts moléculaires de l'exposition trophique des nanoplastiques combinés à l'arsenic sur des huîtres caribéennes (*Isognomon alatus*)

Marc Lebordais[1,2], Zélie Venel[1], Julien Gigault[3], Valerie S. Langlois[2] and Magalie Baudrimont[1]

[1]Université de Bordeaux, CNRS, UMR EPOC 5805, Place du Dr Peyneau, 33120 Arcachon, France

[2]Centre Eau Terre Environnement, Institut national de la recherche scientifique (INRS), 490 rue de la Couronne, G1K 9A9 Québec City, QC, Canada

[3]Université Laval, UMI Takuvik 3376, 1045 avenue de la Médecine, G1V 0A6 Québec City, QC, Canada

Titre de la revue savante : Invited to submit to a Special Issue on *Do Nanoplastics Represent a Risk for Aquatic Organisms? From Bio-Nano-Interactions to Possible Impacts at Population and Community Level* in Nanomaterials. The manuscript was submitted on November 30th, 2020.

Contributions des auteurs et autrices :

Marc Lebordais: methodology, investigation, formal analysis, writing - original draft. **Zélie Venel:** methodology, investigation, writing - review & editing. **Julien Gigault:** funding acquisition, resources, writing - review & editing. **Valerie S. Langlois:** conceptualization, resources, supervision, writing - review & editing. **Magalie Baudrimont:** funding acquisition, project administration, conceptualization, resources, supervision, writing - review & editing.

2.1 Graphical Abstract

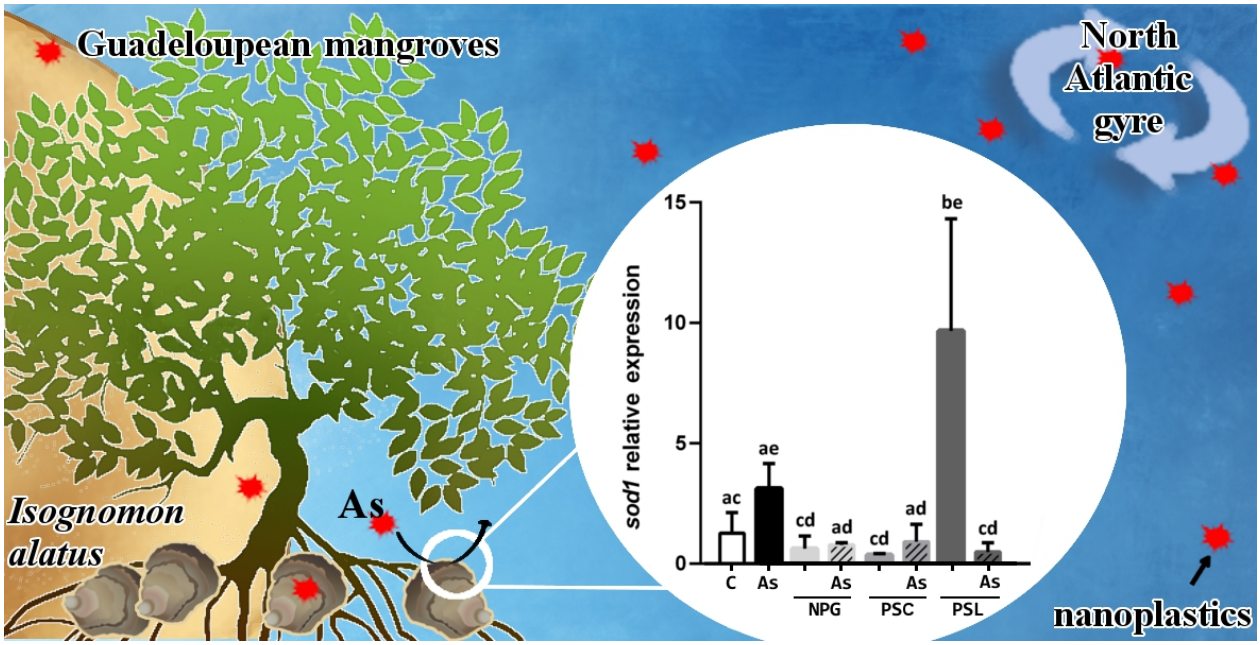

Highlights

- *Isognomon alatus'* gene expression response is activated by nanoplastics containing diet

- Spherical latex and weathered nanoplastics revealed different molecular effects

- Data suggest nanoplastics combined with As has a protective effect compared to the nanoplastics alone

2.2 Abstract

Plastic wastes are an anthropogenic contaminant of these past decades that have been observed to accumulate into oceans. More recently, nanoplastics (NPs) raised concern as they are suspected to cross biological barriers and accumulate into tissues. In addition, NPs are known to adsorb contaminants such as metals. Thus NPs represent an ecotoxicological risk to aquatic organisms, especially for bivalves. This study focuses on the impacts of three very distinct NPs to the Guadeloupean oyster (*Isognomon alatus*) through diet. As such, marine micro algae (*Tisochrysis lutea*) were exposed to carboxylated polystyrene nanoparticles of latex (PSL), crushed pristine polystyrene nanoparticles (PSC), and mixed nanoplastics environmentally weathered from Guadeloupe (NPG). Oysters were ultimately exposed by dietary route to each of the three NPs at 10 and 100 µg L^{-1}, combined or not with 1 mg L^{-1} arsenic in water. We investigated the mRNA levels of targeted genes in gills and visceral mass of *I. alatus*. The gene functions we investigated were endocytosis (*cav*, *cltc*), oxidative stress (*gapdh*, *sod1*, *cat*), mitochondrial metabolism (*cox1*, *12S*), cell cycle regulation (*gadd45*, *p53*, *bax*) and detoxification (*mdr*). Arsenic (As) treatment significantly induced *cav* expression, but once combined with any of the three NPs at both concentrations, basal mRNA levels of *cav* were observed. Similarly, As treatment significantly inhibited *bax* expression but once combined with NPG and PSC at 100 µg L^{-1} a significantly higher mRNA level was measured. This study suggested a protective effect of the interaction between NPs+As.

Keywords : nanoparticles, bivalves, ,gene expression, trophic pathway, metal

2.3 Introduction

Plastic contamination is a worldwide environmental issue, as recognized by the United Nations Environment Programme (UNEP, 2001). Daily used plastic products can last in the environment for several hundred years without being completely degraded (Barnes *et al.*, 2009; Briand 2014). With an average of 8 million tons of plastic waste discarded into oceans each year, Wright and Kelly (2017) estimated an accumulation of 250 million tons by 2025. Aquatic ecosystems act as a natural receptacle for contaminants, including plastics that have been detected from the Arctic polar circle (Lusher *et al.*, 2015) to the Mariana trench (Koelmans *et al.*, 2015; Chiba *et al.*, 2018). Plastic debris are carried by currents that converge to five main ocean areas called gyres (Law *et al.*, 2010). Guadeloupe Island is an example of a terrestrial area exposed to the North Atlantic gyre (7th expedition continent in 2015, Baudrimont *et al.*, 2019). In the gyre, different size of plastic debris can be identified: large microplastics (size < 5 mm; Arthur *et al.*, 2009), microplastics (size < 0.3 mm; Cai *et al.*, 2018) and nanoplastics (size < 0.001 mm; Lambert and Wagner, 2016).

Nanoplastics (NPs) are commonly referred to plastic nanoparticles smaller than 1000 nm in one of the three dimensions of space. NPs originating from industrial synthesis are refered to as primary NPs, whereas those from environmental degradation are called secondary NPs (Koelmans *et al.*, 2015; Lambert and Wagner, 2016). Indeed nanofragmentation of plastic occurs within aquatic ecosystems through physical abrasions and chemical oxidations (e.g., waves, salt and mainly UV; Gigault *et al.*, 2018a; Magrí *et al.*, 2018), thus yielding more available additives used for specific plastic properties (e.g., plasticizers, UV-filters, flame retardants, metals; Lambert and Wagner, 2016; Wright and Kelly, 2017). Eventually as plastics age and fraction into NPs, more polar surfaces are exposed for contaminants to desorb or be adsorbed (Tien and Chen, 2013; Suhrhoff and Scholz-Bottcher, 2016; Wright and Kelly, 2017). For example, Davranche *et al.* (2019) recently documented metallic adsorption on marine NPs. Further analysis revealed that arsenic was one of the most abundant metal adsorbed on plastic debris from Guadeloupean beaches (El Hadri *et al.*, 2020b). Therefore, since most marine species ingest plastic debris regularly (Gall and Thompson, 2015; Lusher *et al.*, 2017) NPs potential toxicity triggered questioning. Indeed NPs have high residence time, surface reactivity and size availability for cellular uptake (Rossi *et al.*, 2013; Manfra *et al.*, 2017) that present a great risk of interaction and bioaccumulation within organisms (Nel *et al.*, 2006; Mattsson *et al.*, 2015; Chae and An, 2017). As such, nanoparticles have been classified as emerging contaminants (Richardson and Kimura, 2020). However, there is a critical lack of data on NPs' fate and

bioavailability, mostly explained by quantification challenges (Quik *et al.*, 2011; Bergmann *et al.*, 2015; Ter Halle *et al.*, 2017). For example, NPs aggregate in seawaters due to higher ionic strength (Hotze et al, 2010; Corsi *et al.*, 2014; Mao *et al.*, 2020). Yet Gigault *et al.* (2018a) newly observed limited aggregation of NPs passing through a salinity gradient. Thus making estuarine areas such as mangroves very relevant systems for NP studies. As a matter of fact, mangroves hold a significant role in ecosystem services (Kulkarni *et al.*, 2018), also, their sensitive functioning provides helpful indicators to study worldwide issues (Mitra, 2013; Carugati *et al.*, 2018).

To tackle ingested NPs toxicity, we studied NP effects alone and combined with arsenic on Caribbean oysters. We conducted our experiment on *Isognomon alatus* wild oysters native from Guadeloupean mangrove swamps since oysters are relevant organisms for ecotoxicological studies. Bivalves have been indeed used for decades as bioindicators of metal contamination in waters (Cajaraville *et al.*, 2000; Baudrimont *et al.*, 2005; Arini *et al.*, 2011). Since they tolerate and accumulate high metal concentrations bivalves are indeed good monitoring organisms (Aguirre-Rubí *et al.*, 2017; Kulkarni *et al.*, 2018). Additionally, plastic exposure of bivalve aquacultures recently raised concerns in regard to their putative role of NPs transfer into the food web (Baun *et al.*, 2008; Wright and Kelly, 2017; Tallec *et al.*, 2020). The trophic exposure is an under-rated NP pathway (Cerdervall *et al.*, 2012; Besseling *et al.*, 2014; Lusher *et al.*, 2015) that we explored through NP-contaminated phytoplankton used to feed *I. alatus* oysters. Indeed filter-feeding bivalves rely on ciliated structures to collect phytoplankton but also organic and inorganic particles (up to 500 nm; Ward and Shumway, 2004; Ward and Kach, 2009). Thus to mimic environmental feeding conditions of *I. alatus*, solutions of the marine micro algae *Tisochrysis lutea* were used to expose oysters to three different NPs. Selected NPs for this study encompassed the synthetic and additives-free carboxylated polystyrene nanoparticles of latex (PSL; Pessoni *et al.*, 2019), the crushed pristine polystyrene nanoparticles (PSC, primary NPs; El Hadri *et al.*, 2020b), and to represent the environmental plastic weathering, a custom Guadeloupean NP mix was prepared (NPG; secondary NPs). Most NP studies have used monodispersed calibrated nanospheres, but these spherical NPs have been considered poorly relevant to address ecotoxicology issues (Alimi *et al.*, 2018; Magrí *et al.*, 2018). Therefore, in the present study we aimed to investigate genes expression changes of *I. alatus* exposed by dietary route to NPs at low concentrations (10 and 100 µg L^{-1}), potentially environmentally representative (Lenz *et al.*, 2016; Besseling *et al.*, 2017). Considering the ecotoxicological relevance of NPG (as a mix of polydispersed NPs with heterogeneous shapes, specific surface area and oxidative degree), we also investigated the NPG putative role towards

arsenic bioaccumulation into *I. alatus* gills and visceral mass. Overall, the main novelty of our study lies in comparing the effects of three relevant NPs, combined or not with arsenic, on *I. alatus* key genes.

2.4 Materials and methods

2.4.1 Nanoplastic dispersions

Plastics used to generate the mixed nanoplastics from Guadeloupe (NPG) were collected in 2016 on the Guadeloupean beaches (16° 21' 06" N; 61° 23' 09" W), naturally aged *in situ* by environmental factors (salt, mechanical abrasion and mainly UV exposure). Polystyrene pristine pellets used to produce crushed nanoparticles (PSC) were commercially purchased from Goodfellow (Lille, France). Both nanoplastic dispersions were prepared according to an optimized protocol (El Hadri *et al.*, 2020a). Plastics pellets were degraded with 99% ethanol in a blade grinder to get a primary powder and later fragmented using a planetary ball mill (El Hadri *et al.*, 2020a). The resultant powder was then dried by lyophilization to remove ethanol, then suspended in milliQ water and filtered on cellulose acetate filters (5-6 µm pore size; VWR, Biare, France). Hydrodynamic diameters of NPG and PSC nanoparticle dispersions were measured by Dynamic Light Scattering (DLS) (**Table 1**) through a contactless (*in situ*) DLS probe at 170 °C on a Vasco flex instrument (Cordouan Technologies®, Pessac, France). The intensity fluctuations as a function of the time were processed as an autocorrelation function. Cumulants algorithm was used to fit this function in order to obtain a size distribution (z-average). The surface charges of particles (potential ζ) were assessed using a Wallis zetameter (Cordouan Technologies®, Pessac, France) (**Table 1**). Details of NPG and PSC dispersions are respectively presented in supplementary files **Fig. S1** and **Fig. S2** (Annexe I). The carboxylated polystyrene nanoparticles of latex (PSL) were synthesized and calibrated by IPREM (Pau, France) with 43 COOH groups per nm² and a z-average of 390 ± 20 nm. Also they were made spherical with a raspberry-like surface texture (Pessoni *et al.*, 2019). Noteworthy, polystyrene was chosen for both PSL and PSC as it is one of five main plastics produced, representing 90% of global demand (Andrady and Neal, 2009). All three nanoplastics particle sizes were suspended and diluted as needed with deionized water (MilliQ, Millipore, 18 MΩcm) in cleaned glass vials. The mass concentration of each nanoplastic dispersion was measured by Total Organic Carbon

(TOC) analysis on a Shimadzu® instrument with a detection limit at 0.05 mg L^{-1}. Spike recovery was performed (yield = 92%) to validate the analysis accuracy.

Table 1 : Main characteristics of prepared nanoparticles (NPG and PSC) measured by DLS *in situ* on a Vasco Flex instrument (Cordouan Technologies®, Pessac, France).

Nanoparticles	z-average (nm) / PDI	Potential ζ (mV) 5 mM NaCl, pH 7
NPG	361 ± 40 nm / 0.210	-30.2 ± 1.1
PSC	354 ± 30 nm / 0.190	-44.0 ± 2.0
PSL	390 ± 20 nm / 0.002	-42.0 ± 2.0

2.4.2 Micro algae and oyster cultures

The micro algae species used to feed the oysters during the acclimation period were *Tisochrysis lutea* (Marie *et al.*, 2006; Tallec *et al.*, 2020) and *Thalassiosira weissflogii* (Strady *et al.*, 2011) obtained from Gujan-Mestras (Lycée polyvalent de la Mer, France). Of note, *T. weissflogii* was only used during oysters acclimation for nutritional purposes (Gonzalez Araya *et al.*, 2012). Both algal cultures were cultivated into glass balloons in F/2 medium (Guillard, 1975) at salinity 26‰ and oxygenated by an air distribution pump through a glass pipette. As recommended by Helm and Bourne (2004), the micro algae were grown at 22 °C under 24:24 artificial light of 100 µmol/m²/s.

This study used native tropical flat oysters as they are representative of mangrove swamps (Saed *et al.*, 2004; Yap *et al.*, 2011). As a matter of fact, mangroves host large biodiversity holding a significant role in ecosystem services. Individuals of *I. alatus* were collected from their natural habitat in Grand Cul-de-sac marin (16°18'58.1460"N; 61°32'1.9379"O), a natural reserve to the north of Pointe-à-Pitre in Guadeloupe. Once brought to the laboratory, they were individually brushed to remove external parasites and stored in 30 L tanks (100 oysters per tank) lined with tiles to fulfill *I. alatus'* need of hanging substrate. The tanks were filled with reconstituted seawater (Instant Ocean®) at 32‰ salinity, oxygenated, and filtered by an aquarium filter pump. Also, 2/3 of the water tanks were renewed every two days during the first week of oysters' acclimation given their high organic matter release. Similar to *I. alatus* native environmental conditions, they were acclimatized at 26 °C with aquarium heaters and under 12:12 (natural light : dark) for 15 days according to A. Arini (personal communication, February

02, 2019). Oysters were fed twice a week with 100 mL of mixed *T. lutea* and *T. weissiflogii* (10 x 10^6 cells/L and 2 x 10^6 cells/L, respectively) per tank.

2.4.3 Experimental design of trophic exposure

A preliminary experiment was conducted to determine *T. lutea* optimal exposure to NP solutions (Supplementary file **Fig. S3**, Annexe I). *T. lutea* solutions were exposed in 10 mL individual glass vials with five replicates. Of note, all the glassware exposed to NPs was previously cleaned using an acid bath of 3% nitric acid, rinsed with distilled water then with 70% ethanol and dried under a fume hood. Cell concentrations were daily measured for 96 h by spectrophotometry at 750 nm. Based on micro algae concentrations variability, we estimated 48 h was the optimal duration to conduct the trophic exposure. Thus, NPG, PSC and PSL were separately added into algal solutions for 48 h at low nominal concentrations of 10 and 100 µg L^{-1} reported to be relevant proxies of NPs environmental concentration (Lenz *et al.*, 2016; Besseling *et al.*, 2017) . Prior to each NP inoculations, the micro algae concentrations were controlled by counting on a Nageotte chamber and brought to 1 x 10^6 cells/mL. Each NP-*T. lutea* solution was exposed to similar abiotic conditions (media, temperature, light) as the acclimation phase previously mentioned. To avoid NP accumulation onto the air pump tubing, the micro algae were oxygenated through an agitation table in the presence of the NPs (Baudrimont *et al.*, 2019).

Among inorganic forms of arsenic, pentoxide arsenic (hereafter referred to As) has been chosen as it is the most abundant form found in oxygenated marine waters (Penrose, 1974; Neff, 1997; Yang *et al.*, 2012; Zhang *et al.*, 2013). A single solution of dissolved As (Merck KGaA®, Germany) was used. Oyster exposure to 1 mg L^{-1} As was conducted through batch injection at the beginning of the exposure (day 0). This As nominal concentration was based on oysters bioaccumulation tolerance and As levels in seawater (Langston, 1984; Zhang *et al.*, 2015; Freitas *et al.*, 2018). To keep the concentration consistent at 1 mg L^{-1} throughout the exposure, water samples were collected in the morning and As levels were quantified. Thus, As concentration was adjusted one day out of two if needed.

The experimental design encompassed (**Figure 2.1**) : a control of reconstituted seawater, a positive As treatment of 1 mg L^{-1}, three single-NP treatments (NPG, PSC, and PSL) at 10 and 100 µg L^{-1}, and a mix of As (1 mg L^{-1}) with each of the NP treatments (As + 10 µg L^{-1} NP and As + 100 µg L^{-1} NP). All treatments were run in quadruplicate with two oysters per 500 mL glass jar.

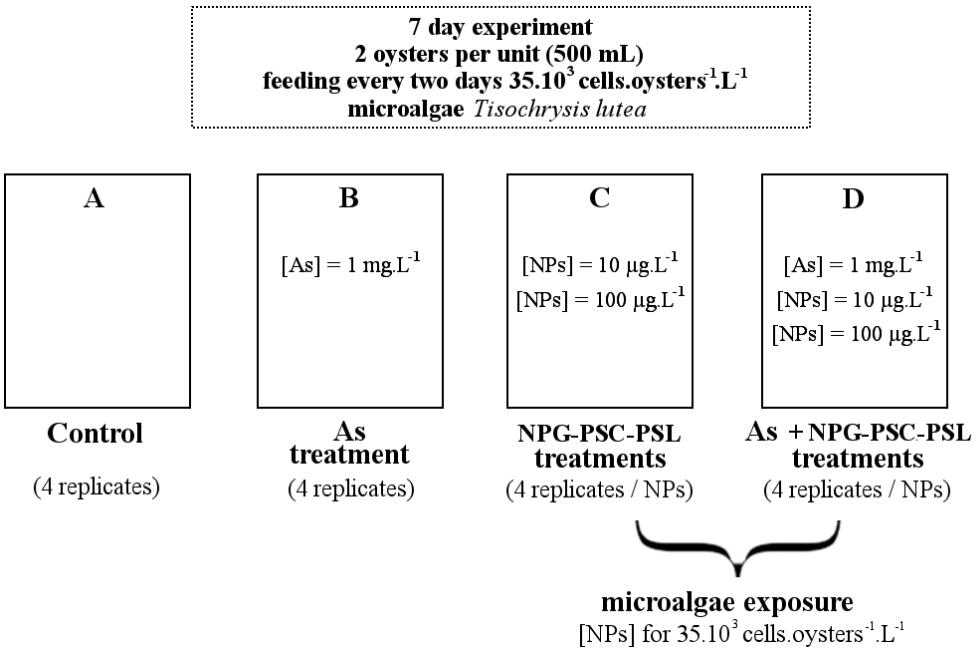

Figure 2.1: Experimental procedure of *I. alatus* trophic exposure. As injections were performed at day 0 in treatments (B) and (D). NPs were added through pre-contaminated micro algae feeding, one day out of two in treatments (C) and (D). NPs refer to individual NPG, PSC and PSL treatments.

Each jar was parafilm-covered to minimize evaporative loss. Water oxygenation was ensured by an air distribution pump. The oysters were under the same abiotic conditions (salinity, temperature and light) as the above-mentioned acclimation period. Oysters of each condition were fed every two days with 35 x 10^3 cells/oyster/L *T. lutea* considered as a relevant environmental concentration (Malet *et al.*, 2008). After one week of dietary exposure, individual oysters were assessed for biometric parameters (Supplementary file **Fig. S4**, Annexe I). Each tissue was manually dried with paper, then weighed (fresh weight). Gills and visceral mass were sampled for arsenic bioaccumulation and molecular assays. Empty shells were also individually measured and weighed. Thus the Condition Index (Lucas and Beninger, 1985) was calculated as follow.

Equation 1:

$$CI = \frac{\text{leftover tissues* weight}}{\text{shells weight}} \times 100$$

*leftover tissues: whole body excluding gills and visceral mass

2.4.4 Water and tissue arsenic quantification by ICP-OES

To evaluate the efficiency of the As dissolution and dilution, a nominal solution of 1 mg L^{-1} was prepared from a 1 g L^{-1} As solution. The 1 mg L^{-1} solution was then acidified with 3% nitric acid to measure the final concentration on an Inductively Coupled Plasma Optical Emission Spectrometry (ICP-OES). To monitor and compensate for the As concentration throughout the exposure week, water samples of 0.5 mL were collected per jar and acidified at 3% nitric acid for ICP-OES analysis.

For tissue analyses, the pooled gills and visceral mass were dried (48 h at 50 °C) and weighted prior to digestion (dry weight). Tissue samples were then acidified with 70% nitric acid (3 mL per sample) and heated at 100 °C for 3 h on a hot plate (Digiprep). After dilution of the digestates with 18 mL of pure water, total As bioaccumulation was measured using an ICP-OES (**Figure 2.2**). Certified biological reference materials (dolt-5, Yang *et al.*, 2014) were systematically analyzed with the samples to ensure that the data obtained were within the certified range.

2.4.5 RNA extraction and cDNA synthesis

Gill and visceral mass tissues were preserved in RNA later at -20 °C right after dissections. For minimal weight purposes, tissues from two oysters were pooled together. Tissues were ground with a Biorad Fastprep® (40 s at 6 movements/s) in 500 µL of RNA lysis buffer, using ceramic pellets (Lysing Matrix D Bulk from MP Biomedicals). Deproteinization was done by adding 500 µL of phenol-chloroform isoamyl alcohol as this organic solvent is very suitable for oyster tissues rich in proteins and fat (Vicient and Delseny, 1999). Then, samples were vortexed and centrifuged for 5 min at 9000 g to separate the organic and the aqueous phases. From there, total RNA was extracted using the Promega kit “SV Total RNA Isolation System” according to the manufacturer. For each gene, specific primer sets were designed using Primer3Plus (**Table S1**, Annexe I). Extracted RNA concentration was measured by using a microplate spectrophotometer at 260 nm and RNA quality was estimated with a Take3 plate (nucleic acids purity ensured by 260/280 ratio ≥ 2), both from BioTek EPOCH®. All samples were diluted to obtain the same RNA concentration (1000 ng in 10 µL) before performing reverse transcription (RT) to synthesize complementary DNA (cDNA) with the Promega kit “GoScript Reverse Transcription System” according to the supplier’s instructions.

Given the non-sequenced genome of *I. alatus*, primers were designed from the reconstituted *I. alatus* transcriptome sequenced by Lemer (2019). The primer details can be found in the Supplementary file **Table S1** (Annexe I). Our genes of interest were representative of five biological functions. Transport pathway related genes included *cav* (cell membrane invagination for endocytosis), and *cltc* (intracellular vesicle transport; Conner and Schmid 2003; Doherty and McMahon 2009). Genes related to cell cycle regulation included *p53* (tumor suppressor; Harris and Levine, 2005), *gadd45* (DNA repair; Salvador *et al.*, 2013), and *bax* (apoptotic activator; Harris and Levine, 2005). Oxidative stress related genes included *sod1* (dismutation of superoxides into O_2 and H_2O_2), *cat* (conversion of H_2O_2 into O_2 and H_2O; Defo *et al.*, 2018), and *gapdh* (reduction and oxidation activities; Tristan *et al.*, 2011; Sirover, 2011). Mitochondrial metabolism related genes included *cox1* (respiratory chain electron transport), normalized by *12S* being indicative of the ribosomic RNA level (Al kaddissi *et al.*, 2012; Arini *et al.*, 2015). Finally detoxification related genes included *mdr* (drugs cell expulsion; Franzellitti and Fabbri, 2006).

2.4.6 qPCR assays and validations

Real-time quantitative polymerase chain reaction (qPCR) was performed with the Promega kit "GoTaq® qPCR Master Mix" containing the 5X buffer, the *Taq* polymerase, $MgCl_2$, dNTP, and SybrGreen dye. Validation of primer's efficiency and specificity was conducted so that 1 µL of the forward and reverse primers (100 µM each) were optimal for conducting the reactions. Together with the qPCR mix, primers were added to 1/10 diluted cDNA. The resulting final volume was poured into white 96-well qPCR plates, including two no-template control wells without cDNA and replaced by RNAse free-water. Plates were sealed and quickly centrifugated, then analyzed by the LightCycler 480 Roche®. Starting with one cycle at 95 °C for 2 min, then 30 amplification cycles at 95 °C for 30 s and 60 °C for 30 s.

Amplification efficiency of qPCR primers was assessed by 10-fold sample serial dilutions. Specificity was determined for each reaction from the dissociation curve of the qPCR products, obtained by following the SyberGreen fluorescent level during gradual heating from 60 to 95 °C. Based on these indicators, non-conforming data were not analyzed (ND). Following the $2^{-\Delta Ct}$ method described by Livak and Schmittgen (2001), genes of interest were standardized by the average cycle thresholds (Ct) from the reference genes *β-actin* and *rpl7* (Lee and Nam, 2016). Given the focus of this study on NP trophic exposure, visceral mass gene expression data are

presented in **Figure 2.3**; whereas gills gene expression data are found in Supplementary file **Fig. S5** (Annexe I).

2.4.7 Statistical analysis

To satisfy the conditions for parametric analyses, raw data were transformed by commonly used functions (inverse square root or decimal logarithm). Normality was then confirmed using the Shapiro-Wilk test and homoscedasticity was confirmed by the Student test (α error = 5%). Transformed data were then compared between each treatment and concentration exposure using a two-way analysis of variance (ANOVA). The significant differences were identified by a post-hoc Tukey HSD test on Prism 8.0 for gene expression and Bonferroni test on SigmaPlot 12.0 for arsenic dosage.

2.5 Results

2.5.1 Oysters biometric parameters and arsenic bioaccumulation

Biometric parameter data are shown in **Fig. S4** (Annexe I). Mortality during the exposure was negligible (< 4%). No significant differences were observed for the total fresh tissue weights and the CI among treatments. Field collected control animals had an average concentration of 75 µg g^{-1} As in gills and 133 µg g^{-1} As in visceral mass (**Figure 2.2**). As-exposed oysters yielded approximately 1.5 times greater As concentrations than the control oysters in both tissues (**Figure 2.2**). However, there were no statistical differences in As concentrations between the As and the NPG+As exposed oysters.

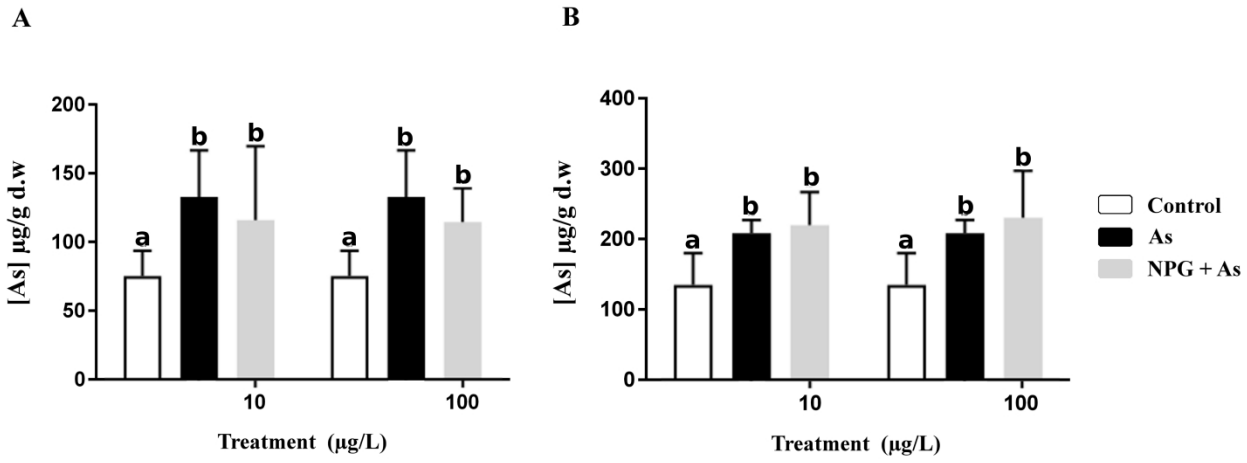

Figure 2.2: Arsenic accumulation in gills (A) and visceral mass (B) (µg/g, dw, mean + sd), after one week of exposure to 0 (control) or 1 mg L^{-1} of As alone or combined with NPG (10 and 100 µg L^{-1}). Different letters denote statistic differences between treatments assessed by two-way ANOVA followed by Bonferonni post-hoc test (n = 4); $p < 0.05$.

2.5.2 Relative gene expression in visceral mass

The expression of a suite of genes involved in five main biological functions; endocytosis, cell cycle regulation, oxidative stress, mitochondrial metabolism and detoxification were assessed in the visceral mass (**Figure 2.3**). The same responses in gills are presented in **Fig. S5**.

Single arsenic treatment

The expression of *cav* was significantly upregulated by the As treatment, but this effect was cancelled in the presence of NPs except for PSC+As at 100 µg L^{-1} (**Figure 2.3 A**). The expression of *bax* was significantly repressed by the presence of As, even in the presence of NPs (**Figure 2.3 C**). No statistical transcriptional changes were seen for *p53* expression between treatments (**Figure 2.3 E**); however, the ANOVA was significant for the test ($p = 0.0009$), which supports *p53* inhibition for the As treatment.

Single nanoplastic treatments

The expression pattern of *gadd45* revealed a significant downregulation for both PSC and PSL at 10 and 100 µg L^{-1} concentrations (**Figure 2.3 D**). The mRNA level of *sod1* was significantly upregulated for PSL at 100 µg L^{-1}, unlike most of the other NP treatments being under expressed (**Figure 2.3 H**).

Nanoplastics + arsenic treatments

The expression of *bax* showed a significant downregulation for NPG+As at both 10 and 100 µg L^{-1}, and only at 10 µg L^{-1} for PSC+As (**Figure 2.3 C**). Since PSL+As could not be detected, it is worth noting *bax* downregulation for PSL also at 10 µg L^{-1}. The same downregulation pattern was shared in *gadd45* for PSC+As and PSL+As treatments at both concentrations (**Figure 2.3 D**). Expression of *cat* showed significant downregulation for PSC+As at 10 µg L^{-1} (**Figure 2.3 F**). Similarly, for *gapdh* expression there was a significant downregulation for NPG+As at 10 µg L^{-1} (**Figure 2.3 G**). The *sod1* expression response for PSL+As at 100 µg L^{-1} was significantly

inhibited compared to the PSL treatment, and interestingly, also significantly lower than for the arsenic treatment (**Figure 2.3H**). Expression of *mdr* was not modulated except for the NPG +As treatment, significantly inhibited at 100 µg L^{-1} (**Figure 2.3 J)**.

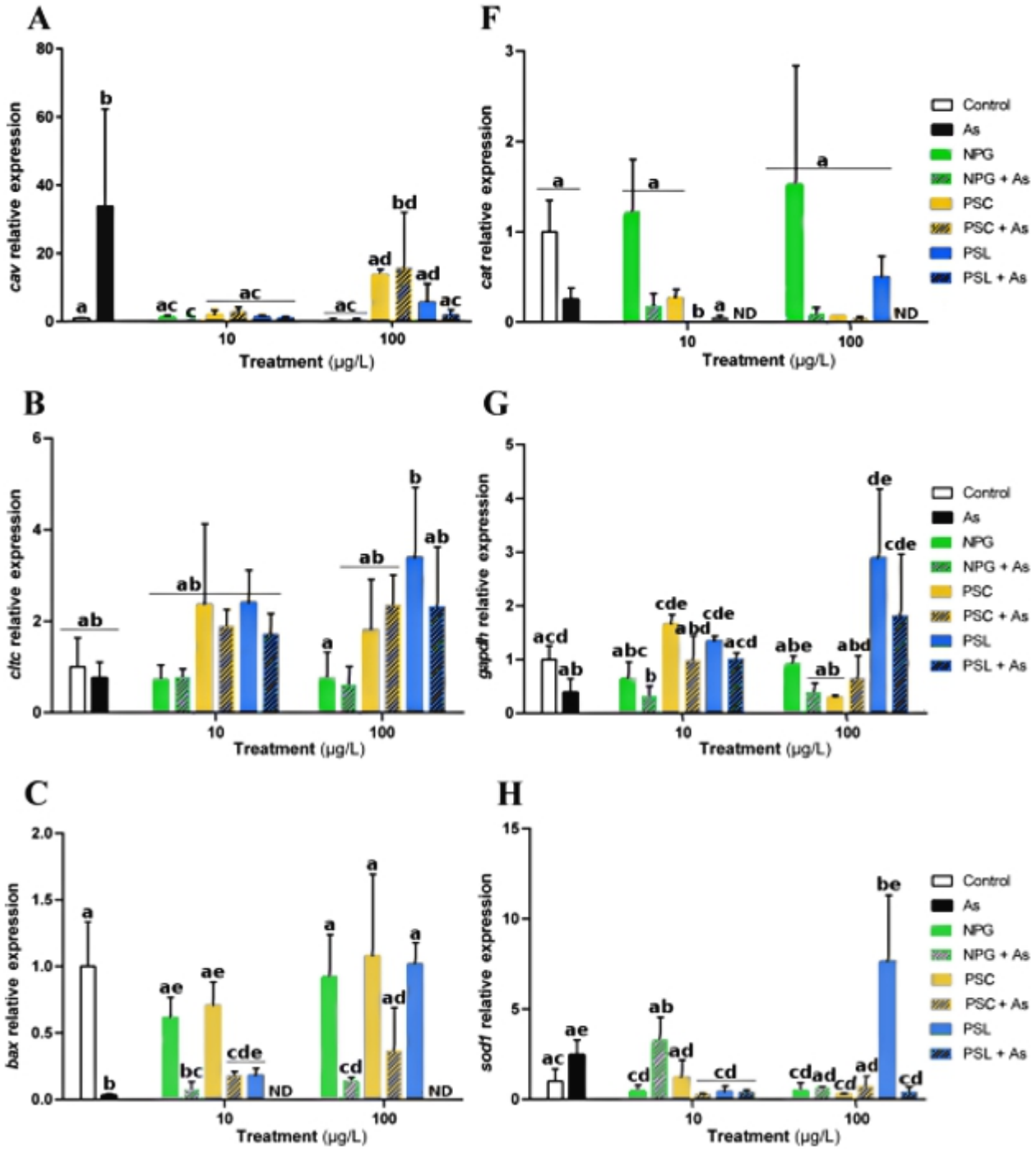

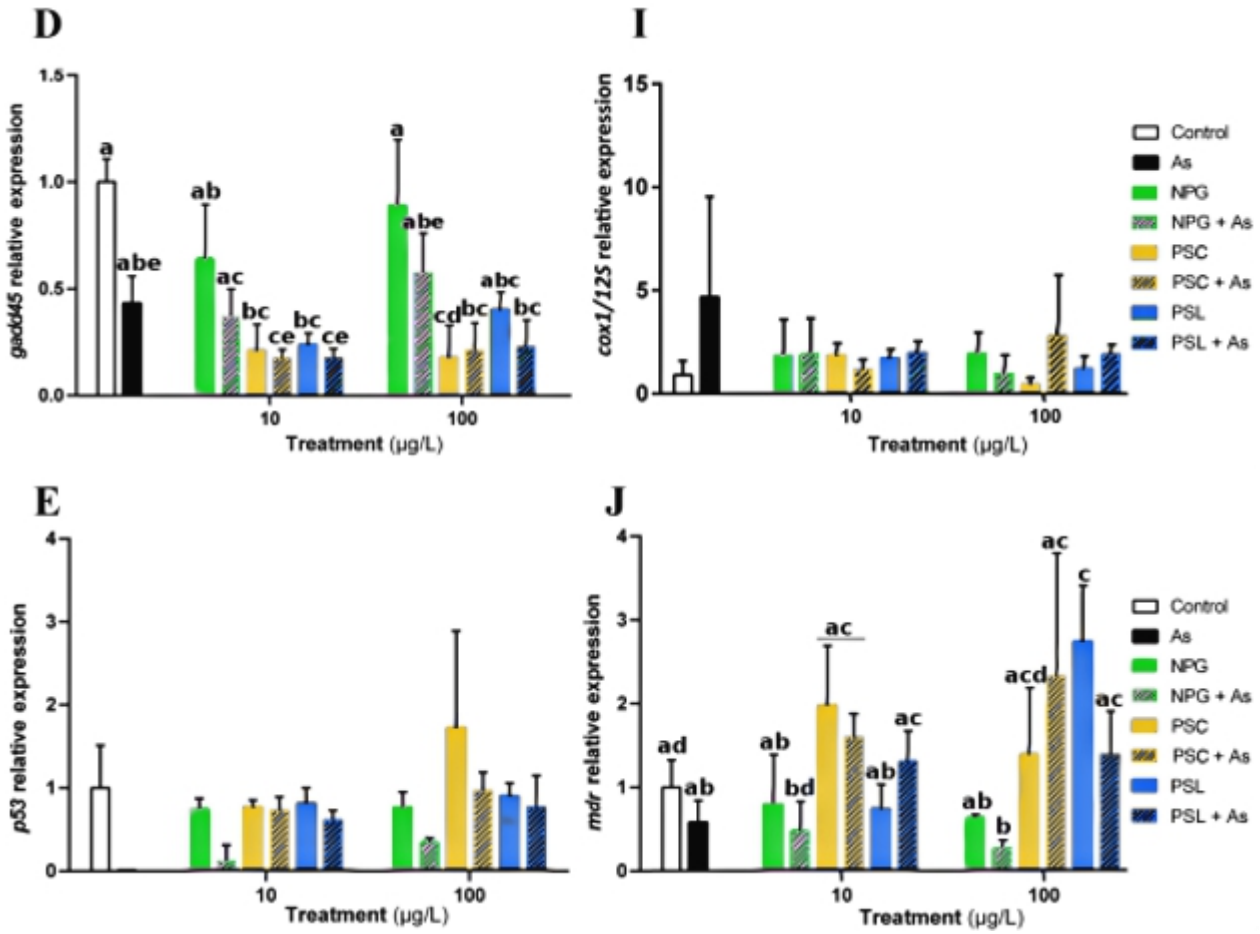

Figure 2.3: Relative gene expressions in *I. alatus* visceral mass after one week exposure to 1 mg L^{-1} As combined or not with 10 and 100 µg L^{-1} NPs. mRNA levels are presented for *cav* (A), *cltc* (B), *bax* (C), *gadd45* (D), *p53* (E), *cat* (F), *gapdh* (G), *sod1* (H), *cox1*/*12S* (I) and *mdr* (J). All the values are presented as the mean + sd (n = 4) normalized by *β-actine* and *rpl7* genes. Different letters denote statistic differences (*p < 0.05*) between treatments assessed by two-way ANOVA followed by Tukey post-hoc test.

2.6 Discussion

2.6.1 Micro algae growth under nanoplastics exposure

Phytoplankton organisms like micro algae are primary producers. They are therefore a keystone in aquatic food webs. Yet NPs are known to interact with micrometric compounds such as micro algae due to their colloidal behaviour in water (Lagarde *et al.*, 2016; Gigault *et al.*, 2018b; Wang *et al.*, 2020). To anticipate NP effects on *T. lutea* growth, a 96 h exposure was conducted with NPG, PSC, PSL solutions at 10 and 100 µg L^{-1} (**Fig. S3**, Annexe I). No significant changes were

observed under any NP treatments. Noteworthy, higher optical density dispersions happened at 72 h for both NP concentrations. Thus we decided to expose *T. lutea* for 48 h to NP solutions prior to feeding oysters. NPs availability in our trophic experiment is believed to be mainly driven by their filtration rate (Green, 2016; Arini *et al.*, 2019). Therefore special attention was given to feed oysters with consistent micro algae concentrations among treatments. NPs were expected to be adsorbed or internalized after 48 h exposure, and to potentially trigger physiological changes on micro algae membrane. To assess the fate of NPG, PSC and PSL at 10 and 100 µg L^{-1}, optical microscopic observations were conducted on NP-*T. lutea*. We did not observe significant effects for any treatments. Yet, in a similar experiment (Lebordais *et al.*, *in prep*) we attested PSL adsorption on *T. lutea* surface for a concentration grade including 10 and 100 µg L^{-1} by Scanning Electron Microscopy (SEM).

2.6.2 Arsenic uptake and bioaccumulation

The statistical analyses conducted on biometric parameters do not show any significant differences for the measured shell length and fresh tissue mass, nor for the calculated CI (**Fig. S4**, Annexe I). Potential variations in As bioaccumulation in tissues can thus not be attributable to differences in biometric parameters.

The total As tissue bioaccumulation measured in controls demonstrated the biogeochemical background of Guadeloupean mangroves. These levels provide us with the environmental As baseline of *I. alatus* in their native habitat. Despite these rather high As values, they are comparable with a reviewed range of bioaccumulated As occurring naturally in bivalves (Neff, 1997, Maher *et al.*, 2018). For each treatment, total As bioaccumulation in gills is around half the As bioaccumulation in the visceral mass. These results confirm the organ's function towards chronic metal exposure with higher As levels in the visceral mass (storage organ; Soegianto *et al.*, 2013, Arini *et al.*, 2014) compared to the gills (transfer organ; Strady *et al.*, 2011; Perrier, 2017). This present study used 1 mg L^{-1} As, which enabled an increase in As bioaccumulation for both tissues after a short term-exposure (one week). No speciation analysis has been conducted as we did not aim to address the As behaviour in this study. Given chemical reactions in seawater, the initial As form (arsenate) underwent speciation changes (Francesconi and Edmonds, 1996; Farrell *et al.*, 2011; Azizur Rahman *et al.*, 2012). Thus it has to be kept in mind that total As results can not be interpreted as equivalent of the initial As. Therefore, As treatment and total As results should be seen as a positive control. Seawater analysis from the oysters' reference site was also conducted. For all sampling stations, total As concentrations measured were below the limit of detection. The chronic exposure of *I. alatus* is most likely responsible for

the tissue bioaccumulation found in controls. Under environmental conditions, oyster exposure to As most likely comes from sediment through waterborne route (Langston, 1984; Zhang *et al.*, 2013; Maher *et al.*, 2018), and phytoplankton through dietary route since micro algae bioaccumulate inorganic As (Ünlü and Fowler, 1979; Neff, 1997; Azizur Rahman *et al.*, 2012). Concentration has been only measured in NPG+As treatments as NPG were the only nanoparticles carrying an initial As burden. Thus NPG was the most indicated NPs to increase the As bioaccumulation in *I. alatus* tissues. Yet, there were no statistical differences in As bioaccumulation between the As and the NPG+As treatments, at 10 and 100 µg L^{-1} NPG concentrations for both tissues. Simlarly, Freitas *et al.* (2018) did not observe an increased As bioaccumulation in clams in the presence of As (0.1 mg L^{-1}) combined to multi-walled carbon nanotubes (0.1 mg L^{-1}). Our results underlined that As bioaccumulations in both tissues was only driven by As treatment. Ultimately, the presence of NPs at these low concentrations did not affect the As total uptake of *I. alatus*.

2.6.3 Effects of arsenic and nanoplastics on gene expression

Single arsenic treatment

Data showed *bax*, *gadd45* and *p53* to be downregulated following As treatments. Tumor suppressors, like P53, are known to induce *gadd45* transcription (Salvador *et al.*, 2013; Arini *et al.*, 2019). Thus, *gadd45* downregulation can be linked to the decrease of P53 transcription factor since the As treatment leads to *p53* inhibition **(Figure 2.3 E)**. As *bax* regulation is generally dependent upon *p53* induction (Harris and Levine, 2005), As treatment could be responsible for *p53* downregulation, ultimately inhibiting *bax* expression **(Figure 2.3 C)**. Indeed, it has already been described in humans that As is able to inhibit the repair of DNA damages, leading to carcinogenic effects (Beyersmann, 2002). Non significative upregulation of *cox1/12S* ratio **(Figure 2.3 I)** for As treatment could suggest an increased mitochondrial metabolism not yet overwhelmed. Indeed, *cox1* induction was also supported by *12S* induction (data not shown), we thus interpret that it did not overcharge the mitochondrial respiratory chain. Our results demonstrate a metal toxicity similar to that observed by *cox1* upregulation in *C. fluminea* hemocytes exposed to ionic Au for 28 days (Arini *et al.*, 2019).

Single nanoplastic treatments

Our results showed significant downregulation of *gadd45* mRNA level for PSC and PSL treatments at both concentrations, except for PSL 100 µg L^{-1} (**Figure 2.3 D**). Given that the main role of *gadd45* is to maintain genomic stability, this gene is strongly regulated by DNA damaging agents like metals but also growth-arresting signals (Salvador *et al.*, 2013). Oxidative stress has also been established by *in vitro* and *in vivo* studies as an early indicator of NP toxicity in freshwater bivalves (Tedesco *et al.*, 2010; Arini *et al.*, 2019). Thus, NP toxicity is mainly exerted through two pathways: either directly by interacting with the cellular contents including DNA, or indirectly by ROS release known for causing nucleotide adducts (Singh *et al.*, 2009; Ruiz *et al.*, 2015). Significant upregulation of *sod1* for PSL treatment at 100 µg L^{-1} (**Figure 2.3 H**) might imply higher ROS production which induces *sod1* expression to compensate for PSL toxicity. Our overall results show different patterns of effects among NPs, thus shedding light on the necessity to use several NPs for ecotoxicological studies. Unlike conventional commercial nanoparticles (Wegner *et al.*, 2012; Rossi *et al.*, 2013; Kulkarni and Feng, 2013), here we used functionalized PSL nanoparticles with no additives to avoid additional toxicity (Pessoni *et al.*, 2019). Indeed most commonly used additives like sodium dodecyl sulfate, Tween® and Triton-X® can induce toxic effects on aquatic organisms (Rosety *et al.*, 2001; Hrenovic and Ivankovic, 2007; Jahan *et al.*, 2008). Recently, it has been demonstrated by Pikuda *et al.* (2019) that toxicity of commercial PSL-COOH on daphnia was coming from its bactericide additive (sodium azide). Additionally, since carboxylated functions ensured PSL stability we propose their higher availability by endocytosis (**Figure 2.3 B**). It can be hypothesized that PSL was either more absorbed or adsorbed by micro algae before being ingested by oysters. Nanoparticles un-stability has indeed been acknowledged for turning aggregates into bigger particles (e.g., MPs), particularly in seawater solutions (Hotze et al, 2010; Gigault *et al.*, 2018a; Mao *et al.*, 2020). Natural Organic Matter has also been addressed to affect PS NPs aggregation depending on the water chemistry and its ions valence (Cai *et al.*, 2018). Moreover Mao *et al.* (2020) observed fewer aggregation from PS NPs in the presence of algal Extracellular Polymeric Substances. Interestingly they also observed fewer aggregation from artificially UV-aged PS NPs since the formation of carbonyl groups enabled to stabilize them. In our experiment, lower stability has been particularly observed for NPG compared to the other NPs. Therefore the aggregation of NPG may have led to fewer interaction with micro algae during the exposure. This could explain their fewer toxicity effects compared to PSC and PSL. As such, our results underline the value to assess NPs stability in the exposure media (Quik *et al.*, 2011; Besseling *et al.*, 2017) and to

further study comparative NP effects. This is also supported by Baudrimont *et al.* (2019) study which revealed a significantly higher production of pseudofeces by *Corbicula fluminea* after 36 h of exposure to 1000 µg L^{-1} environmental NPs, which was not observed under conventional commercial polyethylene NP exposure. These comparative NP exposures along with our current results, suggest different hazardous effects between environmental and conventional plastic nanoparticles. Thereby we would like to raise awareness on the under-estimation of NP ecotoxicity in the literature as most conventional commercial polystyrene nanoplastics are being used

Nanoplastics + arsenic treatments

Expression of *mdr* (**Figure 2.3 J**) revealed opposite responses at 100 µg L^{-1} between PSL treatment's upregulation and NPG+As treatment's downregulation. MXR pumps work as a cytoprotective system by excreting exogenous compounds. Nonetheless, it is sensitive to both physical and chemical stressors (Minier *et al.*, 2000). NP toxicity might be increased by As interaction with NPG since the detoxification process can be inhibited in the presence of metals (El Haj *et al.*, 2019). Similar results were found for encoded MXR-related proteins in *Mytilus galloprovincialis* digestive glands exposed to 0.75 µM Hg^{2+} for 6 days (Franzellitti and Fabbri, 2006). Due to physical and chemical fragmentation factors (Holmes *et al.*, 2014; Koelmans *et al.*, 2015; Dawson *et al.*, 2018), NPG surfaces are heterogeneously degraded and expected to be the most environmentally representative NPs in aquatic ecosystems. As proposed by Lambert and Wagner (2016), Ter Halle *et al.* (2017), and Baudrimont *et al.* (2019) higher reactivity of secondary plastic surfaces enables increased availability for contaminants to be adsorbed onto them. This experiment evaluated NP affinities towards As showing more interaction for NPG and PSL (as expected from NPG degraded surfaces and PSL carboxylated surface groups). Previous studies recorded changes in bivalve closure rhythm under metal exposure, ultimately affecting their filtration (Tran *et al.*, 2003; Pan and Wang, 2012). This stress is most likely to be seen in the transcriptional response of gills, but also in visceral mass tissues. Similar bioavailability of As for *I. latus* most likely explains the converging responses between NPs+As treatments and single As treatment as for cell cycle regulation (*bax*, **Figure 2.3 C**). Yet we observed lower toxicity in NPs+As treatments compared to single As treatments for endocytosis (*cav*, **Figure 2.3 A**) and oxidative stress (*sod1*, **Figure 2.3 H**). Antagonist effects have been recently documented for MP-NP exposures combined with metals (Oliveira *et al.*, 2018; Wen *et al.*, 2018) including As (Freitas *et al.*, 2018). Antagonist effects refer to significantly lower responses in combined contaminant treatments (NPs+As) compared to control and both

individual contaminants (Bhagat *et al.*, 2019). However, we underline here basal mRNA levels for combined NPs+As treatments. We are not aware of any earlier studies showing a decrease of NP's gene expression effects when in the presence of any metal exposure. Therefore, we aim to repeat this experiment with another oyster species to confirm this novel finding.

2.6.4 Models of trophic exposure effects on the studied gene functions

Based on the gene expression, **Figure 2.4** sheds light on the main findings of this present study. Induction arrows show the presence of a biological effect for a given treatment, regardless of genes up- or down- regulation. Prevention arrows represent the absence of a biological effect for NPs+As treatment. Therefore the gene response is equivalent to the control treatment. Then antagonist arrows show the presence of a biological effect for NPs+As treatment. Therefore the gene response is significantly lower than control and absent in NP treatment. In gills (**Figure 2.4 A**), PSC internalization can be hypothesized at 100 µg L^{-1} by *cav* induction. Since a fraction of PSC might be aggregated resulting in bigger particles similar to MPs, a higher PSC concentration might be required to witness their internalization. Polystyrene nanoplastics (PS NPs) were consistent in DNA damage showing no change of toxicity for PSC+As and PSL+As treatments. Also, *bax* regulation by NPG+As treatment at 10 µg L^{-1} was most likely caused by As. Contrary to what was expected, no synergistic effects were observed between As and NPs in combined treatments. At a subcellular level the As treatment alone affected mitochondria homeostasis by *cox1* upregulation, but once in the presence of PS NPs (PSL+As and PSC+As) at 100 µg L^{-1} it prevented *cox1* upregulation. Thus, we hypothesize that PS NPs presence could decrease the As availability. Most likely through As adsorption on NPs, but no affirmation can be done as there were no significant differences. In the presence of As, there was an inhibition of *cat* expression for PSL +As treatments at 10 and 100 µg L^{-1}, contrary to NP single treatments. Moreover, As alone induced oxidative stress revealed by *sod1* expression and so did the PSL treatment at 100 µg L^{-1}. However, once As was combined with PSL (PSL+As treatment), a putative decrease oxidative stress was observed. Therefore, data highlight a potential protective role of PSL against the oxidative stress caused by As.

In visceral mass (**Figure 2.4 B**), data suggest PSC internalization in the presence of As at 100 µg L^{-1} by *cav* induction leading to membrane invagination. PS NPs triggered DNA damage given the *gadd45* expression. Based on their physico-chemical characteristics, PSC and PSL yielded a low and very low endogenous ROS burden, respectively. Thus, DNA damage most likely came from the physical nanoparticle toxicity, excluding additional toxicity from As in

PSC+As and PSL+As treatments. However, an opposite pattern was observed for NPG+As where *bax* mRNA level decreased once NPG was in presence of As. Therefore, As interaction showed different effects among NPs towards cell cycle regulation and apoptosis. Moreover, PSL and NPG expressed an opposite *mdr* response at 100 µg L^{-1}. Indeed, as PSL were very stable an increased exposure seemed to lead to a greater induction response from the cell to expel them. This was in contrast to NPG which might have been too large to be expelled by the *mdr* channel. Oxidative stress was triggered by PSL at 100 µg L^{-1} inducing *sod1* regulation but was prevented in presence of As (PSL+As treatment), while *gapdh* expression was inhibited by NPG+As treatment at 10 µg L^{-1}. Additionally, *cat* expression also was prevented in NPG+As treatment at 10 µg L^{-1} and inhibited in PSC+As treatment at 10 µg L^{-1}. Thus, As presence seemed to prevent the oxidative stress production seen for NPs' single treatments. It has to be kept in mind that NPG were the most weathered NPs, with high porosity and high surface oxidative degree that potentially increased its interaction with As. The same logic applies for PSL by As adsorption on its carboxylated functions. Noteworthy, As treatment induced endocytosis activation by *cav* expression. Again we observed As interaction with NPs, potentially through adsorption leading to the prevention of *cav* expression by NPG+As at 10 µg L^{-1}.

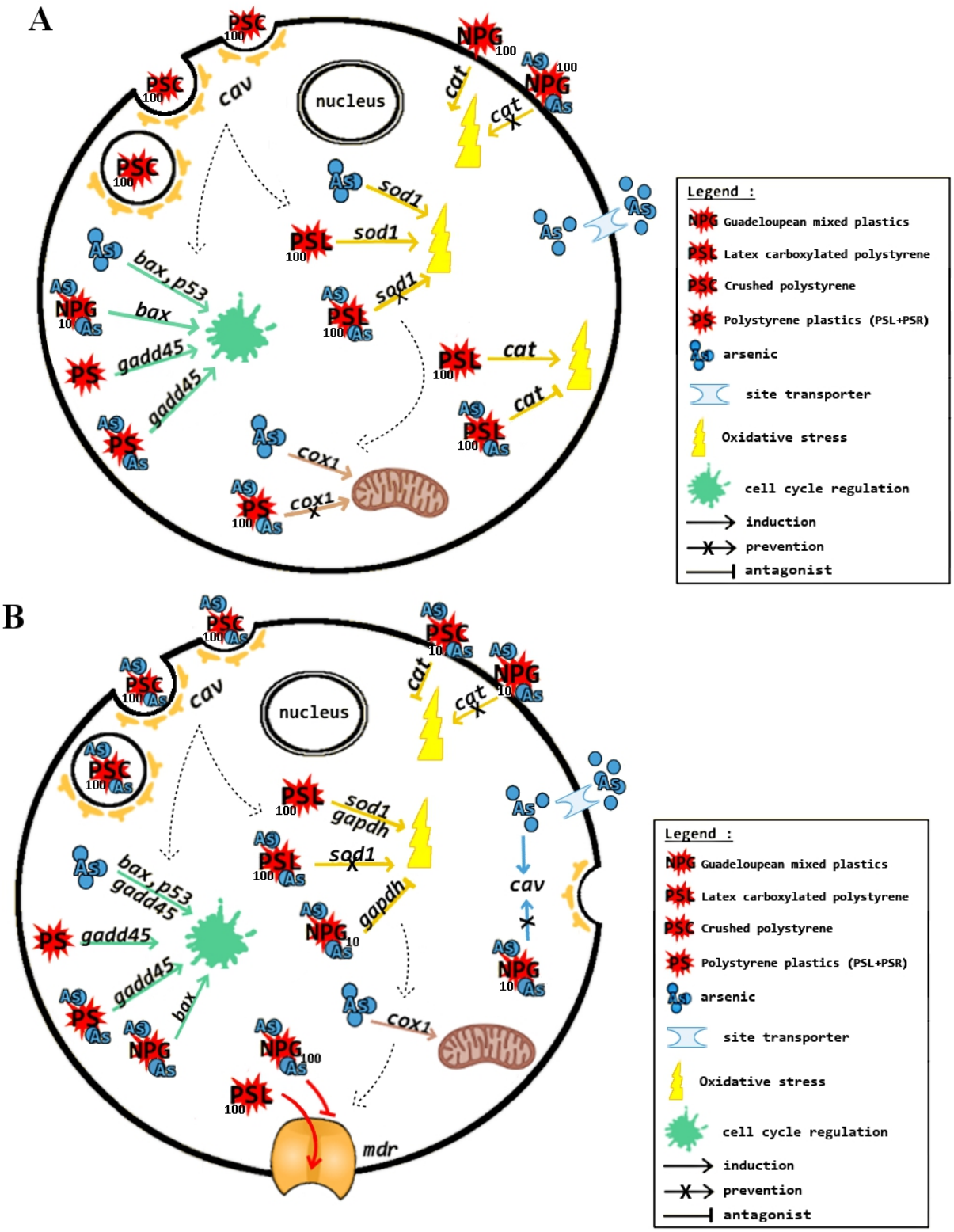

Figure 2.4: Schematics of suggested cellular effects of NPs and As in gills (A) and visceral mass (B) oyster tissues.

2.7 Conclusion

We demonstrated that sublethal exposures of NPs impaired cellular functions at the molecular level on native Guadeloupean oysters. Among our three NP solutions, PSL treatments showed the most consistent toxic effects by triggering oxidative stress and cell cycle regulation in gills and visceral mass tissues. These results shed light on the interest to use PSL additives-free nanoparticles with surface functionalized groups (e.g., carboxyl group) rather than conventional commercial PSL. Similarly but with fewer effects observed, PSC toxicity came most likely from their irregular surface with high specific surface that potentially enabled more adsorption on micro algae surface. Interestingly NPG treatments also showed toxic effects, but fewer than PSL by only triggering oxidative stress in gills. In light of these results, we suggest that studies might include more complex environmental NPs in their study design. Moreover, to our knowledge, we present the first results showing a specific response of NPs+As exposure with protective effect for oxidative stress and for endocytosis. All these results underline the threat of plastics for marine wildlife and the need to study crossed effects between NPs and other contaminants.

2.8 Acknowledgments

The authors would like to thank Adeline Arini for her valuable help to design the experimental protocol and conduct molecular biology investigations, Anthony Bertucci for his help to design gene primers on oysters, Patrice Gonzalez and Cerise Daffe for their formation in molecular biology, Pierre-Yves Gourves for sample mineralization and arsenic analyses. We acknowledge Bruno Grassl, Hind El Hadri and Stephanie Reynaud for providing the free-soap carboxylated polystyrene nanoparticles of latex. The authors also appreciated the unknown referee's helpful comments.

2.9 Fundings

This work was supported by the French National Agency of Research (ANR-1-17-CE34-0008: PEPSEA to JG), the Centre National de la Recherche (CNRS) in the EC2CO INIAME program (MB), the Investments for the Future Program, within the Cluster of Excellence COTE (ANR-1-10-LABX-45 to MB), the E2S-Pau, the Nouvelle-Aquitaine Region (EN-Pi project) and by the Canada Research Chair program (950-232235 to VSL).

Transition the first and second manuscripts

Our most environmentally representative NPs, the NPG, did not increase the total As bioaccumulation in *I. alatus* tissues. After one week of trophic exposure several cellular functions have been affected. Among our three NP treatments, we observed higher effects on *I. alatus* gene expressions for PSL treatment at 100 µg L^{-1}. Combined NPs + As treatments triggered lower responses (for *cat*, *cav, cox1* and *sod1*) compared to single As or NP treatments. Thus, we underlined protective effects of both contaminants exposed together to *I. alatus.*

To confirm that As adsorption on NPs does not increase the total As bioaccumulation for oysters, we conducted the same experiment on *C. virginica* for all three NPs combined with As. We also aimed to compare *I. alatus* gene expression responses with *C. virginica* since both are different oyster species native from wild and farmed habitats, respectively. Thus, we expected to target the conserved effects of NPs and As treatments across oyster interspecificities.

3 DEUXIÈME ARTICLE

Molecular impacts of dietary exposure to nanoplastics combined with arsenic in Canadian oysters (*Crassostrea virginica*) and bioaccumulation comparison with Caribbean oysters (*Isognomon alatus*)

Impacts moléculaires de l'exposition trophique des nanoplastiques combinés à l'arsenic sur des huîtres canadiennes (*Crassostrea virginica*) et comparaison de leur bioaccumulation avec des huîtres caribéennes (*Isognomon alatus*)

Marc Lebordais[1,2], Juan Manuel Gutierrez-Villagomez[2], Julien Gigault[3], Magalie Baudrimont[1] and Valerie S. Langlois[2]

[1]Université de Bordeaux, CNRS, UMR EPOC 5805, Place du Dr Peyneau, 33120 Arcachon, France

[2]Centre Eau Terre Environnement, Institut national de la recherche scientifique (INRS), 490 rue de la Couronne, G1K 9A9 Québec City, QC, Canada

[3] Université Laval, UMI Takuvik 3376, 1045 avenue de la Médecine, G1V 0A6 Québec City, QC, Canada

Titre de la revue savante : Submitted to Chemosphere.

Contributions des auteurs et autrices :

Marc Lebordais: methodology, investigation, formal analysis, writing - original draft. **Juan Manuel G. Villagomez:** methodology, investigation, writing - review & editing. **Julien Gigault:** resources, writing - review & editing. **Magalie Baudrimont:** conceptualization, supervision, writing - review & editing. **Valerie S. Langlois:** funding acquisition, project administration, conceptualization, resources, supervision, writing - review & editing.

3.1 Graphical Abstract

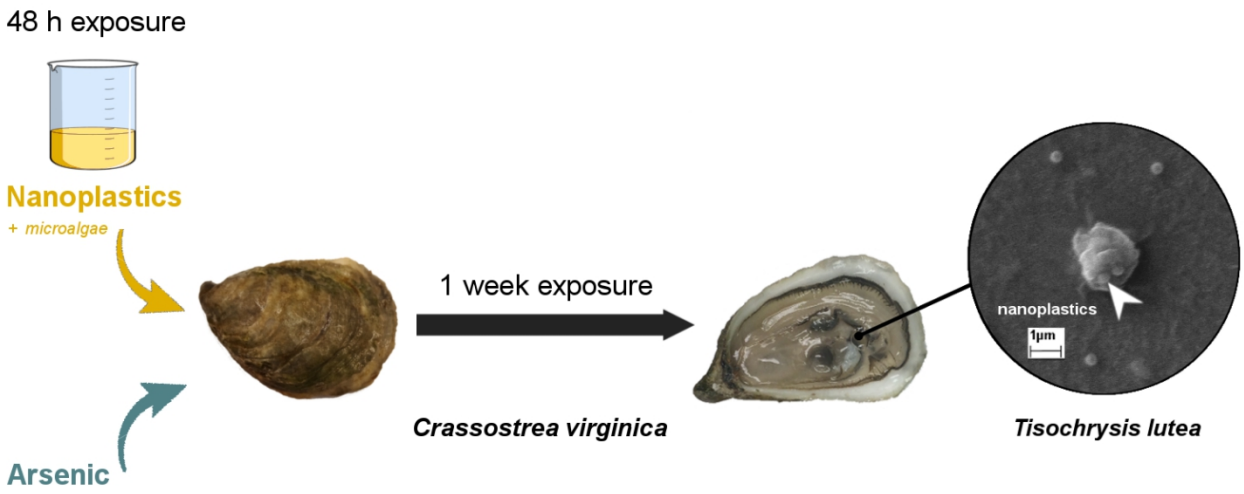

Highlights

- Nanoplastics are adsorbed on micro algae surface starting at 10 µg L^{-1} exposure.
- Nanoplastics triggered apoptotic and mitochondrial metabolism gene responses.
- The combination of nanoplastics with arsenic induced synergetic effects.
- Arsenic bioaccumulation did not increase in the presence of nanoplastics.

3.2 Abstract

Despite the urge need to address the possible impact of plastic debris, up to now, little is known about the translocation of nanoplastics (NPs) through the trophic web. Plus, due to their surface reactivity, NPs could sorb and thus increase metals bioavailability to aquatic filter-feeding organisms (e.g., bivalves). In this study we investigated the dietary exposure route on the oyster *Crassostrea virginica* through micro algae themselves exposed to NPs (PSL, PSC and NPG) at reportedly environmental concentrations combined or not with arsenic (As). Interactive effects of NPs on As bioaccumulation were studied, along with the expression of key genes in gills and visceral mass. The investigated gene functions were endocytosis (*cltc*), oxidative stress (*gapdh*, *sod3*, *cat*), mitochondrial metabolism (*12S*), cell cycle regulation (*gadd45*, *p53*), apoptosis (*bax*, *bcl-2*), detoxification (*cyp1A*, *mdr*, *mt*), and energy storage (*vit*). Results showcased that NP treatments did not impact As bioaccumulation in *C. virginica* tissues. However, NP treatments combined with As triggered synergetic effects on gene expressions. Relative mRNA level of *12S* significantly increased for NPG+As and PSC+As treatments at 10 and 100 µg L^{-1}. Relative mRNA level of *bax* increased for PSL+As and PSC+As treatments at 10 and 100 µg L^{-1} respectively. We also observed that relative As bioaccumulation was significantly higher in *Crassostrea virginica* gills compared to *Isognomon alatus'*. These results are the first comparative molecular effects of NPs alone and combined with As investigated in farmed *C. virginica* oysters. Together with *I. alatus* results we thus shed light on species different sensitivity.

Keywords : nanoparticles, toxicity, bivalves, gene expression, bioaccumulation, Scanning Electron Microscopy

3.3 Introduction

Plastic contamination is of global concern (UNEP, 2001; Bank and Hasson, 2019) and approximately 10% of the annual worldwide plastic production ends up in the oceans (Mattsson *et al.*, 2019). Current estimates indicate that there are 30 million tons of plastic in the oceans, and according to projections by 2025, there will be 220 million tons (Wright and Kelly, 2017). Plastics have become ubiquitous; they can reach all types of aquatic ecosystems, including the Arctic polar circle (Lusher *et al.*, 2015) and the Mariana trench (Koelmans *et al.*, 2015; Chiba *et al.*, 2018). Also, plastic waste is persistent in the environment (Carpenter and Smith, 1972) and can last hundreds of years without being completely degraded (Barnes *et al.*, 2009; Briand 2014).

Physical abrasion, chemical, and photo-oxidations (e.g., waves, salt, UV; Gigault *et al.*, 2018a; Magrí *et al.*, 2018) can lead to plastic fragmentations resulting in the formation of microplastics (MPs) and nanoplastics (NPs). MPs are synthesized or broken plastic pieces smaller than 5 mm (Arthur *et al.*, 2009), while NPs are particles smaller than 1000 nm in one of the three dimensions of space (Lambert and Wagner, 2016; Gigault *et al.*, 2018b). Primary NPs refer to those coming from industrial synthesis and secondary NPs are those resulting from environmental degradation (Koelmans *et al.*, 2015). Both, MPs and NPs, including primary and secondary, are emerging contaminants due to the limited information regarding their toxicity (Richardson and Kimura, 2020). The toxicity of MPs and NPs raises concern globally since most marine species ingest plastic regularly (Gall and Thompson, 2015; Lusher *et al.*, 2017).

Recent evidence showed that organisms could excrete most of the ingested MPs; therefore, minimal translocation into the circulatory system and tissues is expected (Lusher *et al.*, 2013; Sussarellu *et al.*, 2016; Santana *et al.* 2018). However, as plastics age, they lose their physical integrity and their additives (e.g., plasticizers, UV-filters, flame-retardants, metals) become less chemically stable (Lambert and Wagner, 2016; Wright and Kelly, 2017). Also, weathered and nanofragmentated plastics possess more polar surfaces for environmental pollutants to be adsorbed or desorbed (Tien and Chen, 2013; Bhagat *et al.*, 2020). Particularly, marine MPs and NPs can adsorb metals on their surfaces (Ashton *et al.*, 2010; Rochman *et al.*, 2014; Davranche *et al.*, 2019). For example, El Hadri *et al.* (2020a) revealed that arsenic (As) was one of the most abundant metal adsorbed on plastic waste sampled on Guadeloupean beaches (a French island in the Caribbean sea).

Data on NPs' fate and toxicity is limited (Quik *et al.*, 2011; Bergmann *et al.*, 2015; Ter Halle *et al.*, 2017), and they are the least understood plastic fraction, but potentially the most toxic to

biologic systems by tissue bioaccumulation and vectoring chemical contamination (Nel *et al.*, 2006; Mattsson *et al.*, 2015; Chae and An, 2017). Riverine systems are the major input of plastic debris to the open ocean (Mayer and Wells, 2012; Lasareva *et al*., 2017). Therefore, since estuaries link rivers to oceans they are the key interface controlling the fate, transport and accumulation of plastics debris, more specifically for NPs (Galgani *et al.*, 2000; Browne *et al.*, 2010; Sadri and Thompson 2014). Indeed, the change in estuarine systems of ionic strength and natural organic matter (NOM) will control the aggregation of NPs. Aggregation is the main parameter affecting NPs final reactivity in regard to other contaminants. In such systems, mangroves are a specific category where these parameters are intensified (Bouillon, 2011). Moreover, mangroves are essential ecosystems weakened by anthropogenic pressure, thus they are relatively used as a proxy for worldwide environmental issues (Mitra, 2013; Carugati *et al.*, 2018; Kulkarni *et al.*, 2018)

Bivalves are a class of marine and freshwater molluscs. They include oysters, clams, mussels, and most of them are filter feeders (Hancock *et al.*, 2008; Baudrimont *et al.*, 2019) and have been used historically as biomonitoring species to assess exposure to metals (Aguirre-Rubí *et al.*, 2017; Kulkarni *et al.*, 2018). However, recently, plastic exposure to aquaculture bivalves raised concerns about NPs transfer within the food web (Baun *et al.*, 2008; Bouwmeester *et al.*, 2015; Bank and Hansson 2019). Thus, in this study, we conducted a trophic exposure using the eastern oyster (*Crassostrea virginica)* to assess the potentially toxic effects of three distinct NPs and in combination with As. The oyster *C. virginica* is one of the most extensively farmed oyster species in the world. Due to its habitat tolerances ranging from the Gulf of Mexico to Canada's eastern bays (Ozbay *et al.*, 2014), this species is highly commercially valuable and is also commonly used in toxicity assays (McCarthy *et al.*, 2013; Ward *et al.*, 2019; Smith *et al.*, 2020). We used three NP models following a gradient of environmental relevancy : (i) carboxylated polystyrene nanoparticles of latex (PSL) free of additives as it can induce toxicity (Pikuda *et al.*, 2019), (ii) the crushed pristine polystyrene nanoparticles (PSC) that was considered more relevant in size and shape distribution, and finally (iii) nanoplastics environmentally weathered from microplastic debris collected in Guadeloupe. (Lebordais *et al.*, *submitted;* Manuscript #1 of this present M. Sc. thesis). The tropical oyster *I. alatus* is native to Caribbean mangroves that are exposed to the North Atlantic gyre where plastic debris concentrate (7th expedition continent, Baudrimont *et al.*, 2019)..

3.4 Materials and Methods

3.4.1 Preparation of nanoplastic dispersions

In this study, we used three different NP dispersions : (i) spherical carboxylated polystyrene nanoparticles of latex (PSL) synthesized according to a previous protocol (Pessoni *et al*., 2019) free of additives; (ii) the crushed polystyrene nanoparticles (PSC) that were in-laboratory nanofragmented from polystyrene pristine pellets by ball-milling; (iii) and a mixture of nanoplastics produced from microplastic debris environmentally weathered and collected from a beach in Guadeloupe (NPG). The PSC and NPG NP dispersions were prepared according to an optimized protocol (El Hadri *et al.*, 2020b). These NP dispersions have been previously described with further details (Lebordais *et al.*, *submitted*).

To assess NP hydrodynamic diameters and population distributions, dynamic light scattering (DLS) was used. Hydrodynamic diameters of PSC and NPG dispersions were measured using non-invasive backscatter optics at 25 °C on a Zetasizer nano zs instrument (Malvern Panalytical®). The intensity fluctuations by the time were processed as a correlation function. A cumulants algorithm was used to fit this function to obtain a size distribution (z-average) and the polydispersity index (PDI). The z-averages were 692.4 ± 68.55 nm (0.441 PDI) and 1071 ± 30.65 nm (0.755 PDI) for PSC and NPG, respectively. The calibrated z-average of PSL was 390 ± 20 nm (0,002 PDI). The three NPs were suspended in deionized water (MilliQ, Millipore, 18 MΩcm). To measure NP mass concentrations in the three NP dispersions, total organic carbon (TOC) analysis was then performed on a Shimadzu® instrument (Québec, Canada).

3.4.2 Micro algae exposure to carboxylated polystyrene nanosplastics for Scanning Electron Microscopy

To observe the potential interaction between NPs and micro algae surface, we exposed the micro algae *Tisochrysis lutea* (formerly known as *Isochrysis galbana*; Bendif *et al.*, 2014) for 48 h to PSL dispersions at 0 (control), 10, 100, 1000, and 5000 µg L^{-1} and observed it using Scanning Electron Microscopy (SEM). For this, *T. lutea* was purchased from Bigelow National Center for Marine Algae and Microbiota (Maine, USA). The micro algae were aliquoted into previously cleaned glass vials (one per treatment, n = 1) and acclimatized for one week at room temperature under 24:24 artificial light. All micro algae solutions yielded the same concentration (2.1 x 10^6 cells/mL) measured on a Coulter Multisizer II particle counter (Fortin *et al.*, 2000) before starting the exposure. During acclimation and exposition, the *T. lutea* solutions were

homogenized twice a day to mimic estuarine conditions and to avoid sedimentation. Thus, dynamic interactions (adsorption and desorption) were expected to take place between PSL and *T. lutea* surface. Right after the 48 h exposure, *T. lutea* solutions were fixed in 3% glutaraldehyde (Fisher Scientific®, United Kingdom) for 1 h (Bergami *et al.*, 2017). Samples were not previously centrifuged as we suspected PSL precipitation could cover micro algae walls without adsorption interactions. Micro volumes of fixed *T. lutea* were thus dried at room temperature for 30 min in a laminar hood. Later, the samples were gold sprayed and observed under SEM (Carl Zeiss EVO® 50) at 7 kV. All the glassware used in the experiments was cleaned using an acid bath of 3% nitric acid, rinsed with distilled water then with 70% ethanol and dried under a fume hood.

3.4.3 Micro algae and oyster cultures

Marine micro algae species *Chaetoceros calcitrans* and *Tisochrysis lutea* were obtained from Fisheries & Oceans (Tracadie-Sheila, New Brunswick, Canada). *Chaetoceros calcitrans and T. lutea* were cultured in glass balloons with F/2 medium (Guillard, 1975) at 26‰ salinity, and acclimatized at room temperature under 24:24 artificial light of 73 µmol/m²/s.

Individuals of *C. virginica* were acquired at the beginning of fall before the hibernation stage from New Brunswick's raised oysters (Canada). They were selected to have a diameter range from 6.4 to 7.6 cm, meaning all oysters were between 3 to 4 years old. Once brought to the laboratory, they were individually brushed to remove external parasites and placed in 25 L tanks (39 oysters per tank). Tanks contained reconstituted seawater (Instant Ocean®) at 30‰ salinity, oxygenated, and filtered by an aquarium filter pump. Similar to *C. virginica* farming conditions, they were acclimatized at 20 °C (Ward *et al.*, 2019) with aquarium heaters and under 12:12 (light:dark cycles) for nine weeks. During acclimation, the oysters were fed twice a week with a mixt *T. lutea* and *C. calcitrans* (2.5×10^6 cells/L and 1.7×10^6 cells/L, per tank respectively) (Sussarellu *et al.*, 2016; Tallec *et al.*,2020). The algae *C. calcitrans* was used only during oysters acclimation for nutritional purposes (Gonzalez Araya *et al.*, 2012).

3.4.4 Trophic exposure

The micro algae *T. lutea* was used as NPs vector for *C. virginica* dietary exposition to PSL, PSC, and NPG. To that end, the three NP dispersions were separately added into *T. lutea* solutions for 48 h at nominal concentrations of 10 and 100 µg L^{-1} NPs, presumed to be environmentally low (Lenz *et al.*, 2016; Besseling *et al.*, 2014). This exposure time was chosen according to

previous experiments and proven to be effective (Lebordais *et al.*, *submitted*). Before NP dosing, the micro algae concentrations were assessed by a Coulter Multisizer II particle counter (Fortin *et al.*, 2000) and brought to 4.7 x 10^6 cells/mL. NP-*T. lutea* solutions were under the same abiotic conditions as during the acclimation phase. All the *C. virginica* individuals were fed every two days with 2.24 x 10^3 cells/oyster/L of *T. lutea*. The oysters belonging to NP treatments were fed with NP-*T. lutea* at the same micro algae concentration.

To study the complexity of NP interactions with environmental metallic contaminants, we combined each NP treatment with As. Arsenic is one of the most commonly detected metals in the collected Guadeloupean plastics (El Hadri *et al.*, 2020a). Arsenate is the most abundant inorganic form of As found in oxygenated marine waters and also the least toxic one (Francesconi and Edmonds, 1996; Neff, 1997; Yang *et al.*, 2012; Zhang *et al.*, 2013). Therefore, a solution of dissolved arsenate (pentoxide arsenic) was prepared to use during the exposures (US EPA, 2001). On day one, the oysters treated with arsenate (hereafter referred to As treatment) were exposed to a nominal concentration of 1 mg L^{-1} in water (Zhang *et al.*, 2015). The As concentration was chosen based on previous studies (Langston, 1984; Zhang *et al.*, 2015). Water samples were collected one day out of two and the total As was measured. If needed, the As level was adjusted to keep the 1 mg L^{-1} concentration throughout the experiment.

Our experimental design included twelve NP treatments, a negative control (reconstituted seawater) and a positive control (As at 1 mg L^{-1}). Thus, the experiment encompassed three single-NP treatments (NPG, PSC, PSL) at both 10 and 100 µg L^{-1} and three combined-NP treatments (also at 10 and 100 µg L^{-1} for each NPs) with 1 mg L^{-1} of As. One litre jars were filled up to 500 mL with reconstituted seawater and parafilm-covered to lower evaporative loss. Air distribution pumps were set up for water oxygenation. To avoid plastics contact, silicone tubing with glass pipette tips were used in each jar. Salinity, temperature, and light were the same as during acclimation. All treatments were conducted in five independent replicates with one oyster per glass jar.

Oysters were dissected at the end of the one-week diet exposure. Biometric data are reported in supplementary files **Fig. S1** (Annexe II). Shell length was assessed on individual oyster pictures by ImageJ software. Whole-body were manually dried with paper then weighed (fresh weight). Gills and visceral mass tissues were quickly collected and stored at -80 °C for As dosage and subsequent molecular assays. The condition index (CI; Lucas and Beninger, 1985) was calculated by the following equation.

Equation 1:

$$CI = \frac{\text{leftover tissues} * \text{weight}}{\text{shells weight}} \text{ x } 100 \qquad * \text{leftover tissues: whole body excluding gills and visceral mass}$$

3.4.5 Arsenic quantification in water by ICP-OES, in oyster tissues by ICP-MS and bioaccumulation factor comparison

Total $As_{(water)}$ concentration was monitored throughout the one-week exposure. Water samples of 10 mL per jar were collected for control and As treated oysters. Then, the water samples were acidified with 3% nitric acid for inductively coupled plasma optical emission spectrometry (ICP-OES) analysis with a detection limit for As at 0.005 mg L^{-1}.

Total $As_{(tissues)}$ concentration was conducted in gills and visceral mass for *C. virginica*. First dried at 50 °C for 48 h, they were then weighed before digestion. Tissue samples were acidified with 70% nitric acid (3 mL per sample) and heated at 100 °C for 3 h. After dilution of the digestates with milliQ water (1:36), the final volume was 7 mL per sample. Concentrations of total $As_{(tissues)}$ were measured using an inductively coupled plasma mass spectrometry (ICP-MS) with a detection limit for As at 0.02 µg L^{-1}. A standard curve of an As reference solution (SCP Science®, Multi-Element Std) was systematically analyzed with the samples to control the measured concentrations. The single spike recovery method was performed (yield = 101.71%) to validate the analysis accuracy (Wolle and Conklin, 2018).

In previous work, wild-caught *I. alatus* oysters native to the Caribbean Sea were collected from Guadeloupean mangroves (Lebordais *et al.*, *submitted*) and underwent similar acclimation conditions (reconstituted seawater at 26 °C, salinity of 32‰, 12:12 light). They were fed with the marine micro algae *Tisochrysis lutea* and *Thalassiosira weissflogii* for two weeks of acclimation and were subjected to the identical trophic exposure as *C. virginica*. These consistent parameters in controlled exposures allow us to compare the As uptake for each oyster species. Therefore, the potential differences in the As bioaccumulation between *I. alatus* and *C. virginica* should be mainly due to their physiological and natural background differences (Moreira *et al.*, 2018). To compare As bioaccumulation levels between both oyster species, we normalized the concentration from exposed individuals to controls and presented it for gills and visceral mass.

The bioaccumulation factor (BAF) of As was calculated for *C. virginica* and *I. alatus* oysters using Equation 2 (n = 4 per treatment and species). Wet weights were calculated from the measured dry weights with 0.2 and 0.1 corrections factor for gills and visceral mass,

respectively (Klinck *et al.*, 1992; Choi *et al.*, 1993; Kobayashi *et al.*, 1997). The As concentrations measured in exposed oysters were normalized with natural As background from control oysters. Both As concentrations were measured in individual oysters. These relative As concentrations in gills and visceral mass were then averaged to estimate oyster's whole body content. As concentrations in water were measured for each oyster jars.

Equation 2:

$$BAF = \frac{[As]_{wet\ tissue}}{[As]_{water}} \qquad \begin{matrix} [As]_{wet\ tissue} : \text{in } \mu g/kg \\ [As]_{water} : \text{in } \mu g/L \end{matrix}$$

3.4.6 RNA extraction and cDNA synthesis

A similar amount of tissues were individually homogenized with one stainless steel ball (5 mm) per sample in 600 µL of RNA lysis buffer. To that end, a Retsch® mixer mill MM 400 (Fisher Scientific®, Toronto, Canada) was used for 4 min at 20 Hz. Oyster tissues are rich in fat and proteins and to separate these components, 500 µL of Phenol:Chloroform:Isoamyl Alcohol (25:24:1 v/v/v, Sigma-Aldrich®, Oakville, Canada) were added and vortexed before RNA extraction. This organic solvent is indeed highly suitable for insoluble tissue extractions (Vicient and Delseny, 1999). To separate the aqueous phase that contained the RNA, the samples were centrifuged for 1 min at 13,000 rpm. From there, total RNA was extracted using the Quick-RNA™ Miniprep Kit (Zymo Research®) with on-column DNAase I treatment as described in the manufacturer's protocol. The total RNA concentration was measured using a NanoDrop-2000 spectrophotometer (Thermo Fisher Scientific®). The nucleic acid purity was ensured by ratios 260/280 > 1.8 and the RNA integrity of each sample was assessed on a 1% agarose gel. Generally, in eukaryotes the RNA integrity is assessed by the presence of two defined bands representing the 28S and 18S ribosomic RNA (rRNA) (Gutierrez-Villagomez *et al.*, 2019). In the RNA integrity analysis, a single band with no smear was observed in the gels. This is possible due to a "hidden break" in the 28S rRNA of *C. virginica*. Winnebeck *et al.* (2010) documented that for numerous insects and other animal taxa the 28S rRNA splits into two fragments after heat denaturation. Because of what was described as a hidden break, the two 28S rRNA fragments overlap with the 18S rRNA during a gel electrophoresis analysis.

All the samples were diluted to obtain the same RNA concentration (2000 ng in 8 µL). Complementary DNA (cDNA) was prepared using Maxima™ H Minus First Strand cDNA Synthesis Kit with dsDNase (Thermo Fisher Scientific®). A first step of DNA denaturation was conducted with dsDNase according to the supplier's instructions. Then 4 µL of mix including the reverse transcriptase enzyme, buffer and primers were added with 6 µL of water per sample. This second step was performed on a Mastercycler Thermocycler Pro S (ThermoFisher, Ottawa, Canada) following the supplier's protocol. All cDNA was synthesized at the same time for each tissue sample including a no reverse transcriptase control (NRT) and a no template control (NTC). Then the cDNA samples were stored at -20 °C.

3.4.7 qPCR assays and validations

Quantitative polymerase chain reaction (qPCR) was performed to measure relative messenger RNA (mRNA) levels in the following 15 genes: clathrin heavy chain (cltc) to evaluate endocytosis; catalase (*cat*), glyceraldehyde-3-phosphate-deshydrogenase (*gapdh*) and superoxide dismutase Cu/Zn extracellular (*sod3*) to assess oxidative stress; mitochondrial encoded 12S rRNA (*12S*) to measure mitochondrial metabolism; growth arrest DNA damage (*gadd45*) and tumor protein P53 (*p53*) to measure cell cycle regulation; blcl-2-associated X apoptosis regulator (*bax*) and apoptosis regulator (*bcl-2*) to assess apoptosis; cytochrome P450 family 1 sub-family A1 (*cyp1A*), ATP binding cassette sub-family B1 (*mdr*) and metallothionein (*mt*) to assess detoxification; and vitellogenin (*vit*) to evaluate the energy storage. Elongation factor 1 alpha (*ef1α*) and ribosomal protein L7 (*rpl7*) were included as reference genes (Lee and Nam, 2016). Specific primer sets were designed for all genes with primer-BLAST on the NCBI platform (**Table S1**, Annexe II) and synthesized by Sigma-Aldrich®. Primer optimization was conducted by three-fold serial dilutions and temperature gradients. To confirm each gene transcript, PCR was conducted, a single band was observed in a 2% agarose gel and the products were purified using the NucleoSpin™ Gel and PCR Clean-up kit (Takara®). PCR products were sequenced on a ABI 3730xl, Applied Biosystems platform at Centre Hospitalier d'Université Laval (CHUL, Québec, Canada) and analyzed on BioEdit® software so gene transcript sequences could be confirmed by NCBI BLAST. All qPCR reactions were proceeded using Maxima SYBR Green qPCR Master Mix (2X) (Thermo Fisher Scientific®). This reagent includes the Taq DNA polymerase, the SYBR Green I dye, an optimized PCR buffer and dNTPs. Together with the forward and reverse primers (final concentration of 0.3 µM), each mix was prepared in a 15 µL volume. Then 5 µL added of 1:135 diluted cDNA as it was the optimal dilution for conducting the

reactions. The resulting final volumes were poured into individual optical PCR tubes, RNAse- and DNAse-free treated (Invitrogen®).

Gill and visceral mass cDNA samples were analyzed in Real-Time PCR Detection Systems, CFX96 Dx and CFX96 Touch™ respectively (Bio-Rad®). All samples were run in duplicates, including one NTC and one NRT for each analysis. According to the manufacturer's recommendation, the performed cycling conditions were an activation step at 95 °C for 10 min, followed by 40 cycles of denaturation step at 95 °C for 15 sec, and one primer annealing-extension temperature depending on the primer set for 60 sec (**Table S1**, Annexe II). To guarantee the specificity of the primers, after 40 cycles a melt curve was performed from 60 to 95 °C with increments of 0.5 °C per cycle. Single amplified products were obtained per gene. The efficiency of all qPCR reactions was in a 90-110% range and the coefficient of determination (R^2) was systematically ≥ 0.990. To calculate relative gene expression the relative standard curve method was used (Fronhoffs *et al.*, 2002; Gutierrez-Villagomez *et al.*, 2019). Starting quantities (Sq) data were analyzed using the Bio-Rad CFX Manager Software (Bio-Rad®). Gene fold changes were normalized to both reference genes, calculated relative to the control treatment and averaged by replicates (n = 4-5, essayed in duplicates).

3.4.8 Statistical analyses

Analysis of outliers for biometric data, relative mRNA levels and As tissue concentrations were performed using the ROUT method (Q = 1%) in GraphPad Prism 8.0 (Motulsky and Brown, 2006). Raw data were then transformed by commonly used functions (square root, double square root or decimal logarithm) to satisfy parametric conditions in SigmaPlot 12.0. Normality was thus confirmed using Shapiro-Wilk test and homoscedasticity was confirmed by Levene test. Transformed data were compared using a two-way analysis of variance (ANOVA) for biometric data and relative mRNA levels. As bioaccumulation transformed data were only compared using a one-way ANOVA or a Student's t-test. For all data, the significant differences were identified by a post-hoc Tukey HSD test on Prism 8.0. The significance level was set at $\alpha = 0.05$.

3.5 Results and Discussion

3.5.1 Bottom-up complexity of nanoplastic dispersions

We selected monodispersed PSL nanoparticles free of additives to exclude chemicals toxicity. Also, PSL were functionalized with carboxylated groups making them stable and optimal for comparing results with literature in regard to impact determination of NPs (Kim *et al.*, 2017;

Thiagarajan *et al.*, 2019). Previous works already described these PSL (Pessoni *et al.*, 2019; Lebordais *et al.*, *submitted*), hence NPs characterization was focused on PSC and NPG. The PSC nanoparticles were relevant NPs as they have been laboratory nanofragmented from large plastic pellets (El Hadri *et al.*, 2020b). As a result, they were polydispersed and covering the global colloidal size distribution (**Fig. 3.1 A-B**). This parameter is interesting since NPs polydispersity is poorly addressed in ecotoxicological studies (Alimi *et al.*, 2018; Bhagat *et al.*, 2020). Moreover, PSC had higher specific surface area and irregular shapes increasing NP adsorption ability compared to PSL (Quik *et al.*, 2011; Brennecke *et al.*, 2016). However, both PSL and PSC lacked natural aging and exposure to contaminants. To go one step further in the environmental relevancy, the collected Guadeloupean plastics have been naturally exposed to contaminants and weathered by abiotic processes (such as UV light) which increase surface oxidation (Holmes *et al.*, 2014; Andrady, 2017; Dawson *et al.*, 2018; El Hadri *et al.*, 2020b; Mao *et al.*, 2020). Therefore, NPG resulting from plastic debris was most likely to reproduce the heterogeneity of NPs observed in the environment. As such, NPG could include several plastic polymers (e.g., polyethylene, polypropylene, polyvinyl chloride and polystyrene; Gigault *et al.*, 2016; Davranche *et al.*, 2020).

The NPG plastics mixture may also contain a wide variability of additives like pigments (Frias *et al.*, 2010). Noteworthy, pigments absorbance have been previsouly documented to bias the measures of light dispersion (Zook *et al.*, 2011; Geißler *et al.*, 2015). As NPG are detected by dynamic light scattering, they present a Brownian motion in aqueous system and therefore can be defined as NPs (Gigault et *al.*, 2018b). Based on the instensity of light scattered, NPG z-average was 1071 ± 30.65 nm. However, it is well known in the colloidal field that for large size distribution the presence of bigger particles contributes significantly to the intensity of light scattered ($I_\theta \approx r^6$, r the particle radius) compared to smaller particles. Such high polydispersity tend to mask the presence and characterization of lower size distribution in the colloidal dispersions of materials using CONTIN algorithm. (**Fig. 3.1 C-D**). Moreover, NPG dispersions present irregular shapes, high surface oxidation and specific surface area increasing their adsorption properties (El Hadri *et al.*, 2020a). Numerous contaminant and pollutant families can thus interact with environmental NPs, but also change their bioavailability and toxicity (Alimi *et al.*, 2018; Bhagat *et al.*, 2020). Therefore adding environmentally weathered plastics brings relevance to NP ecotoxicological studies.

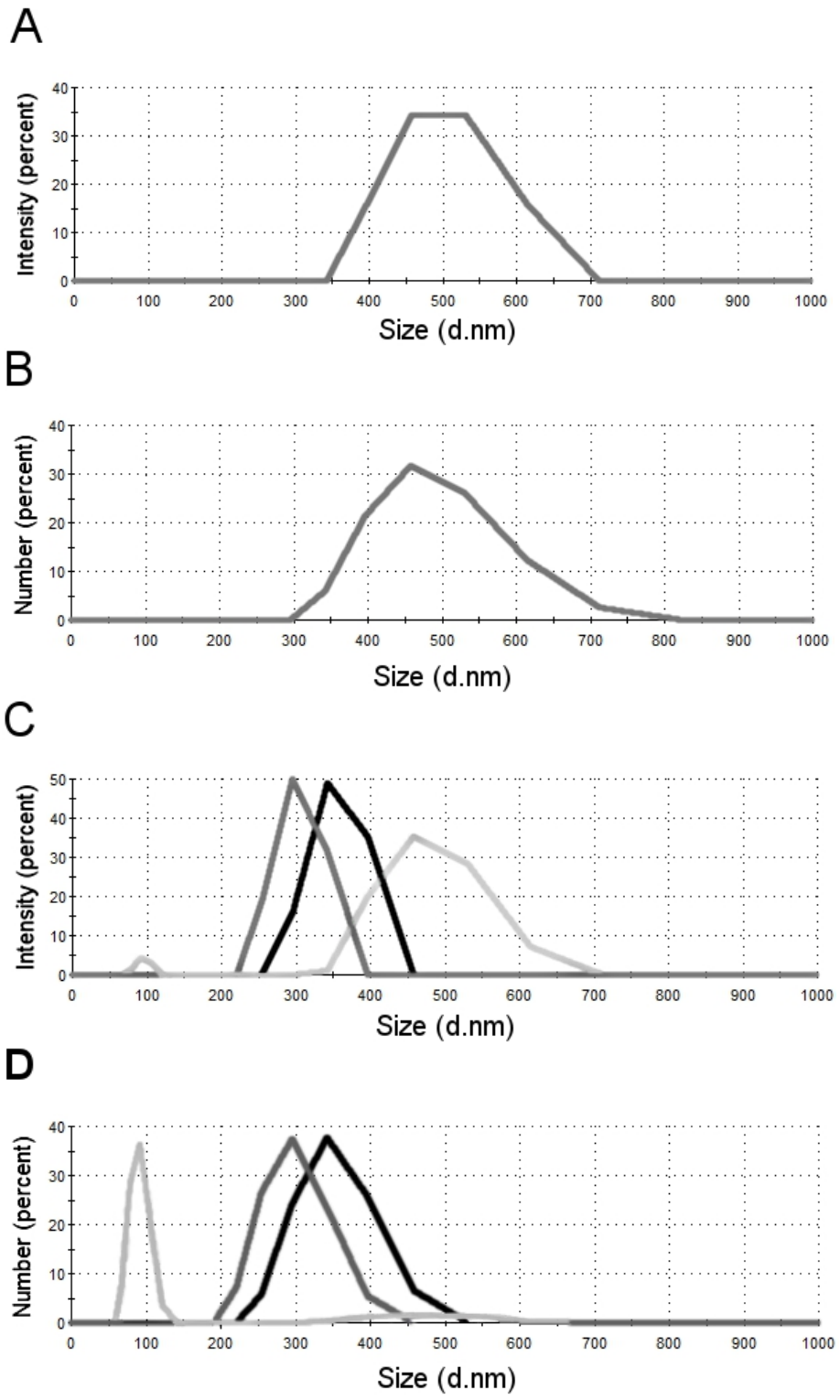

Figure 3.1: Hydrodynamic diameters of NP particles measured by DLS using a Zetasizer nano zs. Size distribution for PSC dispersion with z-average of 692.4 ± 68.55 nm (A) and the corresponding number of nanoparticles (B). Size distribution for NPG dispersion with z-average of 1071 ± 30.65 nm (C) and the corresponding number of nanoparticles (D). Each NPG batch is presented with a different shade of grey.

3.5.2 Adsorption of carboxylated polystyrene nanoplastics on micro algae

The SEM observations highlighted that PSL was adsorbed on *T. lutea* surface in all of the tested concentrations (**Fig. 3.2**). At environmentally realistic NP concentrations, 10 and 100 µg L^{-1}, we observed fewer adsorbed PSL per micro algae (**Fig. 3.2 B-C**) compared to the higher concentrated treatments (**Fig. 3.2 D-E**). Noteworthy, PSL aggregates consistently appeared starting at 1000 µg L^{-1} (**Fig. 3.2 D**). No differences were observed in the number of adsorbed PSL between 1000 and 5000 µg L^{-1}, suggesting a saturation of the particles onto micro algae surfaces. Although these results are representative of a short exposure (48 h) in estuarine-like conditions. Indeed *T. lutea* solutions were homogenized twice a day to mimic dynamic interactions and to avoid sedimentation. In general, we did not notice damage on the micro algae surface. This result is contradictory with Wang *et al.* (2020) that observed fragmented shapes and cracked surfaces onto marine micro algae exposed for 96 h to 200 and 2000 µg L^{-1} of PS NPs (70 nm) associated with molecular and physiological hazards. Such difference can be potentially explained by the presence of surfactant and additives generally used for commercially available PSL (Pikuda *et al.*, 2018). Unlike PSC and NPG, PSL were a valuable NPs model easy to target by SEM given their consistent spherical shape. Also, Pessoni *et al.* (2019) previously demonstrated the PSL carboxylated surface functions should prevent them from forming homoaggregates. Nonetheless, PSL most likely formed heteroaggregates in the presence of NOM noticeable as clear dots in the SEM observations (**Fig. 3.2**). NP aggregations had been observed to change their bioavailability, and thus, to either increase or decrease NP toxicity (Corsi *et al.*, 2014; Zhang *et al.*, 2018). Surprinsigly, despite PSL heteroaggregations and their global negatively charged surface, the SEM images showed that PSL was able to adsorb onto micro algae regardless of natural organic matter's presence and for all the tested concentrations.

.

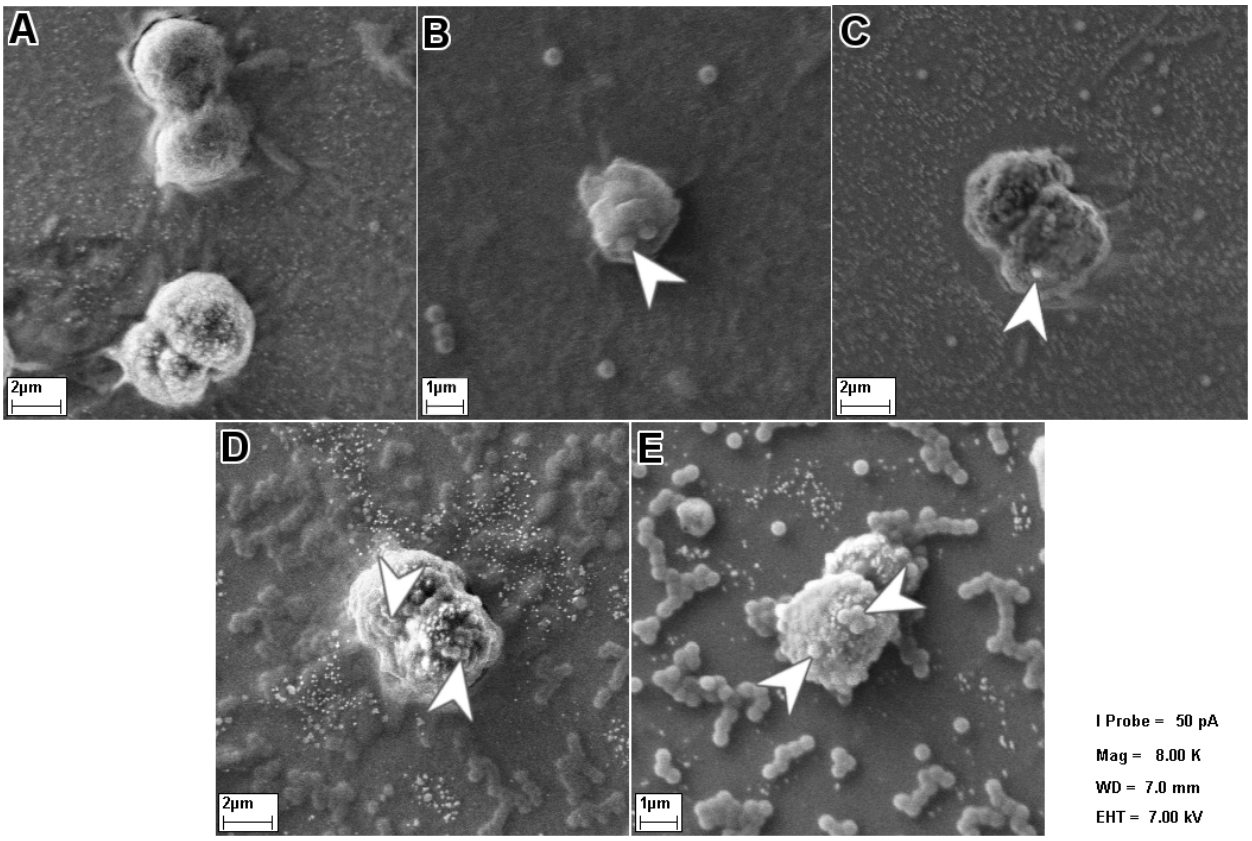

Figure 3.2: Scanning Electron Microscopy (X 8000) observation of carboxylated polystyrene nanospheres of latex (PSL) adsorbed on *T. lutea* exposed for 48 h to 0 µg L^{-1} (A), 10 µg L^{-1} (B), 100 µg L^{-1} (C), 1000 µg L^{-1} (D) and 5000 µg L^{-1} (E). Arrows indicate the presence of adsorbed PSL to micro algae. Of note, only 10 µg L^{-1} and 100 µg L^{-1} were used for the oyster diet exposure.

3.5.3 Oysters physiology and arsenic bioaccumulation

Biometric parameters and arsenic uptake

Crassostrea virginica's biometric data are presented in **Fig. S1** (Annexe II). The registered mortality during the exposure was minor (7%) and statistical differences were only detected for fresh tissue weight (**Fig. S1 A**, Annexe II). Nonetheless, there were no significant differences between the control and other treatments, between both concentrations of the same NP treatment, nor between the As treatment and the NP + As treatments (**Fig. S1 A**, Annexe II).

Crassostrea virginica oysters from control treatment had an average As concentration of 1.6 µg g^{-1} (dry weight) in gills and 3.5 µg g^{-1} in visceral mass (**Figure 3.3**). All As-exposed

oysters (As and NPs + As treatments) displayed statistically similar levels of total As accumulation respectively to each tissue. In addition, they were all significantly different from the control treatment. Thus, the three different NP treatments at 100 µg L^{-1} did not significantly influence the total As accumulation in *C. virginica* after one-week exposure.

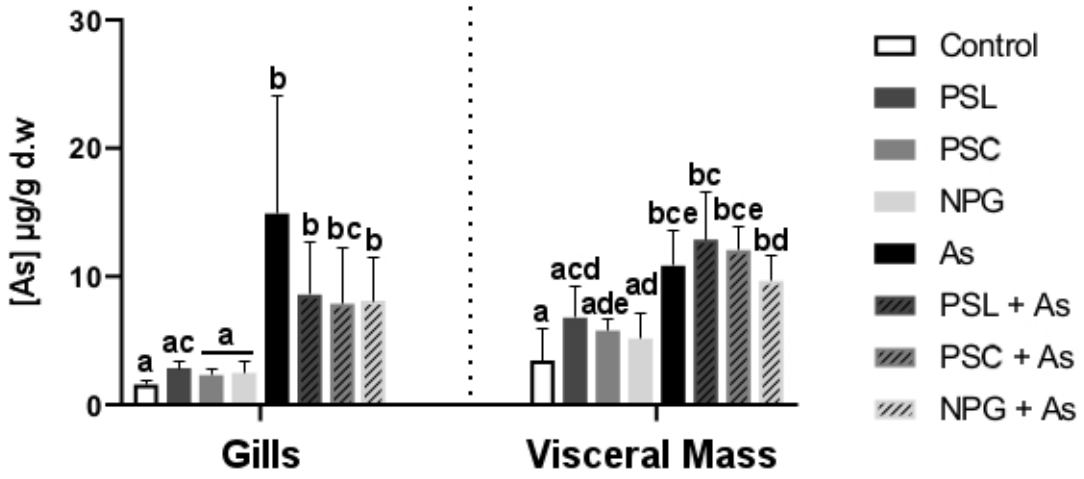

Figure 3.3: Arsenic bioaccumulation (µg/g, dry weight, mean + sd) in *C. virginica* gills and visceral mass (n = 4), after one week of exposure to 1 mg L^{-1} As and/ or 100 µg L^{-1} NPs.

NP quantities were most likely too low to significantly change the total As bioaccumulation by adsorption. We observed similar results when the oyster *I. alatus* was exposed to NPG + As (Lebordais *et al.*, *submitted*). In both oyster experiments NP and As levels were comparable. Similarly, Freitas *et al.* (2018) did not observe higher bioaccumulation of As (0.1 mg L^{-1}) in *Ruditapes philippinarum* clams exposed in combination with multi-walled carbon nanotubes (0.1 mg L^{-1}). Put into perspective, our total As bioaccumulation results in *C. virginica* suggested this experimental design was environmentally realistic. Indeed, these results are consistent with an environmental range of total accumulated As (from 4.1 to 39 µg g^{-1}, dry weight) in *C. virginica* individuals from Gulf of Mexico coastal areas (Wilson *et al.*, 1992). To better assess and compare oysters bioaccumulation, their native background should be considered. The *C. virginica* oysters were farmed at St-Simon bay that is connected to Chaleur bay, where controlled effluents from industrial activities have been discarded. The Human Health Risk Assessment survey (Ministère de la Santé et du Mieux-être du Nouveau Brunswick, 2005) revealed a total As concentration up to 2 $mg.kg^{-1}$ (wet weight) in local mussels. This background

value is consistent with our measured total As levels in *C. virginica* with an average of 0.7 mg.kg^{-1} (wet weight) in gills and 1.4 mg.kg^{-1} in visceral mass for control (data not shown).

Species bioaccumulation factor comparison

In a previous experiment, Caribbean flat oysters *I. alatus* from Guadeloupe mangrove swamps were also exposed in-laboratory to 1 mg L^{-1} of As for one week (Lebordais *et al.*, *submitted*). *I. alatus* and *C. virginica* underwent identical experimental conditions regarding micro algae feeding, salinity, temperature, and light conditions. The relative As bioaccumulation yielded 2-fold change in *I. alatus* tissues compared to controls, while *C. virginica* yielded approximately 5- to 10-fold change in gills and visceral mass, respectively (**Figure 3.4**). There was a significant difference between the gills of *I. alatus* and *C. virginica*. In most aquatic organisms, gills are known to be a transport organ for metallic contaminants (Kraemer *et al.*, 2005; Won *et al.*, 2016, Cao et al; 2018). As gills respond rapidly to metal contamination in water, they have a short-term role in regulation (Langston, 1984; Strady *et al.*, 2011). Ultimately, they are more sensitive through waterborne contamination until metals move into storage organs, like the visceral mass (Soegianto *et al.*, 2013; Arini *et al.*, 2014). As expected, high As concentrations were measured in *I. alatus* oysters exposed in a laboratory setting (Lebordais *et al.*, *submitted*). Nonetheless, relative As levels suggested higher As uptakes for exposed *C. virginica* oysters (**Figure 3.4**).

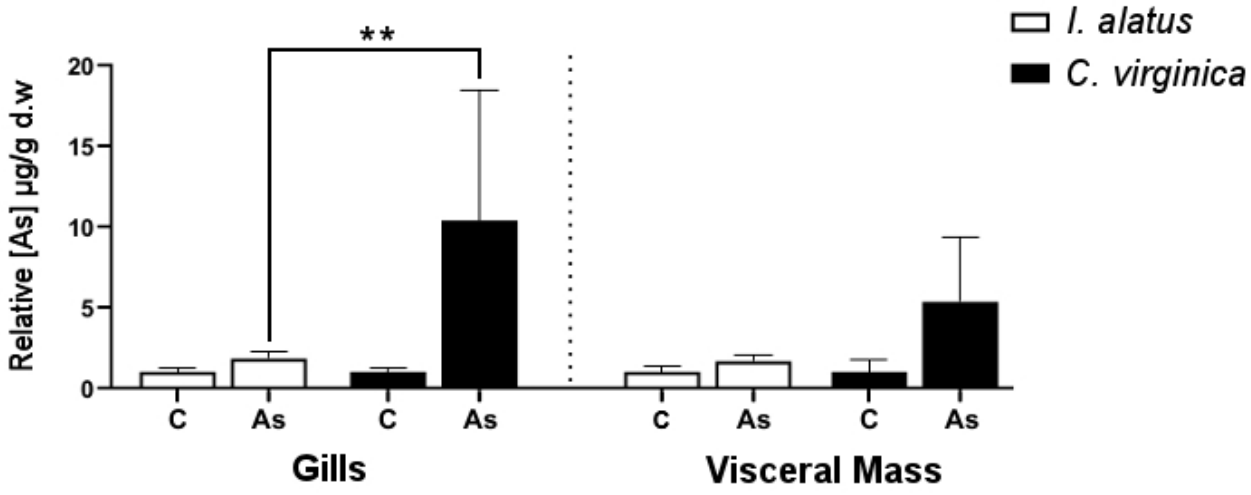

Figure 3.4: Relative arsenic bioaccumulation (µg/g, dry weight, mean + sd) compared between *I. alatus* and *C. virginica* in gills and visceral mass (n = 4), after one week of exposure to 1 mg L^{-1} As. Asterisks show a significant difference (p < 0.01) assessed by Student's t test.

We then calculated the BAF using wet weight for each oyster species. Whole-body BAFs estimated from gills and visceral mass were 13.4 (± 6.1) for *I. alatus* and 57.7 (± 41.9) for *C. virginica*. These BAF values confirmed a higher As uptake for *C. virginica* individuals compared to *I. alatus* suggesting *I. alatus'* physiology is potentially adapted to grow into As-rich environments (Cherkasov *et al.*, 2010; Luo *et al.*, 2014). Regulation, biotransformation, and/or detoxification mechanisms may enable *I. alatus* to tolerate higher As concentrations as revealed by the major As bioaccumulation baseline in the control treatment. Consequently, *C. virginica* is presumably more vulnerable to As exposure than *I. alatus*. Indeed, New Brunswick's nurseries and bays carried most likely minimal As availability to *C. virginica* (as revealed by the low As bioaccumulation baseline in controls). Moreover, BAF standard deviations show noticeable contrast for each species. This difference might be related to oysters filtration rates. *Isognomon alatus* oysters showed consistent BAF values between individuals, while *C. virginica* showed a higher BAF variability between individuals. This high variability could be explained by a putative change in filtration rates between *C. virginica* oysters trying to protect themselves from metal contamination (Tran *et al.*, 2003; Pan and Wang, 2012; Freiras *et al.*, 2018).

The gills and visceral mass of exposed *I. alatus* accumulated 10 and 20 times more As than *C. virginica* tissues, respectively (Lebordais *et al.*, *submitted*). However, As bioaccumulation was already higher in *I. alatus* controls than in exposed *C. virginica* oysters. This major difference could be due to the oyster's respective habitats. The As concentration measured in Guadeloupean seawater was below the limit of detection, and As concentration in upper St. Lawrence estuary (Quebec, Canada) can be up to 1.5 µg L^{-1} for the highest salinity (Tremblay and Gobeil, 1990). There is little variability of As levels in seawater, and according to Neff (1997) the concentration in clean coastal and oceans ranges within 1-3 µg L^{-1}. Thus, it can be considered both species were in waters with naturally similar As concentrations. Nonetheless, sediment plays a key role in As waterborne route for filter-feeding bivalves (Langston, 1984; Zhang *et al.*, 2013; Maher *et al.*, 2018). Consequently, As concentrations in Toucari bay (close to the Guadeloupe island) ranged from 27.8 to 40.9 $mg.kg^{-1}$ in submarine sediment (Johnson and Cronan, 2001); whereas, the average As concentration in Chaleur bay sediment (New Brunswick, Canada) was 11 $mg.kg^{-1}$ (Parsons and Cranston, 2005). Also, As is accumulated by primary producers like phytoplankton being the main As dietary route for marine consumer organisms (Neff, 1997; Azizur Rahman *et al.*, 2012; Maher *et al.*, 2018) and warmer water temperatures can facilitate total As uptake for bivalves (Ünlü and Fowler, 1979; Gutierrez-Galindo *et al.*, 1994). As such, tropical *I. alatus* oysters grew in mangrove swamps that are productive ecosystems with major sediment and phytoplankton inputs (Saed *et al.*, 2004;

Bouillon, 2011; Yap *et al.*, 2011). In contrast, subarctic *C. virginica* oysters were farmed inside floating gears in less rich waters from a Canada's Eastern bay. The age of the oysters should also be considered as it might have influenced the As accumulation results. *C. virginica* oysters were three to four years old, while *I. alatus* oysters were about six years old based on this oyster growth rate in Jamaica mangroves (nearby Guadeloupe island, Siung, 1980). Overall, As concentrations measured in both oyster controls witnessed their natural As burden that is representative of their respective habitat.

3.5.4 Oysters gene responses after exposure

Relative gene expression in gills and visceral mass

We selected a set of genes of interest to target ecotoxicological endpoints gathered in seven biological functions, such as endocytosis (*cltc*), oxidative stress (*cat*, *gapdh*, *sod3*), mitochondrial metabolism (*12S*), cell cycle regulation (*gadd45*, *p53*), apoptosis (*bax*, *bcl-2*), detoxification (*cyp1A*, *mdr*, *mt*), and energy storage (*vit*) (**Table S1**, Annexe II). Of note, we did not detect *vit* in gills after PCR and agarose gel analysis; thus, we only show its results for visceral mass. The **figures 3.5 and 3.6** show the relative mRNA levels results for gills and visceral mass, respectively.

The expression of *12S* significantly increased with PSL treatment at 10 µg L^{-1} compared to the control treatment, but it did not increase at 100 µg L^{-1} (**Figure 3.5 A**). The exposure to PSL + As at 10 µg L^{-1} did not affect significantly the expression of *12S,* suggesting that the induction for PSL treatment at 10 µg L^{-1} was prevented by the presence of As. Similar antagonist effects of As in mixture with PSL were observed in *I. alatus* exposure (Lebordais *et al.*, *submitted*). Ribosomic RNA (rRNA) *12S* is transcribed by the mitochondrial genome. Therefore, *12S* rRNA level is used as a proxy to represent the number of mitochondrial copies in a given tissue (Al kaddissi *et al.*, 2012; Arini *et al.*, 2015). Considering that gills are involved in respiration, their mitochondrial activity can be more sensitive to contaminants like metals (Akberali and Earnshaw, 1982). Significant differences in *12S* expression for As treatment were expected in gills through waterborne route. Instead, the data suggest that As was more available through the dietary route (**Figure 3.6 C**). The expression of *bax* significantly increased in the PSC + As treatment at 100 µg L^{-1} compared to control, As alone and PSC at 100 µg L^{-1} treatments (**Figure 3.5 B**). Also, the *bax* expression for PSL + As treatment significantly increased at 10 µg L^{-1}, but it did not change significantly at 100 µg L^{-1}. In addition, PSL + As at

10 µg L^{-1} significantly increased compared to control, As alone and PSL at 10 µg L^{-1} treatments. Overall, the presence of As in PSC at 10 µg L^{-1} and PSL at 100 µg L^{-1} induced a synergetic *bax* expression. *Bcl-2* gene family are central regulators of programmed cell death. Indeed, the intrinsic pathway for apoptosis relies on upregulation of pro-apoptotic genes like *bax* (Schuler *et al.*, 2000; Chipuk *et al.*, 2010). Seen *bax* regulation integrates internal and external stress signals, its expression gives a relevant proxy to assess contaminant toxicities at the cell level (Yanan 2012). For example, Cao *et al.* (2018) observed a significant increase of *bax* relative mRNA level in *Crassostrea gigas* gills and observed apoptosis at 10 µg L^{-1} of Cd. As such, the combination of As treatment with PSC and PSL most likely induced apoptotic effects in *C. virginica* after one week of exposure. The expression of *gapdh* significantly increased in PSC + As treatment at 10 µg L^{-1} compared to control and PSC at 10 µg L^{-1} treatments (**Figure 3.5 C**). The *gapdh* response can be associated to oxidative stress responses but no further interpretation can be made since its protein is involved in the nucleus, mitochondrial and cytosolic signal pathways (Sirover 2011, Tristan *et al.*, 2011).

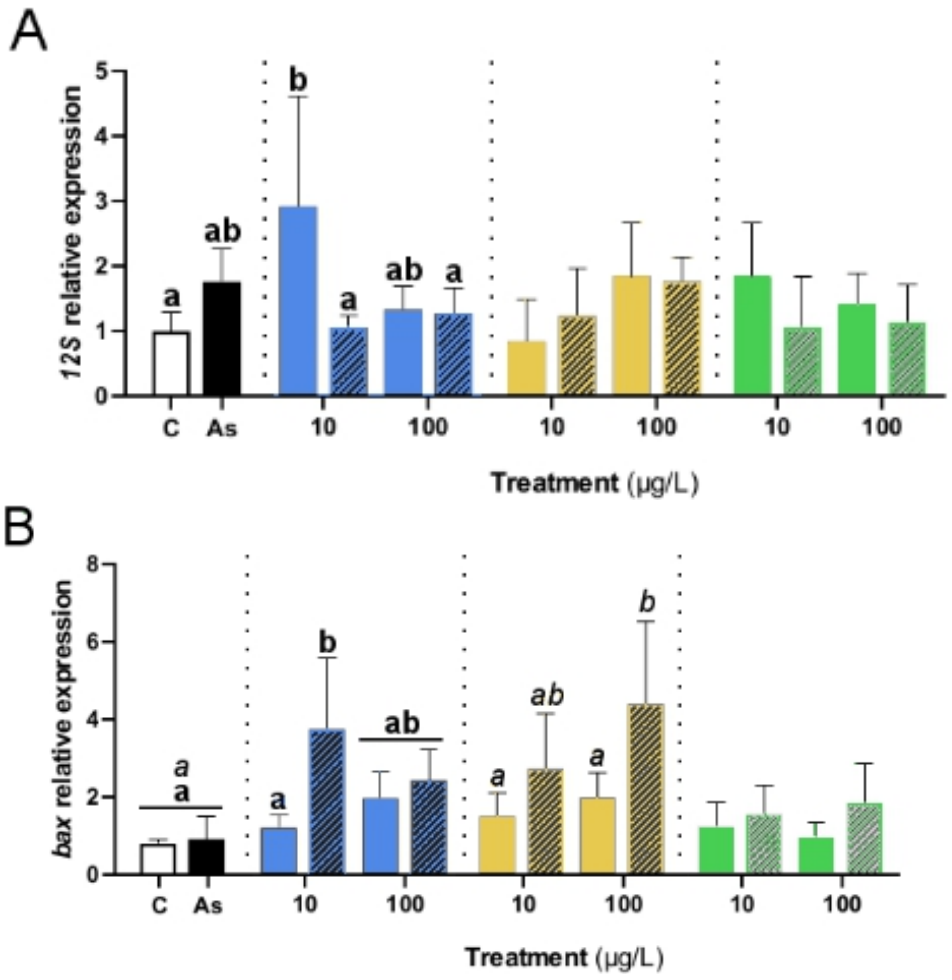

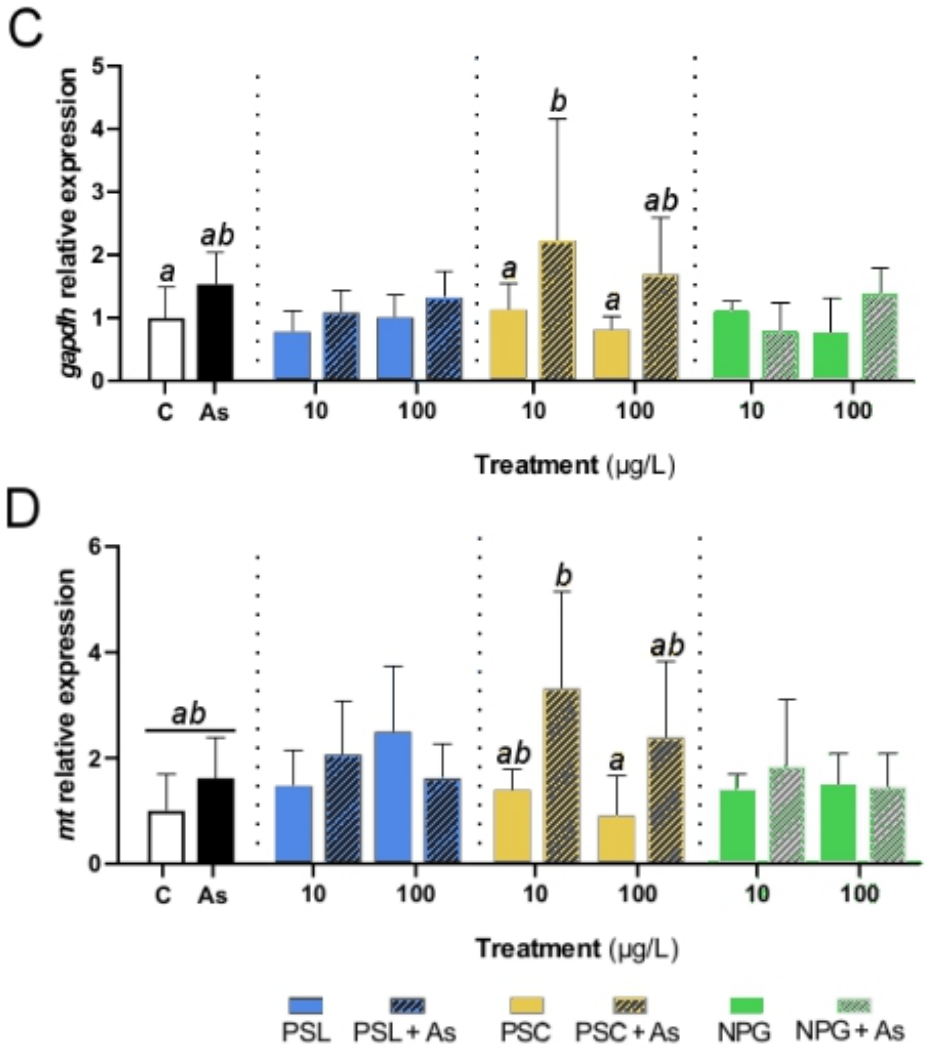

Figure 3.5: Relative gene expressions in *C. virginica* gills after one-week exposure to 1 mg L^{-1} As combined or not with 10 and 100 µg L^{-1} NPs. mRNA levels are presented for *12S* (A), *bax* (B), *gapdh* (C) and *mt* (D). All the values are presented as the mean + sd (n = 4-5) normalized by *ef1α* and *rpl7* genes. Different letters denote significant differences (*p < 0.05*) among treatments assessed by two-way ANOVA followed by Tukey post-hoc test. Bold, italic and capital letters are used for PSL, PSC and NPG treatments respectively.

The expression of *12S* significantly increased for NPG + As treatment at 10 and 100 µg L^{-1} compared to control, As alone and NPG at 10 and 100 µg L^{-1} treatments (**Figure 3.6 C**). Similarly, the expression of *12S* significantly increased in PSC + As treatment at 10 and 100 µg L^{-1} compared to control, to As alone, and PSC (at both concentrations). Thus, the presence of As in NPG + As and PSC + As induced a synergetic *12S* expression. Also, PSL + As treatment significantly increased *12S* expression at 100 µg L^{-1} compared to control, As alone and PSL + As at 10 µg L^{-1} treatments. Based on these gene expression profiles, As treatment alone did not affect mitochondrial metabolism. Yet, in the presence of NPs we can suggest that As was more

effective in impairing mitochondrial respiration. Indeed, metal toxicity can decrease oxygen consumption in mitochondria (Sokolova *et al.*, 2005; Cherkasov *et al.*, 2010). We expected visceral mass to be less sensitive to As exposure regarding mitochondrial gene response (Akberali and Earnshaw, 1982). Nonetheless, we observed significant differences in the mRNA level of *12S* for NPs + As treatments only in visceral mass. These results support stronger effects of As combined with NPs and suggest that diet was the main driver for oysters exposure to NPs. Therefore, the combined NPs + As treatments triggered a synergetic effect that most likely increased the number of mitochondria. The expression of *gadd45* for NPG + As treatment at 100 µg L^{-1} was not significantly different from its control nor the As alone treatment. Yet, it significantly decreased compared to NPG at 100 µg L^{-1}. This indicates that the expression of *gadd45* for NPG treatment at 100 µg L^{-1} was prevented in combination with As. The expression of *p53* for NPG + As treatment at 100 µg L^{-1} did not significantly change compared to the control and the As alone treatments, but its expression significantly increased compared to NPG + As at 10 µg L^{-1} (**Figure 3.6 D**). The expression of *p53* for PSL treatment at 100 µg L^{-1} did not significantly change compared to the control, but its expression significantly increased compared to the PSL + As at 100 µg L^{-1} and to PSL at 10 µg L^{-1} treatments. Thus, PSL treatment at 100 µg L^{-1} in combination with As prevented *p53 gene* expression (**Figure 3.6 E**). Overall, the exposure to As in NPG + As treatment at 100 µg L^{-1} significantly changed *gadd45* and *p53* expressions relatively to NPG treatment for the same concentration. The opposite *gadd45* and *p53* responses to NPG + As treatment might be caused by several negative feedback loops (Harris and Levine, 2005). Considering *gadd45* regulation is (among others) upon P53 transcription factor, its downregulation can be linked to P53 increase (Salvador *et al.*, 2013). The expression of *bcl-2* significantly increased in the PSL treatment at 100 µg L^{-1} compared to control and to PSL at 10 µg L^{-1} treatments (**Figure 3.6 G**). The *bcl-2* expression for PSL at 100 µg L^{-1} also significantly increased compared to As treatment, but not to PSL + As at 100 µg L^{-1}. Thus, the expression of *bcl-2* for PSL treatment at 100 µg L^{-1} was prevented in combination with As. Despite being an anti-apoptotic gene (Aouacheria, 2005), *bcl-2* upregulation has been associated with a significant decrease of red granulocyte percentage in clams blood exposed to MPs (Tang *et al.*, 2019).

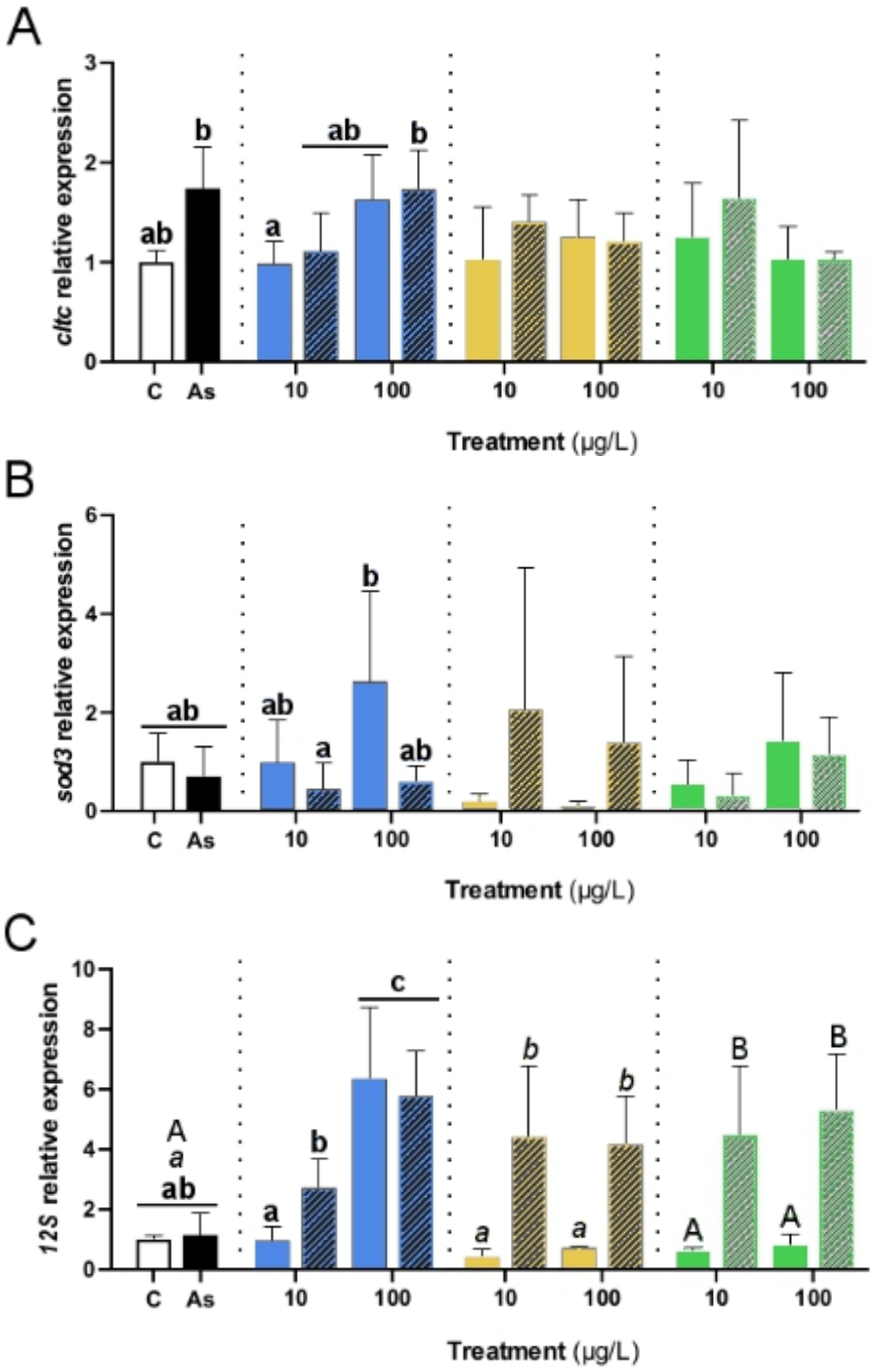
A
cftc relative expression
ab
b
ab
a
b
C
As
10
100
Treatment (µg/L)
B
sod3 relative expression
ab
ab
a
b
ab
C
As
10
100
Treatment (µg/L)
C
12S relative expression
A
a
ab
a
b
c
a
b
a
b
A
B
A
B
C
As
10
100
Treatment (µg/L)

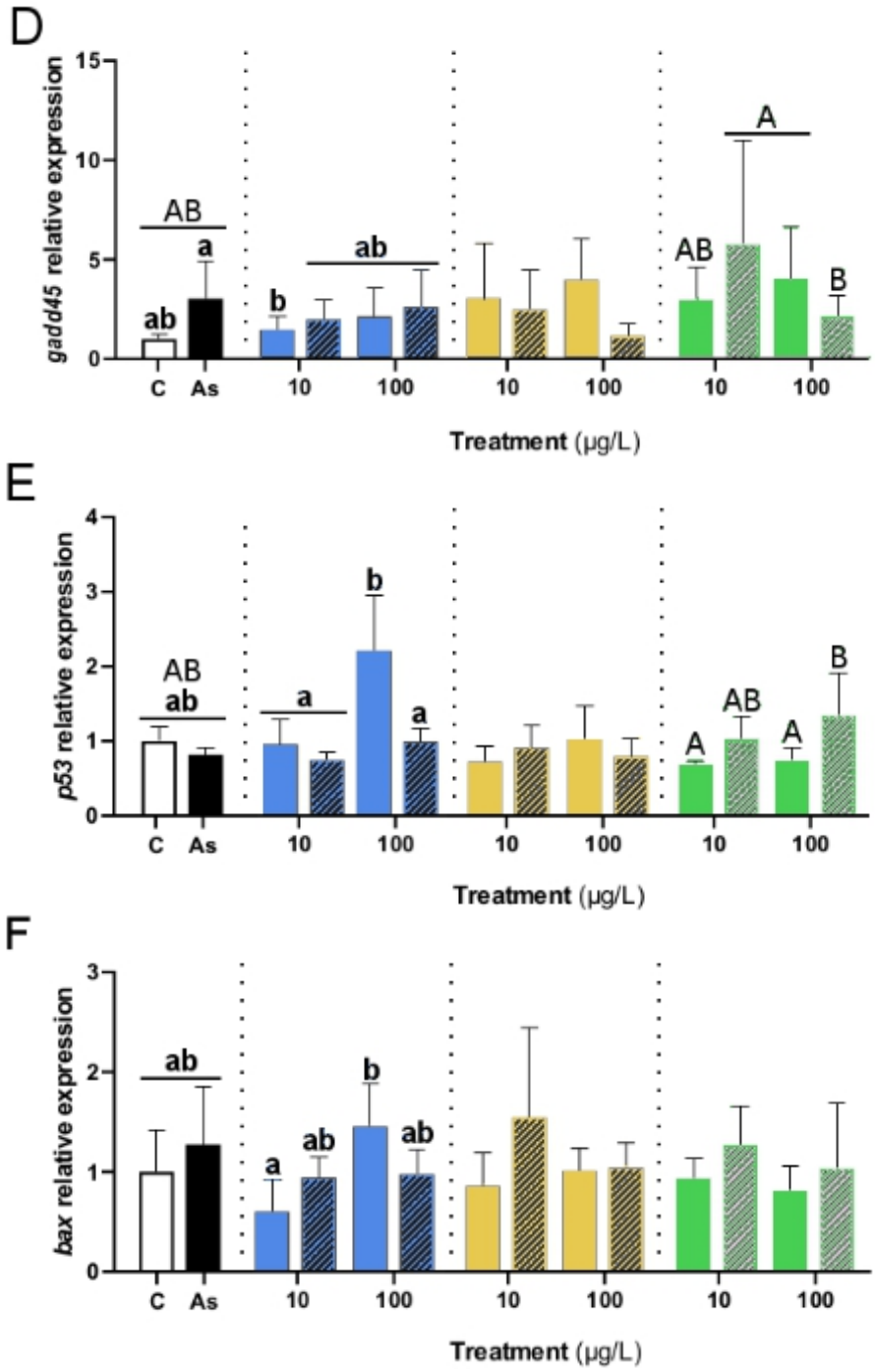
D
gadd45 relative expression
15
10
5
0
AB
a
ab
b
ab
A
AB
B
C
As
10
100
10
100
10
100
Treatment (µg/L)
E
p53 relative expression
4
3
2
1
0
AB
ab
a
b
a
A
AB
A
B
C
As
10
100
10
100
10
100
Treatment (µg/L)
F
bax relative expression
3
2
1
0
ab
a
ab
b
ab
C
As
10
100
10
100
10
100
Treatment (µg/L)

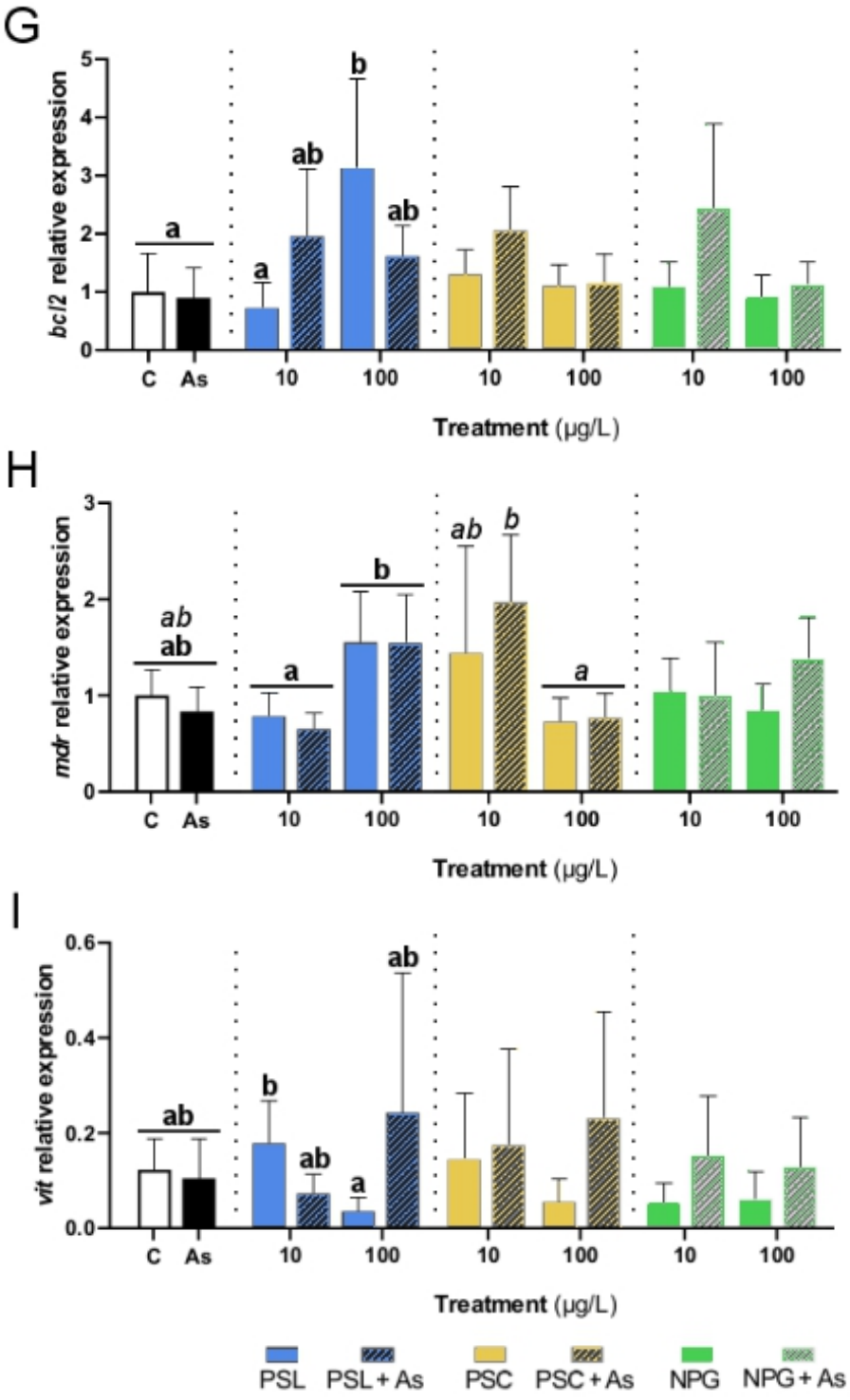

Figure 3.6: Relative gene expressions in *C. virginica* visceral mass after one-week exposure to 1 mg L^{-1} As combined or not with 10 and 100 µg L^{-1} NPs. mRNA levels are presented for *cltc*, (A), *sod3* (B), *12S* (C), *gadd45* (D), *p53* (E), *bax* (F), *bcl-2* (G), *mdr* (H), and *vit* (I). All the values are presented as the mean + sd (n = 4-5) normalized by *ef1α* and *rpl7* genes. Different letters denote significant differences ($p < 0.05$) among treatments assessed by two-way ANOVA followed by Tukey post-hoc test. Bold, italic and capital letters are used for PSL, PSC and NPG treatments respectively.

Combined effects of arsenic with nanoplastics

We observed specific gene responses for combined NPs + As treatments in both tissues. A single antagonist effect was measured (**Figure 3.5 A**), while consistent synergetic effects were measured (**Figures 3.5 B, 3.6 C**). Synergetic effects, according to Bhagat *et al.* (2020) definition, were identified by genes upregulation for NPs + As treatments significantly different from control, As and NP treatments alone. As such, NPG + As and PSC + As synergetic effects on *12S* expression revealed an increase of rRNA level produced by mitochondria that could indicate the induction of mitochondria number in visceral mass (**Figure 3.6 C**). Yet, presumed toxicity on mitochondrial metabolism (e.g., oxidative stress) can not be associated with our results since antioxidant gene responses of *cat*, *sod,* and *gapdh* were not consistent. Interestingly, Freitas *et al.* (2018) measured a significant inhibition of electron transport system activity, with significant inductions of superoxide dismutase and catalase activities in clams exposed to combined multi-walled carbon nanotubes. Synergetic or antagonist effects have been observed for several combined contaminants (Kim *et al.*, 2017; Bhagat *et al.*, 2020) and are most likely related to contaminant changes in bioavailability and/or speciation (Spurgeon *et al.*, 2020). In our experiment *T. lutea* potentially biotransformed As, but only in NPs + As treatments. These As speciation changes might have been reduced by the presence of NPs. Indeed, *T. lutea* was very likely shortly exposed to As before being consumed by *C. virginica*. Thus, As have been potentially metabolized by *T. lutea* as documented for micro algae (Cullen and Reimer, 1989; Azizur Rahman *et al.*, 2012). For instance, phytoplankton and bacteria are major producers of As methylated forms (e.g., dimethylarsinous acid, monomethylarsonous acid; Wood, 1974; Francesconi and Edmonds, 1996; Hellweger and Lall, 2004). However, in the presence of NPs, adsorbed inorganic As is potentially not available for *T. lutea* methylation. According to Farrell *et al.* (2011), adsorption can affect As speciation. These observations matter for toxicity assessment using gene expression responses since As methylated and inorganic forms have distinct molecular targets, bioaccumulation rates and excretion pathways (Dixon, 1997; Petric *et al.*, 2001; Hughes, 2002; Ng, 2005). Thus, we may suggest that As methylated forms present in As treatment, and inorganic As present in NPs + As treatment, triggered different gene expression responses. In this study, putative quantities of As methylated forms in As treatment might be less effective since we observed no significant changes for any investigated gene. Inorganic As forms are known to be more toxic than As methylated forms (Sephar *et al.*, 1980; Neff, 1997; Petric *et al.*, 2001, Ng 2005). Therefore, comparatively to As treatment, higher

amounts of inorganic As available for *C. virginica* could explain synergetic effects measured for NPs + As treatments.

3.6 Conclusions

There is a current lack of relevance in the literature of NPs ecotoxicity that we addressed by comparing the effects of three NP models with a gradient of environmental relevancy. In regards to *C. virginica* gene responses, the most effective NPs treatment combined with As was PSC, while PSL was the most effective NPs treatment conducted alone. Yet, with NPG, all three NPs in presence of As showed synergetic effects in both tissues of *C. virginica*. Our trophic exposure shed light on significant synergetic effects measured in mitochondrial metabolism and apoptosis related genes at low NP concentrations (10 and 100 µg L^{-1}). These are novel results regarding As combination with environmentally representative NPs (NPG). Overall, there were more significant gene responses to NP treatments in visceral mass than in gills. These results suggest that NPs were more available or effective by dietary route as we expected. Furthermore, our BAF results compared between two oyster species revealed higher As uptake for Canadian farmed oysters *C. virginica* than Caribbean wild oysters *I. alatus*. This comparative approach provided valuable data that revealed the effects variability of combined As + NP treaments between two oyster species. Therefore, future studies should target the As speciation to better assess the As forms being adsorbed to NPs and the putative role of micro algae. A longer exposure time at lower As concentration will also be relevant to confirm the gene expressions and bioaccumulation data measured in this study.

3.7 Acknowledgments

We acknowledge Bruno Grassl, Hind El Hadri and Stephanie Reynaud (IPREM) for providing the polystyrene nanoparticles; and Réjean Tremblay (UQAR) for providing micro algae solutions. The authors would like to thank Joy Gaubert (INRS) for help with the molecular assays and Jean-François Dutil (INRS) for help with arsenic analyses. The authors also appreciated the unknown referee's helpful comments.

3.8 Fundings

This work was financially supported by the Agence Nationale de la Recherche (ANR) in the PEPSEA program (ANR-17-CE34-0008-05) to MB and JG, the Centre National de la Recherche

(CNRS) in the EC2CO INIAME program to MB and JG, and the Canada Research Chair program (950-23223) to VSL.

4 DISCUSSION GÉNÉRALE ET CONCLUSION

4.1 Rétrospective sur le modèle expérimental

4.1.1 Le temps d'exposition

Pour nos deux expériences trophiques présentées dans les articles 1 et 2, nous avons utilisé des concentrations en NP de 10 et 100 µg L^{-1}. Ces concentrations se classent dans la gamme basse des expositions de NP pour des expériences similaires (Alimi *et al.*, 2018; Bhagat *et al.*, 2020). Malgré cela, des changements significatifs d'expression de gènes ont pu être mesurés chez *Isognomon alatus* et *Crassostrea virginica* pour plusieurs fonctions biologiques ciblées. Il en va de même pour différentes études qui ont récemment étudié l'impact écotoxicologique des NP chez les bivalves. Par exemple, Brandts *et al.* (2018) ont également mesuré des changements d'expression de gènes révélateurs de stress oxydant et de neurotoxicité chez *Mytilus galloprovincialis* exposée à 50 µg L^{-1} de PS (117 nm) et co-exposée avec la carbamazépine. Shi *et al.* (2020) ont mesuré des effets immunotoxiques et différents stress physiologiques identifiés par analyse transcriptomique chez *Tegillarca granosa* exposée à 290 µg L^{-1} de PS (500 nm) co-exposée avec la sertraline. De même, Tang *et al.* (2020) ont aussi mesuré des effets immunotoxiques et des changements d'expression de gènes liés à l'apoptose chez *Tegillarca granosa* exposée à 1 mg L^{-1} de PS (500 nm) et co-exposée au benzo[a]pyrene ou au 17β-estradiol. À la lumière de ces résultats, il en ressort que les NP (seuls et combinés à d'autres contaminants) induisent des effets physiologiques et des changements moléculaires à des concentrations suggérées comme environnementalement réalistes.

Cependant, la plupart des études menées sur la toxicité des MP et des NP sont des expositions aiguës allant de 48 à 96 h (Bhagat *et al.*, 2020). Les mollusques sont généralement exposés en laboratoire à des temps plus longs allant d'une à deux semaines, voire trois semaines (Xia *et al.*, 2020). Considérant que le temps d'exposition joue un rôle clé pour la toxicité des contaminants, des expositions chroniques sont souvent nécessaires pour évaluer les effets à long terme. Dans le cas des NP, leur accumulation chronique pourrait nuire *in fine* à l'alimentation des huîtres (Ward and Shumway, 2004; Ward and Kach, 2009; Al-Sid-Cheikh *et al.*, 2018). En effet, les NP et agrégats des NP inférieurs à 500 nm peuvent traverser les branchies des huîtres et migrer par la circulation interne jusqu'aux cellules stomacales (voie 1, **Figure 4.1**). Quant aux agrégats de NP compris entre 1 et 6 µm, ils sont directement ingérés au niveau des palpes labiaux et conduits par l'oesophage jusqu'à l'estomac (voie 2, **Figure 4.1**). Au vu de leurs tailles et propriétés d'agrégations, les PSL sont vraisemblablement ingérés par la

voie 1, tandis que les PSC et NPG le sont par la voie 2. Une exposition chronique aux NP peut donc mener à leur potentielle accumulation dans l'estomac des huîtres. De plus, les huîtres ayant un système circulatoire ouvert le transport des NP depuis la circulation interne est facilité jusqu'aux organes vitaux (ex. : coeur, hépatopancréas ; Browne *et al.*, 2008). Ceci augmente alors le risque d'exposition des tissus internes aux NP. Plusieurs études ont en effet documenté l'encombrement physique probable des NP chez les huîtres, mais surtout la toxicité des additifs et/ou des contaminants désorbés pour les cellules (Wegner *et al.*, 2012; Trevisan *et al.*, 2019; Xia *et al.*, 2020).

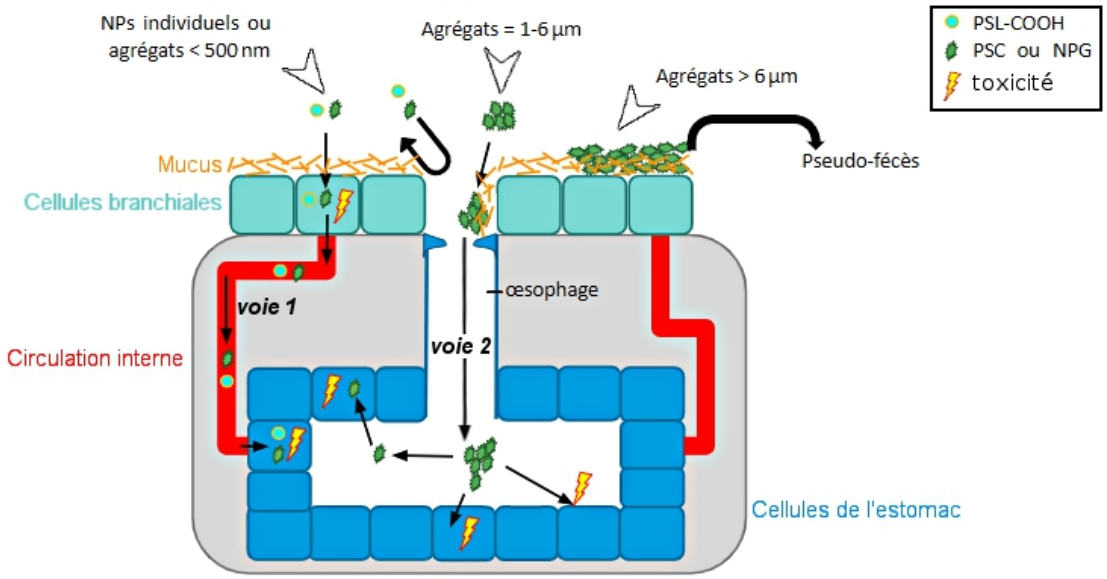

Figure 4.1 : Schéma des voies de contamination en fonction des tailles de NPs chez une huître (Zélie Venel, 2020).

Pour quantifier le nombre de NP accumulés dans les tissus, et suivre leur éventuelle accumulation au cours du temps, des analyses telle que la pyrolyse couplée à la chromatographie gazeuse - spectrométrie de masse sont nécessaires (Bouwmeester *et al.*, 2015). Or cette technique est en cours de développement (Ter Halle *et al.*, 2017). Dans nos deux expériences, nous avons mesuré les effets des NP sur *I. alatus* et *C. virginica* par l'analyse des changements d'expression de gènes. Cette analyse repose sur les quantités d'ARNm produits qui est une réponse à court terme (Achard-Joris *et al.*, 2006). De ce fait, prolonger la durée d'exposition n'aurait pas été pertinent pour notre modèle expérimental. Le choix du temps d'exposition ne doit donc pas être systématique ; au contraire, il doit répondre spécifiquement au

modèle expérimental et à la question de recherche.

4.1.2 Les effets dose-réponse

Les courbes doses-réponses permettent de prouver la toxicité d'un contaminant lorsque celui-ci agit de manière proportionnelle (Schirinzi *et al.*, 2017). Ainsi, pour mieux comprendre la toxicité des NP sur les huîtres, il serait intéressant de conduire une CE_{50} (concentration pour 50% d'effet). Des effets sublétaux tels qu'une décroissance de la masse des tissus, des changements d'activité de la respiration mitochondriale, des hyperplasies dans les branchies et des micronoyaux dus à la génotoxicité sont autant de paramètres pertinents pour compléter les analyses d'expression de gènes (Sokolova *et al.*, 2005; Al Kaddissi *et al.*, 2012; McCarthy *et al.*, 2013). En effet, ces derniers permettraient de confirmer les changements moléculaires mesurés et de quantifier des seuils de sensibilité à plusieurs niveaux biologiques (organisme, tissu, cellule, ADN).

D'ailleurs, dans l'article 1 nous avons testé le potentiel impact des NP sur la croissance des microalgues *Tisochrysis lutea* exposées aux trois NP pendant 96 h (**Figure 4.2**). Cette expérience nous a conforté qu'à 10 et 100 µg L^{-1} de NP la densité optique de *T. lutea* était identique entre les traitements et contrôles jusqu'à 48 h. Ainsi, *I. alatus* et *C. virginica* ont été exposées aux différents traitements de NP sans biais de concentrations en microalgues.

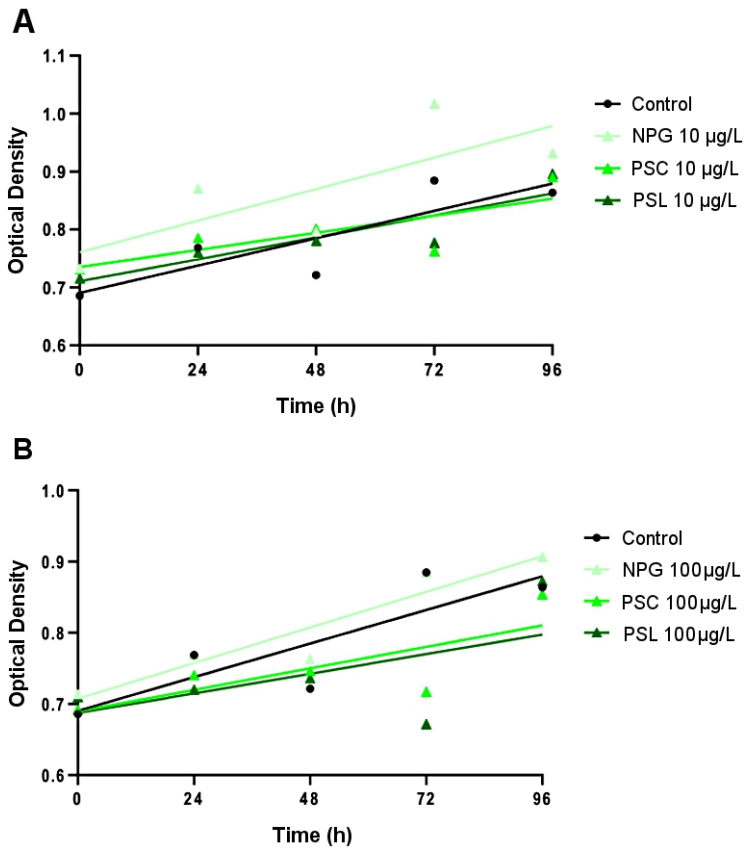

Figure 4.2 : Croissance de *Tisochrysis lutea* en culture pendant 96 h. Régressions linéaires avec valeurs moyennes (n = 5) représentées pour les traitements contrôle (r^2 = 0.74), 10 µg L^{-1} de NP (A) et 100 µg L^{-1} de NP (B). NPG = 0.60, PSC = 0.61, PSL = 0.80 (A). NPG = 0.90, PSC = 0.59, PSL = 0.33 (B).

Pour aller plus loin, une expérience similaire pourrait être menée pour évaluer les CE_{50} des NP exposés à *T. lutea*. En effet, des concentrations plus élevées en NP inhibent la croissance des microalgues (Bergami *et al.*, 2017; Wang *et al.*, 2020). Ces mesures donneraient une valeur comparative entre chaque NP et permettraient ainsi de les classer, par exemple en fonction de leur potentiel d'adsorption. Pour rappel, l'adsorption des PSL a été montrée à la surface de *T. lutea* dans l'article 2 pour 10, 100, 1000 et 5000 µg L^{-1}. De plus, une relation positive a été observée entre la concentration d'exposition en PSL et leur nombre adsorbé en surface de *T. lutea*. Néanmoins, en absence de résultats plus quantitatifs, il n'est pas possible d'estimer la proportionnalité entre la concentration en PSL et leur nombre adsorbé par microalgue. En effet, entre 1000 et 5000 µg L^{-1} de PSL leur nombre adsorbé par microalgue n'était pas différenciable. Il serait donc pertinent de mesurer la concentration seuil pour laquelle un nombre maximal de NP peut s'adsorber en surface des microalgues. C'est pourquoi une expérience dose-réponse

donnerait accès aux concentrations seuils pour chaque NP, et ainsi, renseignerait sur la biodisponibilité d'adsorption des NP en fonction de leur concentration d'exposition.

4.2 Comparaison des deux expériences

4.2.1 Synthèse des résultats

Les effets combinés des NP avec des contaminants métalliques ont récemment été étudiés à travers plusieurs analyses. Parmi elles, l'expression de gènes est relativement documentée dans la littérature (Bhagat *et al.*, 2020). L'expression de gènes est un outil écotoxicologique puissant qui est sensible aux faibles concentrations d'exposition, qui inclut une diversité de réponse des fonctions cellulaires, et qui peut cibler des tissus spécifiques d'intérêt. Les principaux résultats sont comparés entre *I. alatus* et *C. virginica* au terme de leur exposition d'une semaine dans des conditions expérimentales similaires (**Figure 4.3**).

Les fonctions cellulaires représentées (**Figure 4.3**) ont été identifiées à partir des changements significatifs d'expression de gènes dans un tissu donné et pour chaque traitement aux NP seuls ou combinés à l'As. Chez *I. alatus*, il est à souligner que les fonctions impactées par les traitements aux NP ont majoritairement été mesurées dans les branchies. À l'exception des régulations du cycle cellulaire qui sont conservées dans les deux tissus, aussi bien pour les traitements aux NP que pour ceux aux NP + As. En présence d'As, la majorité des fonctions impactées par les traitements aux NP + As ont été mesurées dans les masses viscérales. Quant à *C. virginica*, les traitements aux NP ont agi sur l'apoptose et le métabolisme mitochondrial dans les masses viscérales et les branchies respectivement. Curieusement, en présence d'As (NP + As) nous observons ces deux mêmes fonctions impactées mais dans les tissus inverses. Par ailleurs, les PSL sont les seuls NP qui aient eu des effets sur l'apoptose et le métabolisme mitochondrial. En présence d'As (PSL + As), ces effets ont été maintenus mais ont également été observés pour les autres NP (PSC + As et NPG + As). L'ensemble de ces résultats donnent à voir davantage d'effets chez *I. alatus* que chez *C. virginica* pour les traitements aux NP. Ce contraste pourrait s'expliquer par différentes quantités de NP filtrés par chaque espèce. En effet des réponses d'endocytose ont été mesurées chez *I. alatus* et non chez *C. virginica*. De ce fait, les NP ont potentiellement été davantage biodisponibles pour l'exposition d'*I. alatus*, et aurait donc exercé plus d'effets chez *I. alatus* comparativement à *C. virginica*.

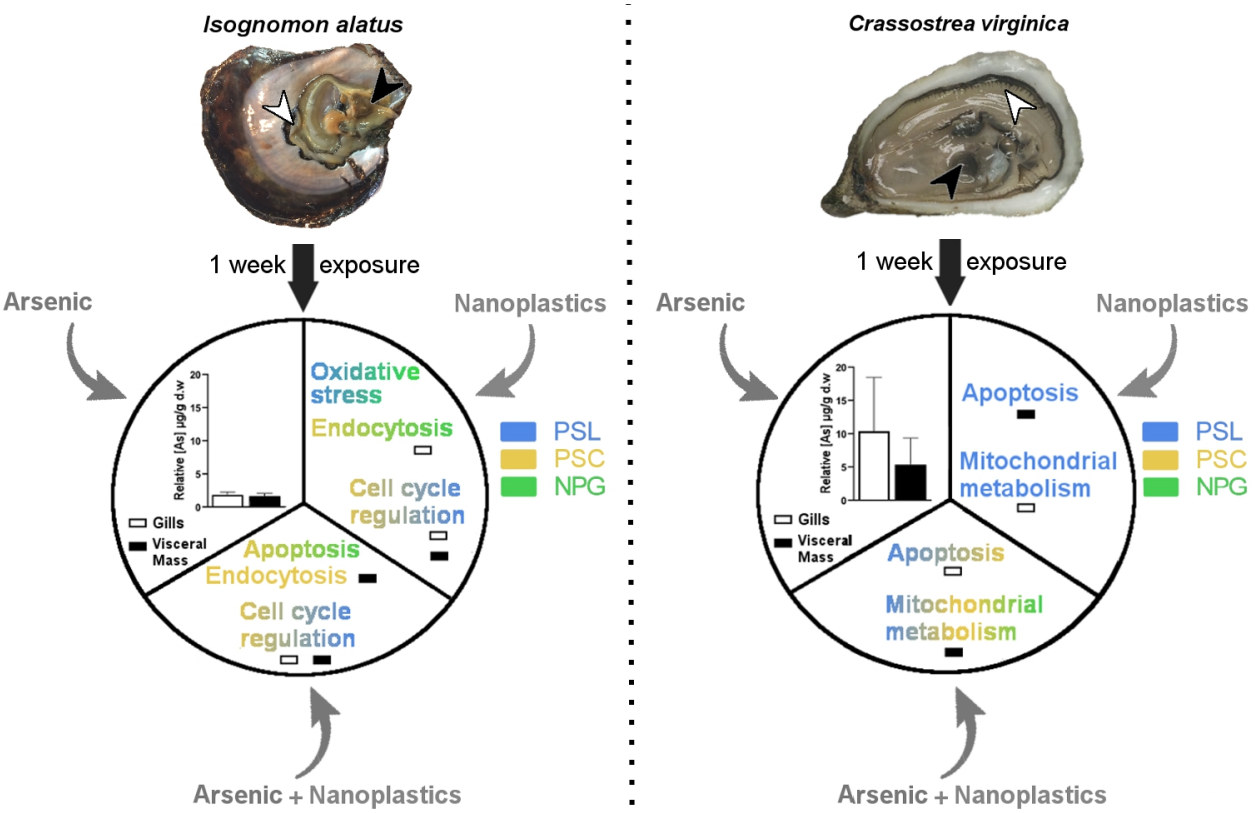

Figure 4.3 : Résultats comparatifs d'*Isognomon alatus* et *Crassostrea virginica* exposées pendant une semaine à l'As (1 mg L^{-1}), aux NP (10 et 100 µg L^{-1}) et combinés aux NP + As.

4.2.2 Limites des interprétations

Bien que les conditions expérimentales le permettent, il ne serait pas pertinent de comparer les effets protecteurs et synergiques mesurés pour les traitements aux NP + As chez *I. alatus* et *C. virginica* respectivement. En effet, nous avons souligné dans l'article 2 que ces deux espèces ont bioaccumulé différentes quantités d'As comme le représentent les concentrations normalisées d'As (µg g^{-1} de poids sec) dans les deux tissus (**Figure 4.3**). Il est néanmoins essentiel d'étudier la toxicité des NP combinés à d'autres contaminants ou polluants. En effet, la toxicité qu'exercent les MP et NP sur les organismes marins est vraisemblablement associée à celles d'autres composés tels que les contaminants métalliques (Wen *et al.*, 2018; Davranche *et al.*, 2019; Zhu *et al.*, 2019). Pour rappel, ces combinaisons peuvent alterner entre effets antagonistes et synergiques suivant les changements de biodisponibilité et/ou de spéciation des contaminants combinés aux NP (Spurgeon *et al.*, 2020). Notre étude comparative permet ainsi

de souligner la diversité des réponses possibles entre deux espèces d'huîtres d'intérêt. Tout en mesurant la complexité d'effets pour deux contaminants combinés et exposés dans des conditions environnementalement réalistes. Face à cette alternance de réponses observées entre *I. alatus* et *C. virginica*, il serait avantageux de mener les futures expériences sur un organisme modèle. La culture en laboratoire d'organismes modèles (indispensables aux études écotoxicologiques; Ashauer and Jager, 2018) permettrait de standardiser les variables biologiques et environnementales pour exclure tout biais expérimental (ex : adaptations comportementales, mécanismes de détoxication différents). Les résultats de ces études menées sur des organismes modèles devraient converger pour les mêmes expositions, et donc aider à mieux identifier les effets combinés des NP aux différentes familles de contaminants et/ou polluants.

5 BIBLIOGRAPHIE

Achard-Joris, M., Gonzalez, P², Marie, V., Baudrimont, M., Bourdineaud, J.P. 2006. Cytochrome c oxydase subunit I gene is up-regulated by cadmium in freshwater and marine bivalves. *Biometals*, 19(3), 237-244.

Aguirre-Rubí, J.R., Luna-Acosta, A., Etxebarría, N., Soto, M., Espinoza, F., Ahrens, M.J., Marigómez, I. 2017. Chemical contamination assessment in mangrove-lined Caribbean coastal systems using the oyster *Crassostrea rhizophorae* as biomonitor species. *Environmental Science and Pollution Research*, 25(14), 13396–13415.

Akberali, H.B., Earnshaw, M.J. 1982. Studies of the effects of zinc on the respiration of mitochondria from different tissues in the bivalve mollusc *Mytilus edulis (L.). Comparative Biochemistry and Physiology Part C: Comparative Pharmacology*, 72(1), 149–152.

Alimi, O.S., Farner Budarz, J., Hernandez, L.M., Tufenkji, N. 2018. Microplastics and Nanoplastics in Aquatic Environments: Aggregation, Deposition, and Enhanced Contaminant Transport. *Environmental Science & Technology*, 52(4), 1704–1724.

Al Kaddissi, S., Legeay, A., Elia, A.C., Gonzalez, P., Floriani, M., Cavalie, I., Massabuau, J.-C., Gilbin, R., Simon, O. 2012. Mitochondrial gene expression, antioxidant responses, and histopathology after cadmium exposure. *Environmental Toxicology,* 29(8), 893–907.

Allen, S., Allen, D., Phoenix, V.R., Le Roux, G., Jiménez, P.D., Simonneau, A., Binet, S., Galop, D. 2019. Atmospheric transport and deposition of microplastics in a remote mountain catchment. *Nature Geoscience*, 12, 339–344.

Al-Sid-Cheikh, M., Rowland, S., Stevenson, K., Rouleau, C., Henry, T. B., Thompson, R.C. 2018. Uptake, whole-body distribution & depuration of nanoplastics by the scallop *Pecten maximus*, at environmentally realistic concentrations. *Environmental Science & Technology*,52(24), 14480-14486.

Andrady, A.L., Neal, M.A. 2009. Applications and societal benefits of plastics. *Philosophical Transactions of the Royal Society of London*, B364, 1977–1984.

Andrady, A.L. 2017. The plastic in microplastics: a review. *Marine Pollution Bulletin*, 119, 12–22.

Aouacheria, A., Brunet, F., Gouy, M. 2005. Phylogenomics of Life-Or-Death Switches in Multicellular Animals: Bcl-2, BH3-Only, and BNip Families of Apoptotic Regulators. *Molecular Biology and Evolution*, 22(12), 2395–2416.

Arini, A., Baudrimont, M., Feurtet-Mazel, A., Coynel, A., Blanc, G., Coste, M., Delmas, F. 2011. Comparison of periphytic biofilm and filtering bivalves metal bioaccumulation (Cd and Zn) to monitor hydrosystem restoration after industrial remediation: a year of biomonitoring. *Environmental Monitoring*, 13, 3386–3398.

Arini, A., Daffe, G., Gonzalez, P., Feurtet-Mazel, A., Baudrimont, M. 2014. Detoxification and recovery capacities of *Corbicula fluminea* after an industrial metal contamination (Cd and Zn): A one-year depuration experiment. *Environmental Pollution*, 192, 74–82.

Arini, A., Gourves, P.-Y., Gonzalez, P., Baudrimont, M. 2015. Metal detoxification and gene expression regulation after a Cd and Zn contamination: An experimental study on *Danio rerio. Chemosphere*, 128, 125–133.

Arini, A., Pierron, F., Mornet, S., Baudrimont, M. 2019. Bioaccumulation dynamics and gene regulation in a freshwater bivalve after aqueous and dietary exposures to gold nanoparticles and ionic gold. *Environmental Science and Pollution Research*, 27(4), 3637–3650.

Arthur, C., Baker, J., Bamford, H. 2009. Proceedings of the International Research Workshop on the Occurrence, Effects, and Fate of Microplastic Marine Debris, 2008. National Oceanic and Atmospheric Administration*, Technical Memorandum NOS-OR&R-30.*

Ashauer, R., Jager, T. 2018. Physiological modes of action across species and toxicants: the key to predictive ecotoxicology. *Environmental Science: Processes & Impacts*, 20(1), 48–57.

Ashton, K., Holmes, L., Turner, A. 2010. Association of metals with plastic production pellets in the marine environment. *Marine Pollution Bulletin*, 60, 2050–2055.

Azizur Rahman, M., Hasegawa, H., Peter Lim, R. 2012. Bioaccumulation, biotransformation and trophic transfer of arsenic in the aquatic food chain. *Environmental Research*, 116, 118–135.

Bank, M.S., Hansson, S.V. 2019. The Plastic Cycle: A Novel and Holistic Paradigm for the Anthropocene. *Environmental Science & Technology*, 53(13), 7177–7179.

Barnes, D.K.A., Galgani, F., Thompson, R.C., Barlaz, M. 2009. Accumulation and fragmentation of plastic debris in global environments. *Philosophical Transactions of the Royal Society B: Biological Sciences*, 364(1526), 1985–1998.

Baudrimont, M., Schäfer, J., Marie, V., Maury-Brachet, R., Bossy, C., Boudou, A., Blanc, G. 2005. Geochemical survey and metal bioaccumulation of three bivalve species (*Crassostrea gigas*, *Cerastoderma edule* and *Ruditapes philipinarum*) in the Nord Médoc salt marshes (Gironde estuary, France). *The Science of the Total Environment*, 337, 265−280.

Baudrimont, M., Arini, A., Guégan, C., Venel, Z., Gigault, J., Pedrono, B., Prunier, J., Maurice, L., Ter Halle, A., Feurtet-Mazel, A. 2019. Ecotoxicity of polyethylene nanoplastics from the North Atlantic oceanic gyre on freshwater and marine organisms (microalgae and filter-feeding bivalves). *Environmental Science and Pollution Research*, 27, 3746−3755.

Baun, A., Hartmann, N.B., Grieger, K., Kusk, K.O. 2008. Ecotoxicity of engineered nanoparticles to aquatic invertebrates: a brief review and recommendations for future toxicity testing. *Ecotoxicology*, 17, 387−395.

Bendif, E.M., Probert, I., Schroeder, D.C., De Vargas, C. 2013. On the description of *Tisochrysis lutea gen. nov. sp. nov.* and *Isochrysis nuda sp. nov.* in the Isochrysidales, and the transfer of Dicrateria to the Prymnesiales (Haptophyta). *Journal of Applied Phycology*, 25, 1763−1776.

Bendif, E.M., Probert, I., Schroeder, D.C., De Vargas, C. 2014. Erratum to: On the description of *Tisochrysis lutea gen. nov. sp. nov.* and *Isochrysis nuda sp. nov.* in the Isochrysidales, and the transfer of Dicrateria to the Prymnesiales (Haptophyta). *Journal of Applied Phycology.*

Bergami, E., Pugnalini, S., Vannuccini, M.L., Manfra, L., Faleri, C., Savorelli, F., Dawson, K.A., Corsi, I. 2017. Long-term toxicity of surface-charged polystyrene nanoplastics to marine planktonic species *Dunaliella tertiolecta* and *Artemia franciscana*. *Aquatic Toxicology*, 189, 159–169.

Bergmann, M., Gutow, L., Klages, M. 2015. *Springer International Publishing*, 325−340.

Besseling, E., Wang, B., Lurling, M., Koelmans, A.A. 2014. Nanoplastic Affects Growth of *S. Obliquus* and Reproduction of *D. Magna*. *Environmental Science Technology* , 48, 12336−12343.

Beyersmann, D. 2002. Effects of carcinogenic metals on gene expression. *Toxicology Letters*, 127(1-3), 63–68.

Bhagat, J., Nishimura, N., Shimada, Y. 2020. Toxicological interactions of microplastics/nanoplastics and environmental contaminants: Current Knowledge and Future Perspectives. *Journal of Hazardous Materials*, 123913.

Bouillon, S. 2011. Storage beneath mangroves. *Nature Geoscience*, 4(5), 282–283.

Bouwmeester, H., Hollman, P.C.H., Peters, R.J.B. 2015. Potential Health Impact of Environmentally Released Micro- and Nanoplastics in the Human Food Production Chain: Experiences from Nanotoxicology. *Environmental Science & Technology*, 49(15), 8932–8947.

Bradac, P., Wagner, B., Kistler, D., Traber, J., Behra, R., Sigg, L. 2010. Cadmium speciation and accumulation in periphyton in a small stream with dynamic concentration variations. *Environmental Pollution*, 158(3), 641–648.

Brandts, I., Teles, M., Gonçalves, A.P., Barreto, A., Franco-Martinez, L., Tvarijonaviciute, A., Martins, M.A., Soares, A.M.V.M., Tort, L., Oliveira, M. 2018. Effects of nanoplastics on *Mytilus galloprovincialis* after individual and combined exposure with carbamazepine. *Science of The Total Environment*, 643, 775–784.

Brennecke, D., Duarte, B., Paiva, F., Cacador, I., Canning-Clode, J. 2016. Microplastics as vector for heavy metal contamination from the marine environment. *Estuarine Coastal and Shelf Science*, 178, 189–195.

Briand, N. 2014. Familles de plastiques et leurs usages. Septième continent. *MobiScience, Briand.*

Browne, M.A., Galloway, T.S., Thompson, R.C. 2010. Spatial Patterns of Plastic Debris along Estuarine Shorelines. *Environmental Science & Technology*, 44(9), 3404–3409.

Cai, L., Hu, L., Shi, H., Ye, J., Zhang, Y., Kim, H. 2018. Effects of inorganic ions and natural organic matter on the aggregation of nanoplastics. *Chemosphere*, 197, 142–151.

Cai, M., He, H., Liu, M., Li, S., Tang, G., Wang, W., Huang, P., Wei, G., Lin, Y., Chen, B., Hu, j., Cen, Z. 2018. Lost but can't be neglected: Huge quantities of small microplastics hide in the South China Sea. *Science of The Total Environment*, 633, 1206–1216.

Cajaraville, M.P., Bebianno, M.J., Blasco, J., Porte, C., Sarasquete, C., Viarengo, A. 2000. The use of biomarkers to asses the impact of pollution in coastal environment of the Iberian Peninsula: a practical approach. *The Science of the Total Environment*, 247, 295−311.

Canesi, L., Ciacci, C., Fabbri, R., Balbi, T., Salis, A., Damonte, G., Cortese, K., Caratto, V., Monopoli, M.P., Dawson, K., Bergami, E., Corsi, I. 2016. Interactions of cationic polystyrene nanoparticles with marine bivalve hemocytes in a physiological environment: Role of soluble hemolymph proteins. *Environmental Research*, 150, 73–81.

Cao, R., Wang, D., Wei, Q., Wang, Q., Yang, D., Liu, H., Dong, Z., Zhang, X., Zhang, Q., Zhao, J. 2018. Integrative Biomarker Assessment of the Influence of Saxitoxin on Marine Bivalves:

A Comparative Study of the Two Bivalve Species Oysters, *Crassostrea gigas*, and Scallops, *Chlamys farreri. Frontiers in Physiology*, 9.

Carpenter, E.J., Smith, K.L. 1972. Plastics on the Sargasso Sea surface. *Science* , 155, 1240−1241.

Carugati, L., Gatto, B., Rastelli, E., Lo Martire, M., Coral, C., Greco, S., Danovaro, R. 2018. Impact of mangrove forests degradation on biodiversity and ecosystem functioning. *Scientific Reports*, 8(1).

Cedervall, T., Hansson, L.A., Lard, M., Frohm, B., Linse, S. 2012. Food chain transport of nanoparticles affects behaviour and fat metabolism in fish. *PloS One* 7, 32254.

Chae, Y., An, Y.-J. 2017. Effects of Micro- and Nanoplastics on Aquatic Ecosystems: Current Research Trends and Perspectives. *Marine Pollution Bulletin*, 124, 624−632.

Cherkasov, A.S., Taylor, C., Sokolova, I.M. 2010. Seasonal variation in mitochondrial responses to cadmium and temperature in eastern oysters *Crassostrea virginica* (Gmelin) from different latitudes. *Aquatic Toxicology*, 97(1), 68–78.

Chiba, S., Saito, H., Fletcher, R., Yogi, T., Kayo, M., Miyagi, S., Ogido, M., Fujikura, K. 2018. Human footprint in the abyss: 30 year records of deep-sea plastic debris. *Marine Policy*, 96, 204–212.

Chipuk, J.E., Moldoveanu, T., Llambi, F., Parsons, M.J., Green, D.R. 2010. The BCL-2 Family Reunion. *Molecular Cell*, 37, 299–310.

Choi, K.-S., Lewis, D.H., Powell, E.N., Ray, S.M. 1993. Quantitative measurement of reproductive output in the American oyster, *Crassostrea virginica* (Gmelin), using an enzyme-linked immunosorbent assay (ELISA). *Aquaculture Research*, 24(3), 299–322.

Conner, S.D., Schmid, S.L. 2003. Regulated portals of entry into the cell. *Nature*, 422, 37–44.

Corsi, I., Cherr, G.N., Lenihan, H.S., Labille, J., Hassellov, M., Canesi, L., Dondero, F., Frenzilli, G., Hristozov, D., Puntes, V., Della Torre, C., Pinsino, A., Libralato, G., Marcomini, A., Sabbioni, E., Matranga, V. 2014. Common Strategies and Technologies for the Ecosafety Assessment and Design of Nanomaterials Entering the Marine Environment. *ACS Nano*, 8(10), 9694–9709.

Covernton, G.A., Collicutt, B., Gurney-Smith, H.J., Pearce, C.M., Dower, J.F., Ross, P.S., Dudas, S.E. 2019. Microplastics in bivalves and their habitat in relation to shellfish aquaculture proximity in coastal British Columbia, Canada. *Aquaculture Environment Interactions*,11, 357–374.

Cullen, W.R., Reimer, K.J. 1989. Arsenic speciation in the environment. *Chemical Reviews*, 89, 713–764.

Davranche, M., Veclin, C., Pierson-Wickmann, A.-C., El Hadri, H., Grassl, B., Rowenczyk, L., Dia, A., Ter Halle, A., Blancho, F., Reynaud, S., Gigault, J. 2019. Are nanoplastics able to bind significant amount of metals? The lead example. *Environmental Pollution*, 249, 940–948.

Dawson, A.L., Kawaguchi, S., King, C.K., Townsend, K.A., King, R., Huston, W.M., Bengtson Nash, S.M. 2018. Turning microplastics into nanoplastics through digestive fragmentation by Antarctic krill. *Nature Communications*, 9(1).

Defo, M.A., Bernatchez, L., Campbell, P.G.C., Couture, P. 2018. Temporal variations in kidney metal concentrations and their implications for retinoid metabolism and oxidative stress response in wild yellow perch (*Perca flavescens*). *Aquatic Toxicology*, 202, 26–35.

Doherty, G.J., McMahon, H.T. 2009. Mechanisms of endocytosis. *Annual Review Biochemistry*, 78, 857–902.

Dixon, H.B.F. 1997. The biochemical action of arsonic acids especially as phosphate analogues. *Advanced Inorganic Chemistry*, 44, 191–227.

Dumbauld, B.R., Ruesink, J.L., Rumrill, S.S. 2009. The ecological role of bivalve shellfifish aquaculture in the estuarine environment: a review with application to oyster and clam culture in West Coast (USA) estuaries. *Aquaculture*, 290,196–223.

El Hadri, H., Gigault, J., Maxit, B., Grassl, B., Reynaud, S. 2020a. Nanoplastic from mechanically degraded primary and secondary microplastics for environmental assessments. *NanoImpact*, 17.

El Hadri, H., Gigault, J., Mounicou, S., Grassl, B., Reynaud, S. 2020b. Trace Element Distribution in Marine Microplastics Using Laser Ablation-ICP-MS. *Marine Pollution Bulletin*, 160, 111716.

El Haj, Y., Bohn, S., Souza, M.M. 2019. Tolerance of native and invasive bivalves under herbicide and metal contamination: an ex vivo approach. *Environmental Science and Pollution Research*, 26, 31198–31206.

Farrell, A.P., Brauner, C.J., Wood, C.M. 2011. Fish Physiology: Homeostasis and Toxicology of Essential Metals. *Elsevier Science*, 31 part B, 300–301.

Feng, L.J., Shi, Y., Li, X.Y., Sun, X.D., Xiao, F., Sun, J.W., Wang, Y., Liu, X.Y., Wang, S.G., Yuan, X.Z. 2020. Behavior of tetracycline and polystyrene nanoparticles in estuaries and their joint toxicity on marine microalgae *Skeletonema costatum*. *Environmental Pollution*, 263, 114453.

Fortin, C., Campbell, P.G.C. 2000. Silver uptake by the green alga *Chlamydomonas reinhardtii in* relation to chemical speciation: Influence of chloride. *Environmental Toxicology and Chemistry*, 19(11), 2769–2778.

Francesconi, K.A., Edmonds, J.S. 1996. Arsenic and Marine Organisms. *Advances in Inorganic Chemistry*, 147–189.

Franzellitti, S., Fabbri, E. 2006. Cytoprotective responses in the Mediterranean mussel exposed to Hg2+ and CH3Hg+. *Biochemical and Biophysical Research Communications*, 351(3), 719–725.

Freitas, R., Coppola, F., De Marchi, L., Codella, V., Pretti, C., Chiellini, F., Morelli, A., Polese, G., Soares, A.M.V.M., Figueira, E. 2018. The influence of Arsenic on the toxicity of carbon nanoparticles in bivalves. *Journal of Hazardous Materials*, 358, 484–493.

Frias, J., Sobral, P., Ferreira, A.M. 2010. Organic pollutants in microplastics from two beaches of the Portuguese coast. *Marine Pollution Bulletin*, 60, 1988–1992.

Fronhoffs, S., Totzke, G., Stier, S., Wernert, N., Rothe, M., Brüning, T., Koch, B., Sachinidis, A., Vetter, H., Ko, Y. 2002. A method for the rapid construction of cRNA standard curves in quantitative real-time reverse transcription polymerase chain reaction. *Molecular and Cellular Probes*, 16, 99–110.

Galgani, F., Leaute, J., Moguedet, P., Souplet, A., Verin, Y., Carpentier, A., Goraguer, H., Latrouite, D., Andral, B., Cadiou, Y., Mahe, J.C., Poudlard, J.C., Nerisson, P. 2000. Litter on the Sea Floor Along European Coasts. *Marine Pollution Bulletin, 40(6), 516–527.*

Gall, S.C., Thompson, R.C. 2015. The impact of debris on marine life. *Marine Pollution Bulletin*, 92(1-2), 170–179.

Geißler, D., Gollwitzer, C., Sikora, A., Minelli, C., Krumrey, M., Resch-Genger, U. 2015. Effect of fluorescent staining on size measurements of polymeric nanoparticles using DLS and SAXS. *Analytical Methods*, 7(23), 9785–9790.

Gies, E.A., LeNoble, J.L., Noël, M., Etemadifar, A., Bishay, F., Hall, E.R., Ross, P.S. 2018. Retention of microplastics in a major secondary wastewater treatment plant in Vancouver, Canada. *Marine Pollution Bulletin*, 133, 553−561.

Gigault, J., Balaresque, M., Tabuteau, H. 2018a. Estuary-on-a-chip: unexpected results for nanoparticles fate and transport. *Environmental Science: Nano.*

Gigault, J., Ter Halle, A., Baudrimont, M., Pascal, P.-Y., Gauffre, F., Phi, T.-L., El Hadri, H., Grassl, B., Reynaud, S. 2018b. Current opinion: What is a nanoplastic? *Environmental Pollution*, 235, 1030–1034.

Gonzalez Araya, R., Mingant, C., Petton, B., Robert, R. 2012. Influence of diet assemblage on *Ostrea edulis* broodstock conditioning and subsequent larval development. *Aquaculture*, 364–365, 272–280.

Green, D.S. 2016. Effects of microplastics on European flat oysters, *Ostrea edulis* and their associated benthic communities. *Environmental Pollution*, 216, 95–103.

Guillard, R.R.L. 1975. Culture of phytoplankton for feeding marine invertebrates. *Culture of Marine Invertebrate Animals*, 26–60.

Gutierrez-Galindo, E.A., Flores Muñoz, G., Villaescusa Celaya, J.A., Arreola Chimal, A. 1994. Spatial and temporal variations of arsenic and selenium in a biomonitor (*Modiolus capax*) from the Gulf of California, Mexico. *Marine Pollution Bulletin*, 28(5), 330–333.

Gutierrez-Villagomez, J.M., Martyniuk, C.J., Xing, L., Langlois, V.S., Pauli, B.D., Blais, J., Trudeau, V.L. 2019. Transcriptome Analysis Reveals that Naphthenic Acids Perturb Gene Networks Related to Metabolic Processes, Membrane Integrity, and Gut Function in *Silurana (Xenopus) tropicalis* Embryos. *Frontiers in Marine Science*, 6, 533.

Hancock, R. 2008. Recognising research on molluscs. *Australian Museum*. Archived from the original on 2009-05-03. Retrieved on 2009-03-09.

Handy, R.D., Owen, R., Valsami-Jones, E. 2008. The ecotoxicology of nanoparticles and nanomaterials: current status, knowledge gaps, challenges, and future needs. *Ecotoxicology*, 17(5), 315–325.

Harris, S., Levine, A. 2005. The p53 pathway: positive and negative feedback loops. *Oncogene*, 24, 2899–2908.

Hassan, P.A., Rana, S., Verma, G. 2015. Making sense of Brownian motion: colloid characterization by dynamic light scattering. *Langmuir*, 31, 3–12.

Hellweger, F.L., Lall, U. 2004. Modeling the Effect of Algal Dynamics on Arsenic Speciation in Lake Biwa. *Environmental Science & Technology*, 38(24), 6716–6723.

Helm, M.M., Bourne, N. 2004. Hatchery culture of bivalves. A practical manual. *FAO Fisheries Technical Paper*, 471, 177.

Holmes, L.A., Turner, A., Thompson, R.C. 2012. Adsorption of trace metals to plastic resin pellets in the marine environment. *Environmental Pollution*, 160(1), 42−48.

Holmes, L.A., Turner, A., Thompson, R. 2014. Interactions between trace metals and plastic production pellets under estuarine conditions. *Marine Chemistry*, 167, 25–32.

Hotze, E.M., Phenrat, T., Lowry, G.V. 2010. Nanoparticle Aggregation: Challenges to Understanding Transport and Reactivity in the Environment. *Journal of Environment Quality*, 39(6), 1909.

Hrenovic, J., Ivankovic, T. 2007. Toxicity of anionic and cationic surfactant to *Acinetobacter junii* in pure culture. *Open Life Sciences*, 2(3), 405–414.

Hughes, M. 2002. Arsenic toxicity and potential mechanisms of action. *Toxicology Letters*, 133, 1–16.

Jahan, K., Balzer, S., Mosto, P. 2008. Toxicity Of Nonionic Surfactants. *WIT Press*, 110, 281–290.

Johnson, A., Cronan, D.S. 2001. Hydrothermal Metalliferous Sediments and Waters Off the Lesser Antilles. *Marine Georesources & Geotechnology*, 19(2), 65–83.

Kim, D., Chae, Y., An, Y.J. 2017. Mixture toxicity of nickel and microplastics with different functional groups on *Daphnia magna*. *Environmental Science & Technology*, 51, 12852–12858.

Klinck, J.M., Powell, E.N., Hofmann, E.E., Wilson, E.A., Ray, S.M. 1992. Modeling oyster populations: the effect of density and food supply on production. *Proc. Adv. Mar. Tech. Conf.*, 5, 85–105.

Kobayashi, M., Hofmann, E.E., Powell, E.N., Klinck, J.M., Kusaka, K. 1997. A population dynamics model for the Japanese oyster, *Crassostrea gigas. Aquaculture*, 149(3-4), 285–321.

Koelmans, A.A., Besseling, E., Shim, W.J. 2015. Nanoplastics in the Aquatic Environment. Critical Review. *Marine Anthropogenic Litter*, 325–340.

Kraemer, L.D., Campbell, P.G.C., Hare, L. 2005. Dynamics of Cd, Cu and Zn accumulation in organs and sub-cellular fractions in field transplanted juvenile yellow perch (*Perca flavescens*). *Environmental Pollution*, 138(2), 324–337.

Kulkarni, S.A., Feng, S.S. 2013. Effects of Particle Size and Surface Modification on Cellular Uptake and Biodistribution of Polymeric Nanoparticles for Drug Delivery. *Pharmaceutical Research*, 30(10), 2512–2522.

Kulkarni, R., Deobagkar, D., Zinjarde, S. 2018. Metals in mangrove ecosystems and associated biota: A global perspective. *Ecotoxicology and Environmental Safety*, 153, 215–228.

Lagarde, F., Olivier, O., Zanella, M., Daniel, P., Hiard, S., Caruso, A. 2016. Microplastic interactions with freshwater microalgae : hetero-aggregation and changes in plastic density appear strongly dependent on polymer type. *Environmental Pollution*, 215, 331–339.

Lambert, S., Wagner, M. 2016. Characterisation of nanoplastics during the degradation of polystyrene. *Chemosphere*, 145, 265−268.

Langston, W.J. 1984. Availability of arsenic to estuarine and marine organisms: A field and laboratory evaluation. *Marine Biology*, 80, 143–154.

Law, K.L., Moret-Ferguson, S., Maximenko, N.A., Proskurowski, G., Peacock, E.E., Hafner, J., Reddy, C.M. 2010. Plastic Accumulation in the North Atlantic Subtropical Gyre. *Science*, 329(5996), 1185–1188.

Lebordais, M., Venel, Z., Gigault, J., Langlois, V.S., Baudrimont, M. 2020. Molecular impacts of dietary exposure to nanoplastics combined with arsenic in the Caribbean mangrove oysters (*Isognomon alatus*). *Manuscript submitted for publication*.

Lee, S.Y., Nam, Y.K. 2016. Evaluation of reference genes for RT-qPCR study in abalone Haliotis discus hannai during heavy metal overload stress. *Fisheries and Aquatic Sciences*, 19(1), 21.

Lemer, S. 2019. Assembled and translated transcriptomes. Harvard Dataverse.

Lenz, R., Enders, K., Nielsen, T.G. 2016. Microplastic exposure studies should be environmentally realistic. *Proceedings of the National Academy of Sciences*, 113(29), E4121–E4122.

Livak, K.J., Schmittgen, T.D. 2001. Analysis of relative gene expression data using real-time quantitative PCR and the $2^{-\Delta\Delta CT}$ method. *Methods*, 25, 402–408.

Lucas, A., Beninger, P.G. 1985. The use of physiological condition indices in marine bivalve aquaculture. *Aquaculture*, 44(3), 187–200.

Luo, L., Ke, C., Guo, X., Shi, B., Huang, M. 2014. Metal accumulation and differentially expressed proteins in gill of oyster (*Crassostrea hongkongensis*) exposed to long-term heavy metal-contaminated estuary. *Fish & Shellfish Immunology*, 38(2), 318–329.

Lusher, A.L., McHugh, M., Thompson, R.C. 2013. Occurrence of microplastics in the gastrointestinal tract of pelagic and demersal fish from the English Channel. *Marine Pollution Bulletin*, 67(1-2), 94–99.

Lusher, A.L., Tirelli, V., O'Connor, I., Officer, R. 2015. Microplastics in Arctic polar waters: the first reported values of particles in surface and sub-surface samples. *Scientific Reports*, 5, 14947.

Lusher, A.L., Welden, N.A., Sobral, P., Cole, M. 2017. Sampling, isolating and identifying microplastics ingested by fish and invertebrates. *Analytical Methods*, *9*(9), 1346-1360.

Magrí, D., Sánchez-Moreno, P., Caputo, G., Gatto, F., Veronesi, M., Bardi, G., Catelani, T., Guarnieri, D., Athanassiou, A., Pompa, P.P., Fragouli, D. 2018. Laser Ablation as a Versatile Tool To Mimic Polyethylene Terephthalate Nanoplastic Pollutants: Characterization and Toxicology Assessment. *ACS Nano.*

Maher, W., Waring, J., Krikowa, F., Duncan, E., Foster, S. 2018. Ecological factors affecting the accumulation and speciation of arsenic in twelve Australian coastal bivalve molluscs. *Environmental Chemistry*, 15(2), 46.

Malet, N., Sauriau, P.G., Ryckaert, M., Malestroit, P., Guillou, G. 2008. Dynamics and sources of suspended particulate organic matter in the Marennes-Oléron oyster farming bay: insights from stable isotopes and microalgae ecology. *Estuarine Coastal and Shelf Science*, 78, 576–586.

Manfra, L., Rotini, A., Bergami, E., Grassi, G., Faleri, C., Corsi, I. 2017. Comparative ecotoxicity of polystyrene nanoparticles in natural seawater and reconstituted seawater using the rotifer *Brachionus plicatilis*. *Ecotoxicology and Environmental Safety*, 145, 557–563.

Mao, Y., Li, H., Huangfu, X., Liu, Y., He, Q. 2020. Nanoplastics display strong stability in aqueous environments: Insights from aggregation behaviour and theoretical calculations. *Environmental Pollution*, 258, 113760.

Marie, V., Gonzalez, P., Baudrimont, M., Boutet, I., Moraga, D., Bourdineaud, J.P., Boudou, A. 2006. Metallothionein gene expression and protein levels in triploid and diploid oysters *Crassostrea gigas* after exposure to cadmium and zinc. *Environmental Toxicology and Chemistry*, 25, 412–418.

Mattsson, K., Hansson, L.A., Cedervall, T. 2015. Nano-Plastics in the Aquatic Environment. *Environmental Science : Processes & Impacts*, 17, 1712−1721.

McCarthy, M.P., Carroll, D.L., Ringwood, A.H. 2013. Tissue specific responses of oysters, *Crassostrea virginica*, to silver nanoparticles. *Aquatic Toxicology*, 138-139, 123–128.

Minier, C., Borghi, V., Moore, M.N., Porte, C. 2000. Seasonal variation of MXR and stress proteins in the common mussel, *Mytilus galloprovincialis*. *Aquatic Toxicology*, 50, 167–176.

Ministère de la Santé et du Mieux-être du Nouveau Brunswick, février 2005. Evaluation des risques à la santé humaine. Annexe A - Etude sur la santé dans la région de Belledune.

Mitra, A. 2013. Sensitivity of mangrove ecosystem to changing climate. *India: Springer*, 62, 43–157.

Molin, M., Ulven, S.M., Meltzer, H.M., Alexander, J. 2015. Arsenic in the human food chain, biotransformation and toxicology – Review focusing on seafood arsenic. *Journal of Trace Elements in Medicine and Biology*, 31, 249–259.

Moreira, A., Freitas, R., Figueira, E., Volpi Ghirardini, A., Soares, A.M.V.M., Radaelli, M., Guida, M., Libralato, G. 2018. Combined effects of arsenic, salinity and temperature on *Crassostrea gigas* embryotoxicity. *Ecotoxicology and Environmental Safety*, 147, 251–259.

Motulsky, H.J., Brown, R.E. 2006. *BMC Bioinformatics*, 7(1), 123.

Nalder, T.D., Miller, M.R., Packer, M.A. 2015. Changes in lipid class content and composition of *Isochrysis sp.* (T-Iso) grown in batch culture. *Aquaculture International*, 23(5), 1293–1312.

Neff, J.M. 1997. Ecotoxicology of arsenic in the marine environment. *Environmental Toxicology and Chemistry*, 16(5), 917–927.

Nel, A., Xia, T., Madler, L., Li, N. 2006. Toxic Potential of Materials at the Nanolevel. *Science* , 311, 622−627.

Ng, J.C. 2005. Environmental Contamination of Arsenic and its Toxicological Impact on Humans. *Environmental Chemistry*, 2(3), 146.

O'Brine, T., Thompson, R.C. 2010. Degradation of plastic carrier bags in the marine environment. *Marine Pollution Bulletin*, 60, 2279–2283.

Oliveira, P., Barboza, L.G.A., Branco, V., Figueiredo, N., Carvalho, C., Guilhermino, L. 2018. Effects of microplastics and mercury in the freshwater bivalve *Corbicula fluminea* (Müller, 1774): Filtration rate, biochemical biomarkers and mercury bioconcentration. *Ecotoxicology and Environmental Safety*, 164, 155–163.

Ozbay, G., Reckenbeil, B., Marenghi, F., Erbland, P. 2014. Eastern oyster (*Crassostrea virginica*) aquaculture and diversity of associated species.*Oysters: Biology, Consumption, and Ecological Importance.* NOVA Publishing. Book, 128.

Pan, K., Wang, W.-X. 2012. Reconstructing the Biokinetic Processes of Oysters to Counteract the Metal Challenges: Physiological Acclimation. *Environmental Science & Technology*, 46(19), 10765–10771.

Paquin, P.R., Gorsuch, J.W., Apte, S., Batley, G.E., Bowles, K.C., Campbell, P.G.C., Delos, C.G., Di Toro, D.M., Dwyer, R.L., Galvez, F., Gensemer, R.W., Goss, G.G., Hogstrand, C., Janssen, C.R., McGeer, J.C., Naddy, R.B., Playle, R.C., Santore, R.C., Stubblefield, W.A., Wood, C.M., Wu, K. B. 2002. The biotic ligand model: a historical overview*. Comparative Biochemistry and Physiology Part C: Toxicology & Pharmacology*, 133(1-2), 3–35.

Parsons, M.B., Cranston, R.E. 2005. Distribution, transport, and sources of metals in marine sediments near a coastal lead smelter in northern New Brunswick. Metals in the Environment Around Smelters at Rouyn-Noranda, Québec, and Belledune, New Brunswick: Results and Conclusions of the GSC-MITE Point Sources Project*. Bulletin*, 584.

Penrose, W.R. 1974. Arsenic in the marine and aquatic environments: Analysis, occurrence and significance. *CRC Critical Reviews in Environmental Control*, 4, 465–482.

Perrier, F. 2017. Nano contamination d'organismes aquatiques par des particules inorganiques: transfert trophique et impacts toxiques (thèse de doctorat, Université de Bordeaux, France).

Pessoni, L., Veclin, C., El Hadri, H., Cugnet, C., Davranche, M., Pierson-Wickmann, A.C., Gigault, J., Grassl, B., Reynaud, S. 2019. Soap- and metal-free polystyrene latex particles as a nanoplastic model. *Environmental Science: Nano*, 6, 2253–2258.

Petrick, J.S., Jagadish, B., Mash, E.A., and Aposhian, H.V. 2001. Monomethylarsonous acid (MMAIII) and arsenite: LD50 in hamsters and in vitro inhibition of pyruvate dehydrogenase. *Chemical Research in Toxicology*, 14, 651–656.

Pikuda, O., Xu, E.G., Berk, D., Tufenkji, N. 2018. Toxicity Assessments of Micro- and Nanoplastics Can Be Confounded by Preservatives in Commercial Formulations. *Environmental Science & Technology Letters*, 6(1), 21–25.

Qiao, R., Lu, K., Deng, Y., Ren, H., Zhang, Y. 2019. Combined effects of polystyrene microplastics and natural organic matter on the accumulation and toxicity of copper in zebrafish. *Science of the Total Environment*, 682, 128–137.

Quik, J.T.K., Vonk, J.A., Hansen, S.F., Baun, A., Van De Meent, D. 2011. How to assess exposure of aquatic organisms to manufactured nanoparticles? *Environment International*, 37(6), 1068–1077.

Richardson, S.D., Kimura, S.Y. 2020. Water Analysis: Emerging Contaminants and Current Issues. *Analytical Chemistry*, 92(1), 473–505.

Rochman, C.M., Hoh, E., Hentschel, B.T., Kaye, S. 2013. Long-term field measurement of sorption of organic contaminants to five types of plastic pellets: implications for plastic marine debris. *Environmental Science & Technology*, 47(3), 1646–54.

Rochman, C.M., Hentschel, B.T., Teh, S.J. 2014. Long-term sorption of metals is similar among plastic types: Implications for plastic debris in aquatic environments. *PloS One*, 9, 85433.

Rosety, M., Ordóñez, F.J., Rosety Rodríguez, M., Rosety, J.M., Rosety, I., Carrasco, C., Ribelles, A. 2001. Acute toxicity of anionic surfactants sodium dodecyl sulphate (SDS) and linear alkylbenzene sulphonate (LAS) on the fertilizing capability of gilthead (*Sparus aurata L.*) sperm. *Histology and Histopathology*, 16(3), 839–843.

Rossi, G., Barnoud, J., Monticelli, L. 2013. Polystyrene Nanoparticles Perturb Lipid Membranes. *Physical Chemistry Letters*, 5(1), 241–246.

Ruiz, P., Katsumiti, A., Nieto, J.A., Bori, J., Jimeno-Romero, A., Reip, P., Arostegui, I., Orbea, A., Cajaraville, M.P. 2015. Short-term effects on antioxidant enzymes and long-term genotoxic and carcinogenic potential of CuO nanoparticles compared to bulk CuO and ionic copper in mussels *Mytilus galloprovincialis. Marine Environmental Research*, 111, 107–120.

Sadri, S.S., Thompson, R.C. 2014. On the quantity and composition of floating plastic debris entering and leaving the Tamar Estuary, Southwest England. *Marine Pollution Bulletin*, 81(1), 55–60.

Saed, K., Ismail, A., Omar, H., Kusnan, M. 2004. Heavy metal depuration in flat tree oysters *Isognomon alatus* under field and laboratory conditions. *Toxicological and Environmental Chemistry*, 86, 171–179.

Salvador, J.M., Brown-Clay, J.D., Fornace, A.J. 2013. Gadd45 in Stress Signaling, Cell Cycle Control, and Apoptosis. *Experimental Medicine and Biology*, 793, 1–19.

Santana, M.F.M., Moreira, F.T., Pereira, C.D.S., Abessa, D.M.S., Turra, A. 2018. Continuous Exposure to Microplastics Does Not Cause Physiological Effects in the Cultivated Mussel *Perna perna*. *Archives of Environmental Contamination and Toxicology*, 74, 594–604.

Schirinzi, G.F., Pérez-Pomeda, I., Sanchís, J., Rossini, C., Farré, M., Barceló, D. 2017. Cytotoxic effects of commonly used nanomaterials and microplastics on cerebral and epithelial human cells. *Environmental Research*, 159, 579–587.

Schuler, M., Bossy-Wetzel, E., Goldstein, J.C., Fitzgerald, P., Green, D. R. 2000. p53 Induces Apoptosis by Caspase Activation through Mitochondrial Cytochrome c Release. *Journal of Biological Chemistry*, 275(10), 7337–7342.

Shi, W., Han, Y., Sun, S., Tang, Y., Zhou, W., Du, X., Liu, G. 2020. Immunotoxicities of microplastics and sertraline, alone and in combination, to a bivalve species: size-dependent interaction and potential toxication mechanism. *Journal of Hazardous Materials*, 396, 122603.

Singh, N., Manshian, B., Jenkins, G.J.S., Griffiths, S.M., Williams, P.M., Maffeis, T.G.G., Wright, C.J., Doak, S.H. 2009. Nanogenotoxicology: The DNA damaging potential of engineered nanomaterials. *Biomaterials,* 30, 3891–3914.

Sirover, M.A. 2011. On the functional diversity of glyceraldehyde-3-phosphate dehydrogenase: Biochemical mechanisms and regulatory control. *Biochimica et Biophysica Acta - General Subjects*, 1810(8), 741–751.

Siung, M. 1980. Studies on the biology of *Isognomon alatus* Gmelin (Bivalvia : Isognomonidae) with notes on its potential as a commercial species. *Bulletin of Marine Sciences*, 30(1), 90–101.

Soegianto, A., Winarni, D., Handayani, U.S., Hartati. 2013. Bioaccumulation, Elimination, and Toxic Effect of Cadmium on Structure of Gills and Hepatopancreas of Freshwater Prawn *Macrobrachium sintangese* (De Man, 1898). *Water, Air, & Soil Pollution*, 224(5).

Sokolova, I.M., Sokolov, E.P., Ponnappa, K.M. 2005. Cadmium exposure affects mitochondrial bioenergetics and gene expression of key mitochondrial proteins in the eastern oyste*r Crassostrea virginica* Gmelin (Bivalvia: Ostreidae). *Aquatic Toxicology*, 73(3), 242–255.

Smith, D., Gaspar, T.R., Levi-Polyachenko, N., Kuthirummal, N., Sakar, S., Ringwood, A.H. 2020. The Bioreactivity and Sunlight Potentiation of Hybrid Polymer Nanoparticles in Oysters, *Crassostrea virginica. Environmental Science & Technology*, 54, 16, 10031–10038.

Spehar, R.L., Fiandt, J.T., Anderson, R.L., DeFoe, D.L. 1980. Comparative toxicity of arsenic compounds and their accumulation in invertebrates and fish. *Archives of Environmental Contamination and Toxicology*, 9(1), 53–63.

Spurgeon, D.J., Lahive, E., Schultz, C.L. 2020. Nanomaterial transformations in the environment: effects of changing exposure forms on bioaccumulation and toxicity. *Small*, 2000618.

Strady, E., Schäfer, J., Baudrimont, M., Blanc G. 2011. Tracing cadmium contamination kinetics and pathways in oysters (*Crassostrea gigas*) by multiple stable Cd isotope spike experiments. *Ecotoxicology and Environmental Safety*, 74(4), 600–606.

Suhrhoff, T.J., Scholz-Bottcher, B.M. 2016. Qualitative impact of salinity, UV radiation and turbulence on leaching of organic plastic additives from four common plastics - A lab experiment. *Marine Pollution Bulletin*, 102 (1), 84−94.

Sussarellu, R., Suquet, M., Thomas, Y., Lambert, C., Fabioux, C., Pernet, M.E.J., Le Goïc, N., Quillien, V., Mingant, C., Epelboin, Y., Corporeau, C., Guyomarch, J., Robbens, J., Paul-Pont, I., Soudan, P., Huvet, A. 2016. Oyster reproduction is affected by exposure to polystyrene microplastics. *Proceedings of the National Academy of Sciences*, 113(9), 2430–2435.

Tallec, K., Paul-Pont, I., Boulais, M., Le Goïc, N., González-Fernández, C., Le Grand, F., Bideau, A., Quéré, C., Cassone, A.L., Lambert, C., Soudant, P., Huvet, A. 2020. Nanopolystyrene beads affect motility and reproductive success of oyster spermatozoa *(Crassostrea gigas). Nanotoxicology*, 1–19.

Tang, Y., Rong, J., Guan, X., Zha, S., Shi, W., Han, Y., Du, X., Wu, F., Huang, W., Liu, G. 2019. Immunotoxicity of microplastics and two persistent organic pollutants alone or in combination to a bivalve species. *Environmental Pollution*, 258, 113845.

Tedesco, S., Doyle, H., Blasco, J., Redmond, G., Sheehan, D. 2010. Oxidative stress and toxicity of gold nanoparticles in *Mytilus edulis*. *Aquatic Toxicology*, 100, 178–186.

Ter Halle, A., Jeanneau, L., Martignac, M., Jardé, E., Pedrono, B., Brach, L., Gigault, J. 2017. Nanoplastics in the North Atlantic Subtropical Gyre. *Environmental Science & Technology*, 5, 51(23), 13689–13697.

Thiagarajan, V., Iswarya, V., Seenivasan, R., Chandrasekaran, N., Mukherjee, A. 2019. Influence of differently functionalized polystyrene microplastics on the toxic effects of P25 TiO2 NPs towards marine algae *Chlorella sp*. *Aquatic Toxicology*, 207, 208–216.

Tien, C., Chen, C.S. 2013. Patterns of metal accumulation by natural river biofilms during their growth and seasonal succession. *Archives of Environmental Contamination and Toxicology*, 64, 605–616.

Tran, D., Ciret, P., Ciutat, A., Durrieu, G., Massabuau, J.C. 2003. Estimation of potential and limits of bivalve closure response to detect contaminants: Application to cadmium. *Environmental Toxicology and Chemistry*, 22(4), 914–920.

Tremblay, G.-H., Gobeil, C. 1990. Dissolved arsenic in the St Lawrence Estuary and the Saguenay Fjord, Canada. *Marine Pollution Bulletin*, 21(10), 465–469.

Trevisan, R., Voy, C., Chen, S., Di Giulio, R.T. 2019. Nanoplastics decrease the toxicity of a complex PAH mixture but impair mitochondrial energy production in developing zebrafish. *Environmental Science & Technology*, 53, 8405–8415.

Tristan, C., Shahani, N., Sedlak, T.W., Sawa, A. 2011. The diverse functions of GAPDH: Views from different subcellular compartments. *Cellular Signalling*, 23(2), 317–323.

UNEP. 2001. Marine litter - trash that kills, *United Nations Environment Programme*.

Ünlü, M.Y., Fowler, S.W. 1979. Factors affecting the flux of arsenic through the mussel *Mytilus galloprovincialis*. *Marine Biology*, 51, 209–219.

US Environmental Protection Agency. 2001. Chemical speciation of arsenic in water and tissue by hydride generation quartz furnace atomic absorption spectrometry. *US EPA, Method 1632, Revision A, Office of Water, Washington, DC*. EPA-821-R-01-006.

Vicient, C.M., Delseny, M. 1999. Isolation of Total RNA from *Arabidopsis thaliana* Seeds. *Analytical Biochemistry*, 268(2), 412–413.

Wallner-Kersanach, M., Theede, H., Eversberg, U., Lobo, S. 2000. Accumulation and Elimination of Trace Metals in a Transplantation Experiment with *Crassostrea rhizophorae*. *Archives of Environmental Contamination and Toxicology*, 38(1), 40–45.

Wang, S., Liu, M., Wang, J., Huang, J., Wang, J. 2020. Polystyrene nanoplastics cause growth inhibition, morphological damage and physiological disturbance in the marine microalga *Platymonas helgolandica. Marine Pollution Bulletin*, 158, 111403.

Ward, J.E., Shumway, S.E. 2004. Separating the grain from the chaff: particle selection in suspension- and deposit-feeding bivalves. *Journal of Experimental Marine Biology and Ecology*, 300(1-2), 83–130.

Ward, J.E., Kach, D.J. 2009. Marine aggregates facilitate ingestion of nanoparticles by suspension-feeding bivalves. *Marine Environmental Research*, 68(3), 0–142.

Ward, J.E., Zhao, S., Holohan, B., Mladinich, K.M., Griffin, T.W., Wozniak, J., Shumway, S.E. 2019. Selective ingestion and egestion of plastic particles by the blue mussel (*Mytilus edulis*) and eastern oyster (*Crassostrea virginica*): implications for using bivalves as bioindicators of microplastic pollution. *Environmental Science & Technology*, 53, 15, 8776–8784.

Wegner, A., Besseling, E., Foekema, E.M., Kamermans, P., Koelmans, A.A. 2012. Effects of nanopolystyrene on the feeding behavior of the blue mussel (*Mytilus edulis L.*). *Environmental Toxicology and Chemistry*, 31(11), 2490–2497.

Wen, B., Jin, S.-R., Chen, Z.-Z., Gao, J.-Z., Liu, Y.-N., Liu, J.-H., Feng, X.-S. 2018. Single and combined effects of microplastics and cadmium on the cadmium accumulation, antioxidant defence and innate immunity of the discus fish (*Symphysodon aequifasciatus*). *Environmental Pollution*, 243(A), 462–471.

Wilson, E.A., Powell, E.N., Wade, T.L., Taylor, R.J., Presley, B.J., Brooks, J.M. 1992. Spatial and temporal distributions of contaminant body burden and disease in Gulf of Mexico oyster populations: The role of local and large-scale climatic controls. *Helgoländer Merresunters.* 46:201–235.

Winnebeck, E.C., Millar, C.D., Warman, G.R. 2010. Why Does Insect RNA Look Degraded? *Journal of Insect Science*, 10(159), 1–7.

Wolle, M.M., Conklin, S.D. 2018. Speciation analysis of arsenic in seafood and seaweed: Part II—single laboratory validation of method. *Analytical and Bioanalytical Chemistry*, 410(22), 5689–5702.

Won, E.-J., Kim, K.-T., Choi, J.-Y., Kim, E.-S., Ra, K. 2016. Target organs of the Manila clam *Ruditapes philippinarum* for studying metal accumulation and biomarkers in pollution monitoring: laboratory and in-situ transplantation experiments. *Environmental Monitoring and Assessment*, 188(8).

Wood, J.M. 1974. Biological cycles for toxic elements in the environment. *Science*, *183*(4129), 1049–1052.

Wright, S.L., Kelly, F.J. 2017. Plastic and Human Health: A Micro Issue? *Environmental Science & Technology*, 51, 6634–6647.

Xia, B., Zhang, J., Zhao, X., Feng, J., Teng, Y., Chen, B., Sun, X., Zhu, L., Sun, X., Qu, K. 2020. Polystyrene microplastics increase uptake, elimination and cytotoxicity of decabromodiphenyl ether (BDE-209) in the marine scallop Chlamys farreri. *Environmental Pollution*, 258, 113657.

Yanan, D. 2012. Integrated biomarker and molecular responses in marine bivalve following exposure to environmental contaminants: Implications for human and environmental health. Thesis of Plymouth University, United Kingdom.

Yang, H.C., Fu, H.L., Lin, Y.F., Rosen, B.P. 2012. Pathways of Arsenic Uptake and Efflux. *Current Topics in Membranes,* 69, 325–358.

Yap, C.K., Azmizan, A.R., Hanif, M.S. 2011. Biomonitoring of Trace Metals (Fe, Cu, and Ni) in the Mangrove Area of Peninsular Malaysia Using Different Soft Tissues of Flat Tree Oyster *Isognomon alatus. Water Air Soil Pollution*, 218, 19–36.

Zhang, W., Wang, W.-X., Zhang, L. 2013. Arsenic speciation and spatial and interspecies differences of metal concentrations in mollusks and crustaceans from a South China estuary. *Ecotoxicology*, 22(4), 671–682.

Zhang, W., Guo, Z., Zhou, Y., Liu, H., Zhang, L. 2015. Biotransformation and detoxification of inorganic arsenic in Bombay oyster *Saccostrea cucullata*. *Aquatic Toxicology*, 158, 33–40.

Zhang, Q., Qu, Q., Lu, T., Ke, M., Zhu, Y., Zhang, M., Zhang, Z., Du, B., Pan, X., Sun, L., Qian, H. 2018. The combined toxicity effect of nanoplastics and glyphosate on *Microcystis aeruginosa* growth. *Environmental Pollution*, 243, 1106–1112.

Zhu, J., Zhang, Q., Li, Y., Tan, S., Kang, Z., Yu, X., Lan, W., Cai, L., Wang, J., Shi, H. 2018. Microplastic pollution in the Maowei Sea, a typical mariculture bay of China. *Science of The Total Environment*, 658, 62–68.

Zook, J.M., Rastogi, V., MacCuspie, R.I., Keene, A.M., Fagan, J. 2011. Measuring Agglomerate Size Distribution and Dependence of Localized Surface Plasmon Resonance Absorbance on Gold Nanoparticle Agglomerate Size Using Analytical Ultracentrifugation. *ACS Nano*, 5(10), 8070–8079.

6 ANNEXE I

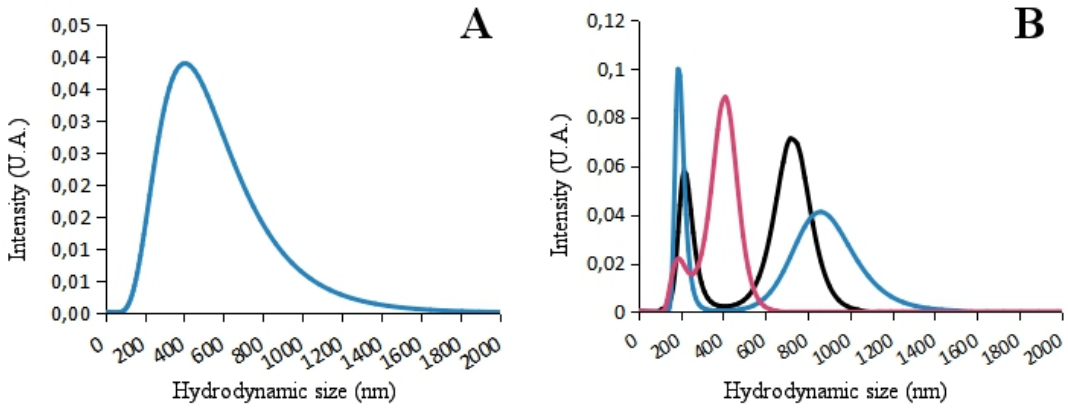

Figure S1 : Size distribution of NPG nanoparticles measured by DLS on a Vasco Flex (using Sparse Bayesian Learning algorithm) showing the hydrodynamic size for overall nanoparticles in the dispersion (A), and the size distribution for each NPG batch presented with a different colour (B).

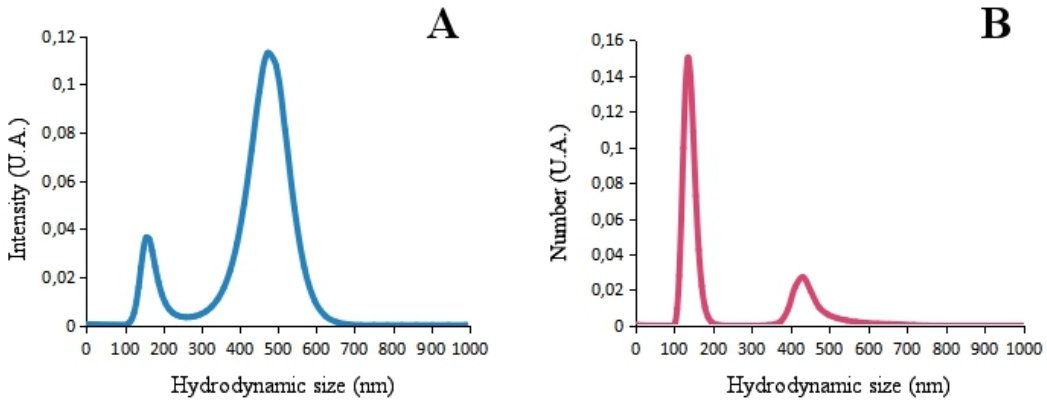

Figure S2 : Size distribution of PSC nanoparticles measured by DLS on a Vasco Flex (using Sparse Bayesian Learning algorithm) showing the hydrodynamic size for overall nanoparticles in the dispersion (A), and the size distribution (B).

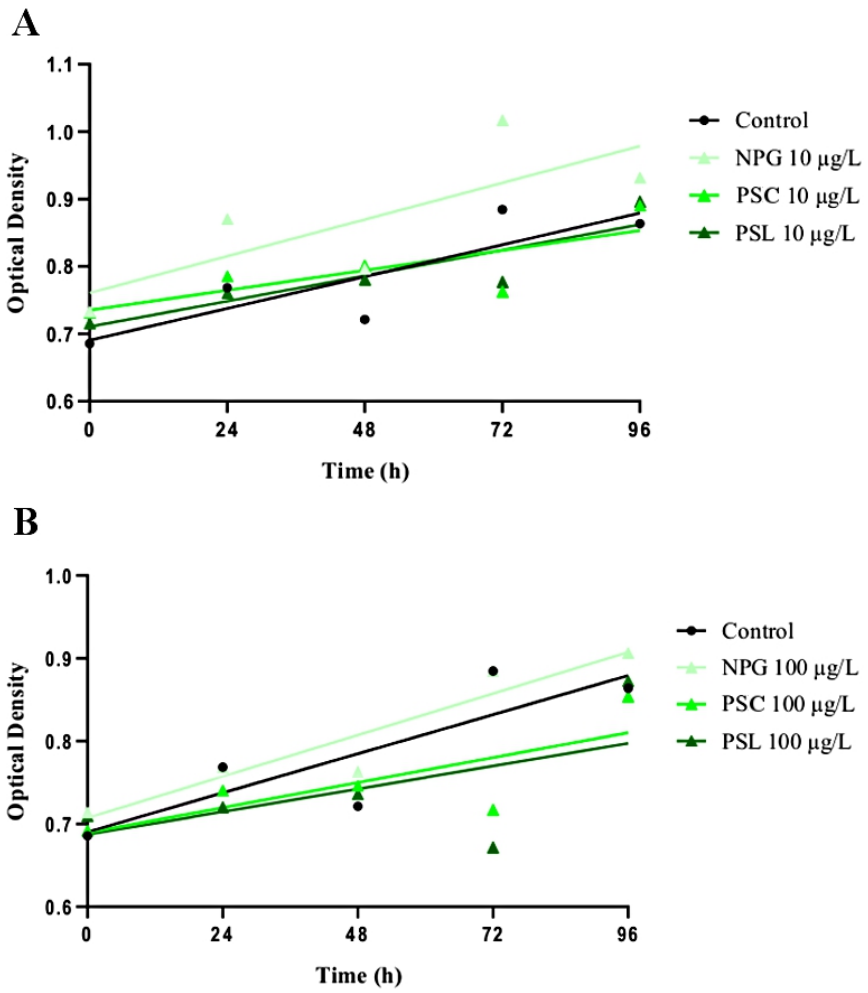

Figure S3 : *T. lutea* growth cultured in F/2 medium for 96 h. Linear regressions with mean points (n = 5) are represented for 10 µg L^{-1} NP treatments (A) and 100 µg L^{-1} NP treatments (B). Regression coefficients (A) are control = 0.74, NPG = 0.60, PSC = 0.61, PSL = 0.80. Regression coefficients (B) are control = 0.74, NPG = 0.90, PSC = 0.59, PSL = 0.33.

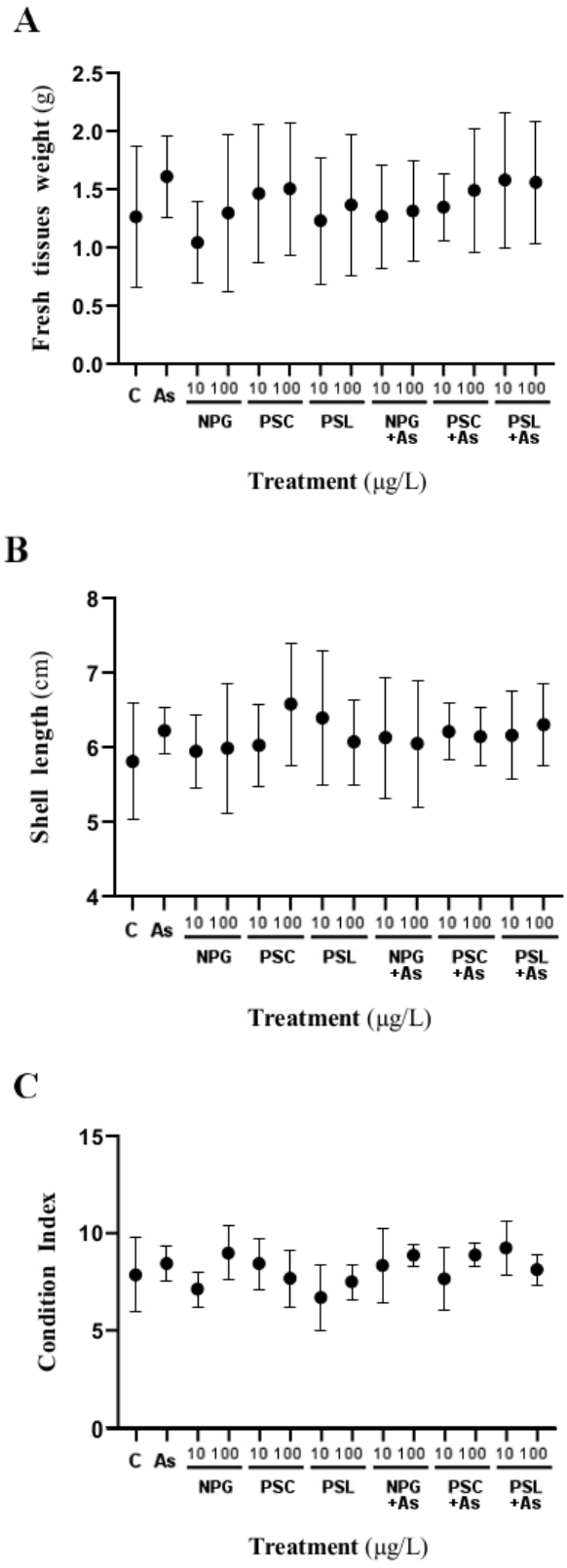

Figure S4 : Comparisons of *I. alatus* biometric parameters after one week exposure (n = 4). Fresh tissues weight in g (A), shell length in cm (B), and Condition Index (C).

Table S1. Primers used for quantifying gene expression by qPCR.

Genes of interest	Full gene names Forward (F) Reverse (R) primers	Associated cell functions
*β-actine**	Actin beta F : AACGAGCGATTCAGATGTCC R : CGATTCCTGGGTACATGGTT	Microfilaments
*rpl7**	Ribosomal protein L7 F : CCCAGGAAGGTCATGCAGTT R : TCCCAGAGCCTTCTCGATGA	Ribosomal sub-unit
cav	Caveolin F : CGTCGAGATCCAGACCTGTT R : ACAGCATTGACTGCGTATGG	Endocytosis and vesicle transport
cltc	Clathrin heavy chain F : AGACTCAGGACCCAGAGGAC R : ATCACACGGGTTCTATCGGC	
bax	bcl2 associated X apoptosis regulator F : AACTGGGGCAGAGTTGGATG R : AATTGCTTCCCAGCCTCCTC	Cell cycle regulation
gadd45	Growth arrest DNA damage F : TTGGCTTGACAAAAGTGCCG R : CTGACAACCTGCATCTCGGT	
p53	Tumor protein p53 F : CGATGATCGGGTTCAGCAGA R : GAGCTCTCTCAACACAGCCA	
cat	Catalase F : CGAGGCTAGCCCAGACAAAA R : TTGGGGAAATAGTTGGGGGC	
gapdh	Glyceraldehyde-3-phosphate dehydrogenase F : CACGGCAACACAGAAGGTTG	

	R : CCCTTCTGAAGTCGGCAAGT	Oxidative stress
sod1	Superoxide dismutase Cu/Zn F : AGACTGCGTCACATGCTTCA R : GCGTCATGTAGGGGATCTGG	
cox1	Mitochondrial encoded cytochrome c oxidase 1 F : GTTGCCTTGGTCGCTAGACT R : GAGCGTCTTGGGCTTAGTCA	Mitochondrial metabolism
12S	Mitochondrial encoded 12S rRNA F : TCAGGTGTTACACAGCCGTC R : GCAGGCGTTTTAATCCCGTC	
mdr	ATP Binding Cassette Subfamily F : GCATGTTGCAAGCCTGTCAA R : CAGTCAACTCAAGCAACCGC	Detoxification

* : reference genes

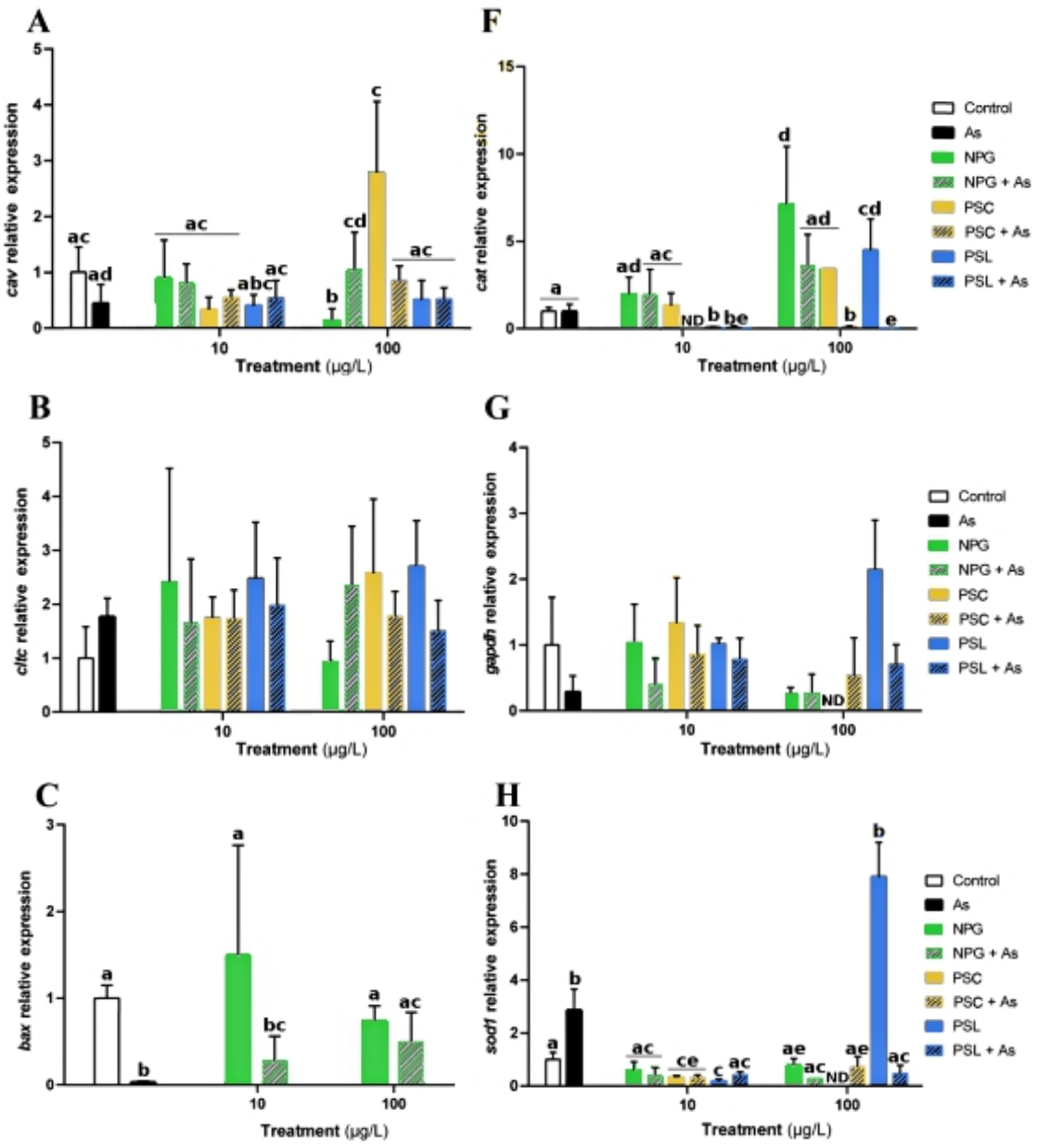
A
cav relative expression
Treatment (µg/L)
B
cftc relative expression
Treatment (µg/L)
C
bax relative expression
Treatment (µg/L)
F
cat relative expression
Treatment (µg/L)
G
gapdh relative expression
Treatment (µg/L)
H
sodf relative expression
Treatment (µg/L)
Control
As
NPG
NPG + As
PSC
PSC + As
PSL
PSL + As

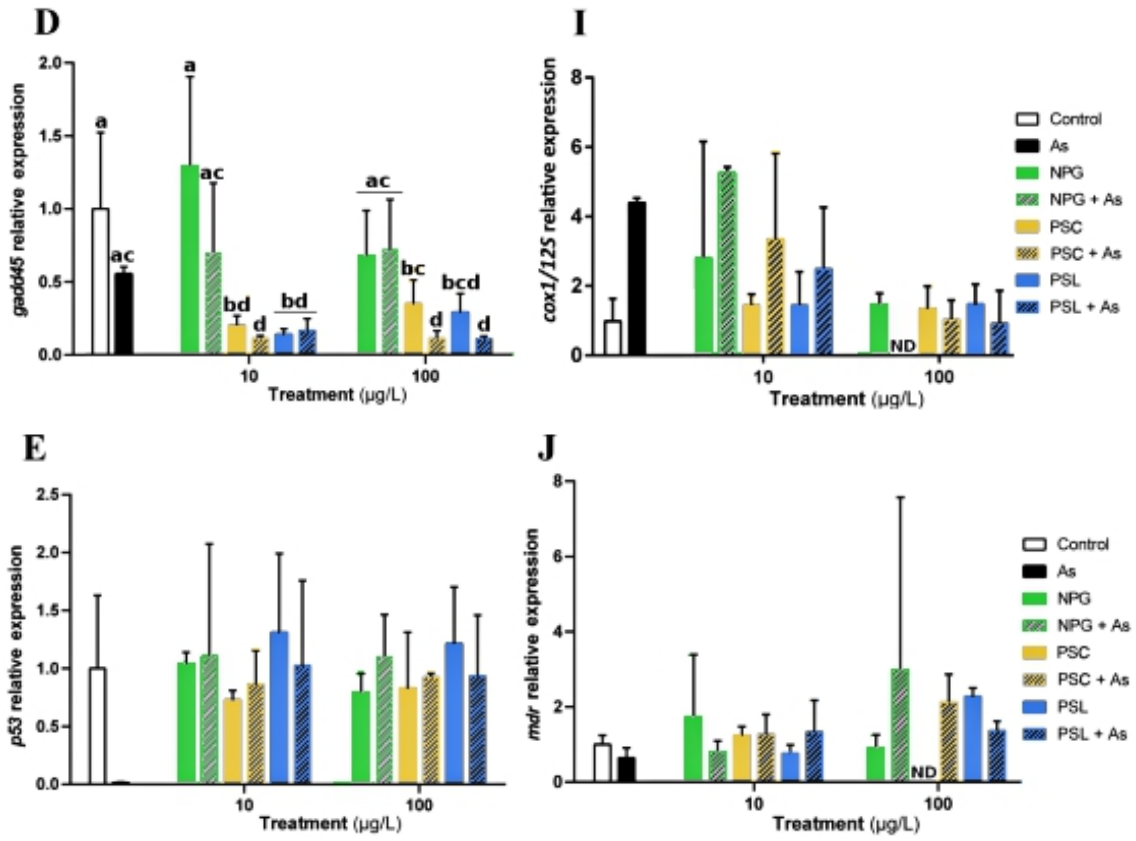

Figure S5 : Relative gene expressions in *I. alatus* gills after one week exposure to 1 mg L^{-1} As combined or not with 10 and 100 µg L^{-1} NPs. mRNA levels are presented for *cav* (A), *cltc* (B), *bax* (C), *gadd45* (D), *p53* (E), *cat* (F), *gapdh* (G), *sod1* (H), *cox1*/*12S* (I) and *mdr* (J). All the values are presented as the mean + sd (n = 4) normalized by *β-actine* and *rpl7* genes. Different letters denote significant differences ($p < 0.05$) between treatments assessed by two-way ANOVA followed by Tukey post-hoc test.

7 ANNEXE II

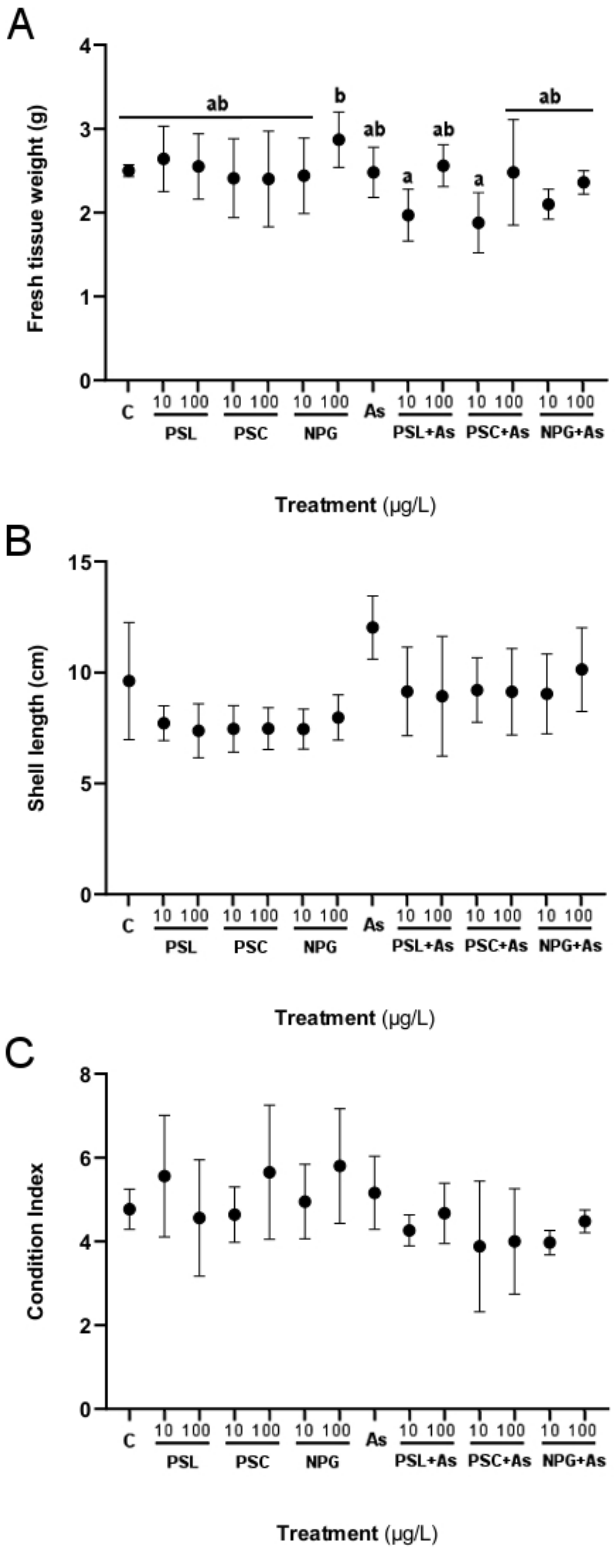

Figure S1 : Comparisons of *C. virginica* biometric parameters after one week exposure. Fresh tissue weight in g (A), shell length in cm (B), Condition Index (C). Different letters denote significant differences between treatments ($p < 0.05$) assessed by two-way ANOVA followed by Tukey post-hoc test (n = 4-5)

Table S1. *C. virginica* targeted gene functions and optimized primer sets temperatures for qPCR

Associated cell functions	Gene names	Abbreviations	Forward (F) Reverse (R) primers	Primers product length	Optimized extension temperatures
Translation elongation factor	Elongation factor 1 alpha	*ef1α**	F : AGGCTGACTGTGCTGTGTTG R : CTCACGGGTTTGTCCGTTTG	83 pb	64 °C
Ribosomal sub-unit (60S)	Ribosomal protein L7	*rpl7**	F : AAGCTGGCAATTTCTTCGTCC R : AGCATGTGAACTGTAGCCTTGT	169 pb	64 °C
Endocytosis	Clathrin heavy chain	*cltc*	F : AGACTCAGGACCCAGAGGAC R : ATCACACGGGTTCTATCGGC	191 pb	66 °C
Oxidative stress	Catalase	*cat*	F : GCAGTGTGTCCACGATAACCA R : TCTCTCCTCGGGCTTCAACA	199 pb	61 °C
	Glyceraldehyde-3-phosphate dehydrogenase	*gapdh*	F : GACCTGAACGGCAAACTCAC R : AGATGCGGACTTGATGGCT	132 pb	64 °C
	Superoxide dismutase Cu/Zn extracellular	*sod3*	F : CCTTGGACGCTCTTTGGCTA R : AGAACAGCGCGCATAGTCAT	147 pb	60 °C

Mitochondrial metabolism	Mitochondrial encoded 12S rRNA	*12S*	F : CATTGGACTGGTTTCAAGGAGG R: CCGTTTTGGTGGAGGATTAGCA	133 pb	65 °C
Cell cycle regulation	Growth arrest DNA damage	*gadd45*	F : GGGTGATGCTGTGTGTGATG R : AGGTCGTTGTCTTTGGGGTT	199 pb	64 °C
	Tumor protein P53	*p53*	F : ATGAAGACTCGTACACCCTCAC R : TCTCTGCTTGAACTACCACCTC	198 pb	57 °C
Apoptosis	Bcl-2-associated X apoptosis regulator	*bax*	F : AGTAAACCCGAGTGCAAACCA R : GACCCCAGTTGTAAACACCATC	80 pb	64 °C
	Apoptosis regulator	*bcl-2*	F : TGGATTGACCAACACGGAGG R : CAATGCCCCTAGAACCACTACA	135 pb	64 °C
Detoxification	Cytochrome P450 family 1 sub-family A1	*cyp1A*	F : CGTCACCGTCAAACTTCTCCT R : TCCCTCCCACATACCACCAC	189 pb	64 °C
	ATP Binding Cassette sub-family B1	*mdr*	F : TACTGTGGCTTTCTGTCCCC R : GATCGCTGCAAACACTTCCTC	133 pb	62 °C
	Metallothionein	*mt*	F : TGGACCCGGATGTAAGTGTG		

			R : GGAGAACGCCTCTCATTGGT	178 pb	64 °C
Energy storage	Vitellogenin	*vit*	F : AGGGGAGTTCATCGTTCGTTT R : CGCAATCCTTGGTGTCTGGT	136 pb	64 °C

9 * : reference genes

10

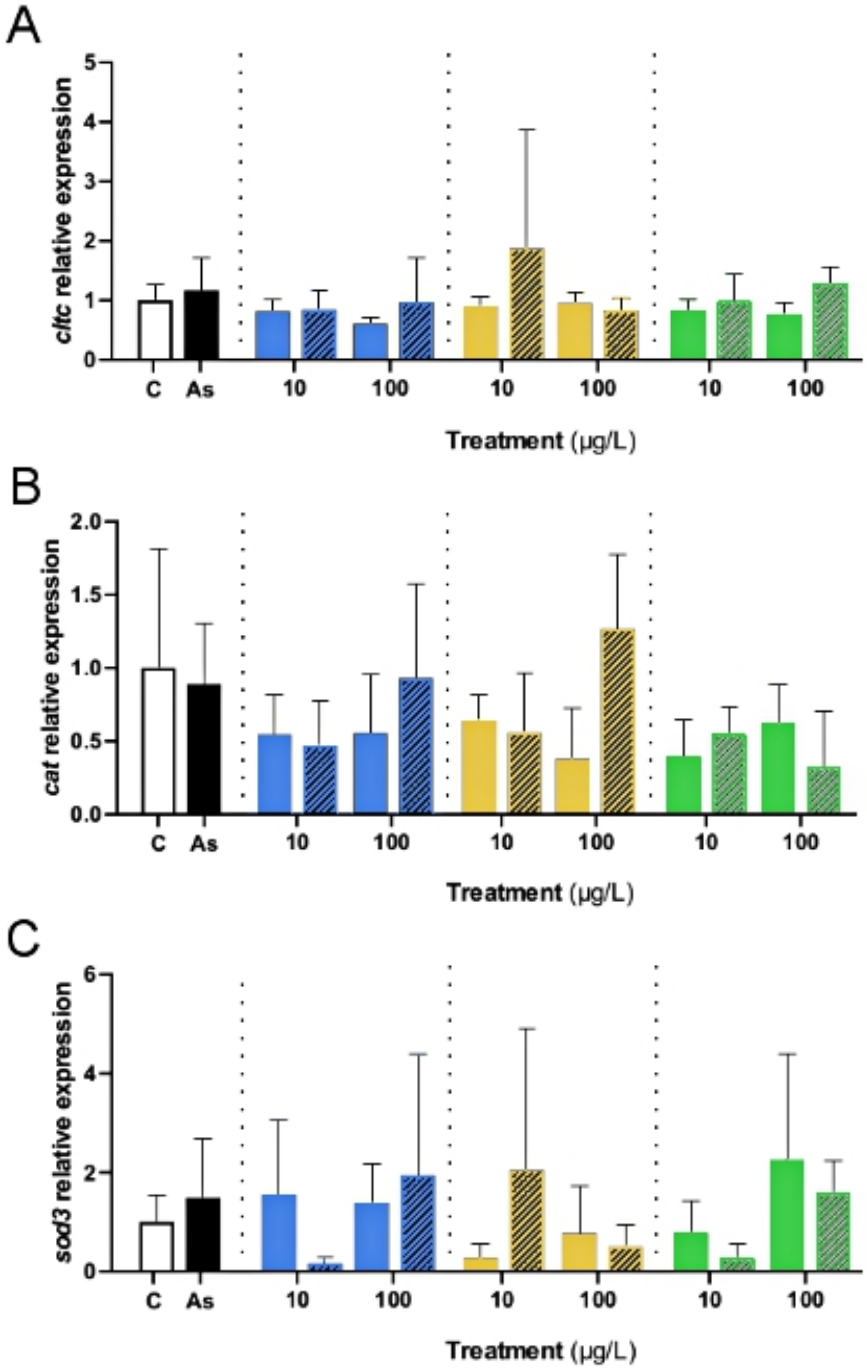
A
cftc relative expression
0
1
2
3
4
5
C
As
10
100
10
100
10
100
Treatment (µg/L)
B
cat relative expression
0.0
0.5
1.0
1.5
2.0
C
As
10
100
10
100
10
100
Treatment (µg/L)
C
sod3 relative expression
0
2
4
6
C
As
10
100
10
100
10
100
Treatment (µg/L)

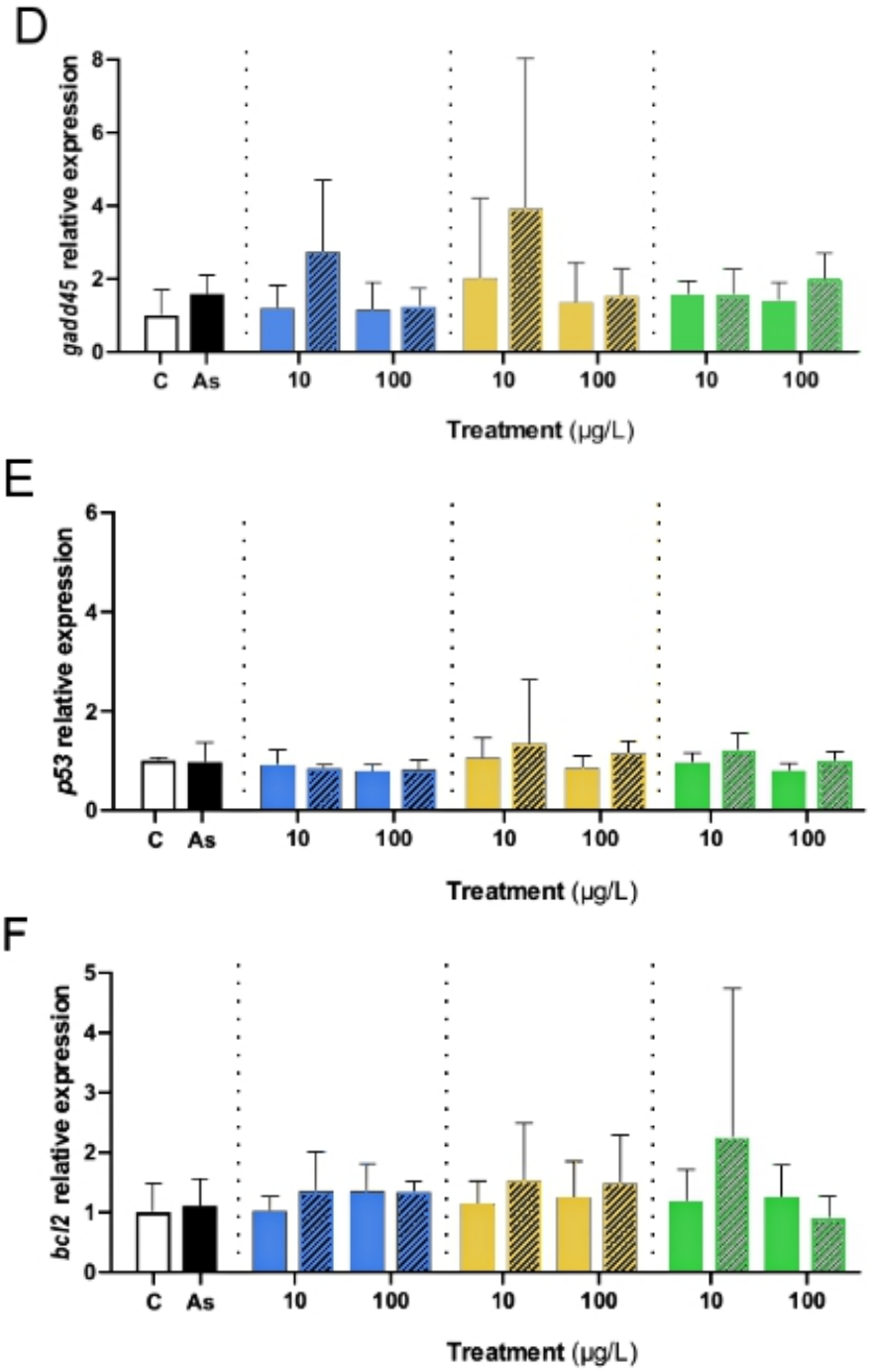
D
gadd45 relative expression
0
2
4
6
8
C
As
10
100
10
100
10
100
Treatment (µg/L)
E
p53 relative expression
0
2
4
6
C
As
10
100
10
100
10
100
Treatment (µg/L)
F
bcl2 relative expression
0
1
2
3
4
5
C
As
10
100
10
100
10
100
Treatment (µg/L)

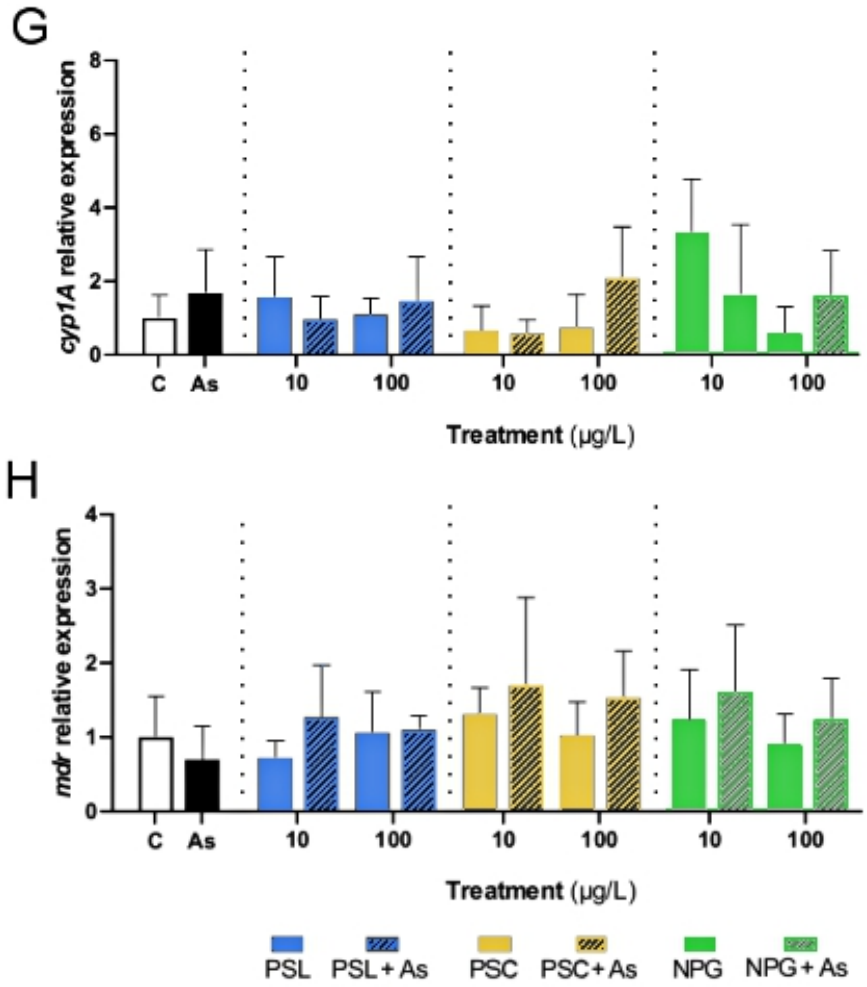

Figure S2 : Relative gene expressions in *C. virginica* gills after one week exposure to 1 mg L^{-1} As combined or not with 10 and 100 µg L^{-1} NPs. mRNA levels are presented for *cltc* (A), *cat* (B), *sod3* (C), *gadd45* (D), *p53* (E), *bcl-2* (F), *cyp1A* (G) and *mdr* (H). All the values are presented as the mean + sd (n = 4-5) normalized by *ef1α* and *rpl7* genes. No significant differences ($p < 0.05$) were assessed by two-way ANOVA.

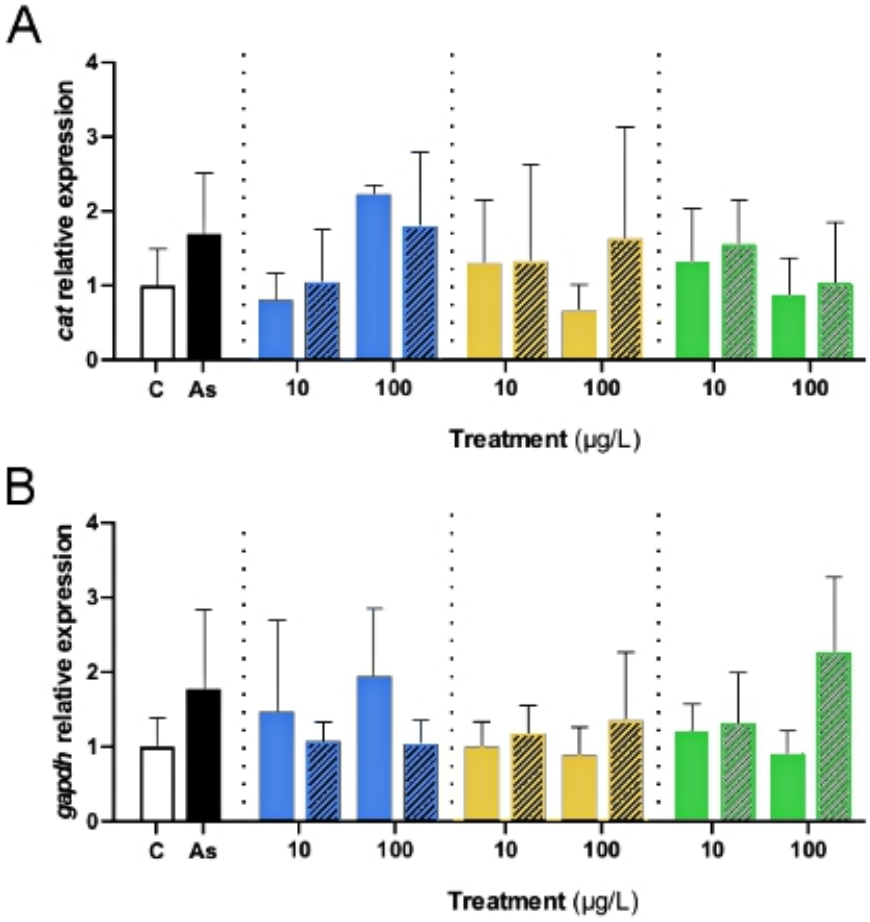
A
cat relative expression
0
1
2
3
4
C
As
10
100
10
100
10
100
Treatment (µg/L)
B
gapdh relative expression
0
1
2
3
4
C
As
10
100
10
100
10
100
Treatment (µg/L)

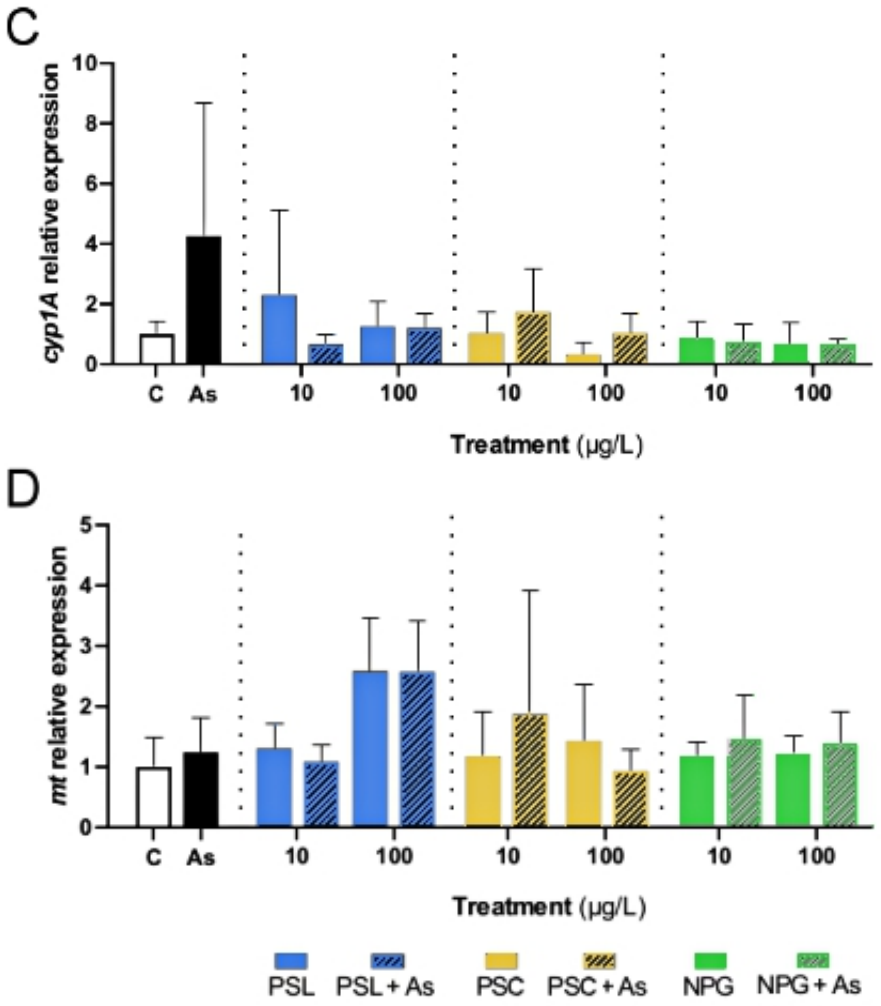

Figure S3 : Relative gene expressions in *C. virginica* visceral mass after one week exposure to treatments. mRNA levels are presented for, *cat* (A), *gapdh* (B), *cyp1A* (C) and *mt* (D). All the values are presented as the mean + sd (n = 4-5) normalized by *ef1α* and *rpl7* genes. No significant differences ($p < 0.05$) were assessed by two-way ANOVA.